FOUR JOINTED BOX ONE, A NOVEL PRO-ANGIOGENIC PROTEIN IN

COLORECTAL CARCINOMA.

BY

Nicole Theresa Al-Greene

Dissertation

Submitted to the Faculty of the

Graduate School of Vanderbilt University

in partial fulfillment of the requirements

for the degree of

DOCTOR OF PHILOSOPHY

In Cell and Developmental Biology.

December, 2013

Nashville Tennessee

Approved:

R. Daniel Beauchamp

Susan Wente

James Goldenring

Albert Reynolds

i

DEDICATION

To my parents, Karen and John, who have helped me in every way possible,

every single day.

ACKNOWLEDGMENTS.

I was lucky enough to be allowed to perform research as an undergraduate in the lab of Ken Belanger. I will be forever grateful for that opportunity that sparked my love of research. Equally important was my time as a technician in Len Zon's lab where I confirmed the fact that I needed to go graduate school and earn my degree. During my time at Vanderbilt I have been helped by so many individuals, and the collaborative nature of everyone I have met with is truly an amazing aspect of the research community here. I am especially thankful for all the technical help and insightful conversations I have had with Natasha Deane, Anna Means, Claudia Andl, Tanner Freeman, Connie Weaver, Keeli Lewis, Jalal Hamaamen, Jenny Zi, John Neff, Christian Kis, Andries Zjistra, Trennis Palmer, Joseph Roland, and Lynn LaPierre. My committee of Jim Goldenring, Al Reynolds, Stacey Huppert, and Susan Wente were essential in both the development and testing of my training these past years. Naturally this work would not have been possible without my mentor, Dan Beauchamp, a man who always inspires me with both his wisdom and his humility. I will never forget our first meeting after I joined the lab when I boldly stated "I'm ready, tell me what to do". He responded with a chuckle, saying that was entirely up to me. His keen ability to gently guide while allowing me to

stumble and learn was remarkable. He was always encouraging, supportive, empathetic, and enthusiastic all at once, which made even the most frustrating of times bearable.   It was truly a gift to work with him and I am forever grateful.

Finally I would like to thank my family. My brother Shawn, and sister-in-law Chrissy have blessed me with a niece and nephew who have provided much joy and comic relief over the past seven years. My parents, Karen and John, who have gone above and beyond the call of duty ever since I could remember, and I'm sure long before that. You have always inspired me to do my best, cheered with me when I have succeeded, and consoled me when I failed. Words cannot ever express my gratitude.

TABLE OF CONTENTS

LIST OF TABLES

LIST OF FIGURES

x

LIST OF ABBREVIATIONS

15-PGDH   15-hydroxyprostaglandin dehydrogenase

ACF   aberrant crypt foci

AOM   azoxymethane

APC   adenomatous polyposis coli

CD24   cluster of differentiation 24

COX   cyclooxygenase

COX-1   cyclooxygenase 1

COX-2   cyclooxygenase 2

CRC   colorectal cancer

CYR61   cysteine-rich angiogenic inducer 61

DS   dachsous (Drosophila)

DSCH1   dachsous 1 (Homo sapiens)

DSS   dextran sodium sulfate

EGF   epidermal growth factor

EP1   prostaglandin E receptor 1

EP2   prostaglandin E receptor 2

EP3   prostaglandin E receptor 3

EP4   prostaglandin E receptor 4

ERK1/2   extracellular signal related kinase 1/2

FAT4   FAT4 (Homo sapiens)

FGF   fibroblast growth factor

FIH   factor inhibiting HIF1

FJ   four jointed (Drosophila)

FJX1	four jointed box one (Homo sapiens)
FT	fat (Drosophila)
GI	gastrointestinal
HIF1-α	hypoxia inducible factor 1
hCG	human chorionic gonadotropin
HRE	hypoxia response elements
HUVEC	human umbilical vein endothelial cells
HMEC-1	human microvascular endothelial cells
IL-1	interleukin 1
LLC	Lewis lung carcinoma cell line
LPS	lipopolysaccharide
MAPK	ERK mitogen-activate protein kinase
MCC	H. Lee Moffitt Cancer Center
NFk$\ss$	nuclear factor kappa $\ss$
NSAIDs	non-steroidal anti-inflammatory drugs
p38 MAPK	mitogen associated protein kinase
PCP	planar cell polarity
PDGF	platelet derived growth factor
PHD	prolyl hydroxylases
PI3K	phosphatidylinositol 3-kinase
PG	prostaglandin
PGE2	prostaglandin E2
PGE-M	11α-hydroxy-9,15-dioxo-2,3,4,5-tetranor-prostane-1,20-dioc acid
PGD$_2$	prostaglandin D2
PGF$_{2\alpha}$	prostaglandin F$_{2\alpha}$

PGH$_2$ prostaglandin H2

PGI$_2$ prostaglandin I2

PNGaseF   peptide N-glycosidase F

ROS   reactive oxygen species

TGFα   transforming growth factor α

TNF-α   tumor necrosis factor α

TxA$_2$ thromboxane A$_2$

VEGF   vascular endothelial growth factor

PHD   prolyl hydroxylase enzme

VEGF   vascular endothelial growth factor

VHL   von-Hippel Lindau

VUMC   Vanderbilt Medical Center

.

CHAPTER I.

INTRODUCTION

Significance of colorectal cancer

Colorectal cancer (CRC) represents the third leading cause of cancer related deaths for both men and women in the United States [1]. In 2013 alone, it is estimated that 150,000 new cases will be diagnosed and 50,000 individuals will die from disease [1]. There are multiple factors involved in the development of CRC. For example, there are known genetic mutations that occur during disease progression from normal colonic epithelium through aberrant crypt foci (ACF) formation, to eventual carcinoma development (Fig. 1) [2]. Mutation of the *adenomatous polyposis coli gene* (*APC*) is a key initial event in the development of CRC, while *Kristen rat sarcoma viral oncogene* (*KRAS), SMAD family member 4 (SMAD4), and tumor protein 53 (*p53) mutations are involved in the later stages of disease. In addition to genetic alterations, increased inflammation has also been linked to CRC development. Cyclooxygenase 2 (COX-2) is an inflammatory related gene whose expression is increased as early as the adenoma stage (~50%) with the majority of carcinomas expressing high levels (~90%). Identification of these changes in gene expression has given insight into the biology of CRC and the derivation of targeted therapies. However an incomplete understanding of the downstream regulatory components exists. Further, some therapies, including COX-2 targeted anti-inflammatory agents have undesirable side effects. Ongoing research is aimed at trying to enhance

our knowledge of how such drugs work *in vivo* to provide rationale for the development of new reagents that potentially exhibit more specific disease treatment as well as less toxicity in patients.
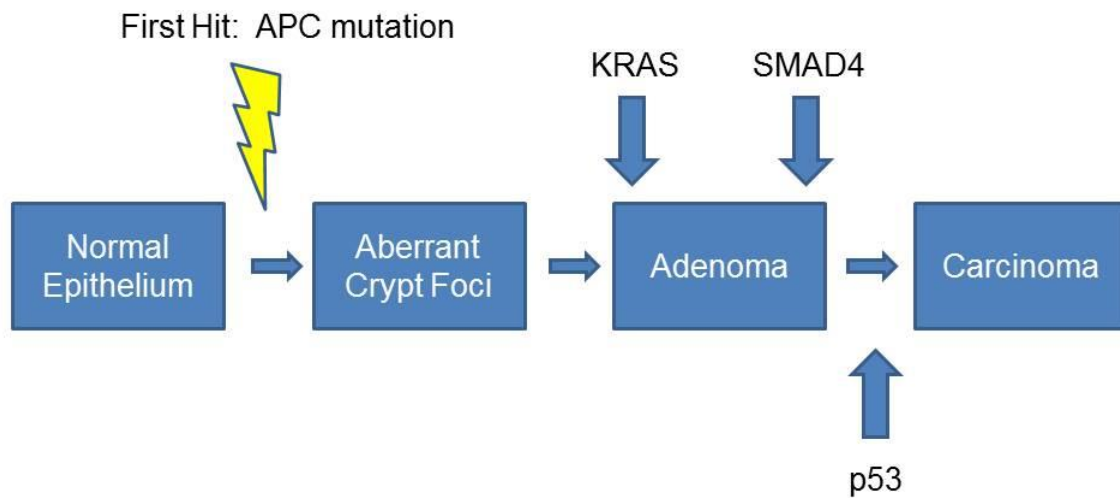
Figure 1. Diagram of known genetic mutations involved in CRC progression. Modified version of known genetic mutations (*adenomatous polyposis coli gene* (*APC*), *Kristen rat sarcoma viral oncogene* (*KRAS*), *SMAD family member 4 (SMAD4), and tumor protein 53* (*p53*)) that occur during disease progression from normal colonic epithelium through adenoma to carcinoma formation first proposed by Burt Vogelstein and colleagues [2].

Cyclooxygenases, angiogenesis, and colorectal cancer

Chronic inflammation has been linked to the development and progression of multiple cancers, including CRC. One of the major pathways linked to inflammation involves the cyclooxygenase enzymes. Targeting these enzymes has shown promise in CRC therapies but causes significant side effects. Cyclooxygenase enzymes 1 and 2 (COX-1, COX-2) represent the rate-limiting step in the conversion of arachidonic acid to prostaglandins (Figure 2). COX-1 is found in normal colonic mucosa and thought to have a homeostatic role whereas COX-2 is expressed at low levels, but rapidly induced in response to inflammatory signals. Arachidonic acid is first converted by COX-1 and COX-2 into prostaglandin H2 (PGH_2). PGH_2 is subsequently metabolized by prostaglandin synthases into prostanoids, including prostaglandin E2 (PGE_2), prostaglandin D2 (PGD_2), prostaglandin $F_{2\alpha}$ ($PGF_{2\alpha}$), prostaglandin I2 (PGI_2) or thromboxane A_2 (TxA_2). An important physiological antagonist of prostaglandins is the prostaglandin degrading enzyme 15-hydroxyprostaglandin dehydrogenase (15-PGDH). 15-PGDH catalyzes the oxidization of a key hydroxyl group on the prostaglandins to a ketone which renders the prostaglandins biologically inactive [3]. Prostanoids have been implicated in tumor growth through modulation of survival factors, angiogenesis, and immune surveillance. PGE_2 is the predominant prostaglandin found in colonic tissue and has been shown to signal through at least four different prostaglandin receptors (prostaglandin E receptors 1-4, EP1-4).

Of the genes involved in the arachidonic acid pathway, much focus has

been placed on COX-2 and its regulation of PGE_2 production in CRC. Elevation of both COX-2 protein and PGE_2 has been detected in CRC as compared to normal mucosa [4-8]. Although *in vivo* levels of PGE_2 have been reported, data suggests that actual levels in patients are difficult to accurately assess. Thus the urinary metabolite 11α-hydroxy-9,15-dioxo-2,3,4,5-tetranor-prostane-1,20-dioc acid (PGE-M) was identified as a more reliable biomarker for PGE_2 production *in vivo* [9]. Increased levels of urinary PGE-M have been associated with larger polyps in CRC patients [10,11]. High expression of COX-2 in CRC patients has also been associated with poor patient prognosis leading to studies that targeted this enzyme in CRC. [12].
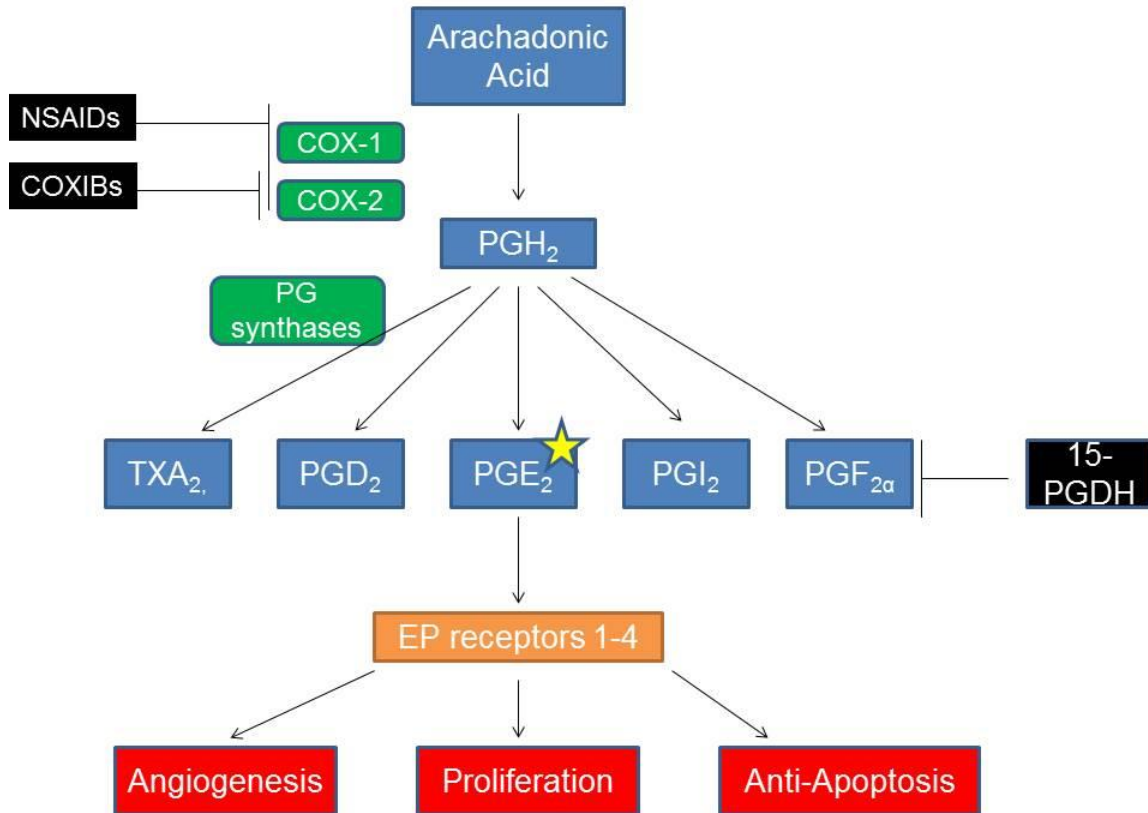
Figure 2. The arachidonic acid signaling pathway. Green symbols represent conversion enzymes, blue symbols represent substrates/products, orange symbols represent prostaglandin receptors, red symbols represent biological activities, and black symbols represent pharmacological or naturally occurring pathway antagonists.

Mouse models represent an important biological tool for understanding regulatory pathways in CRC and for preclinical studies targeting these pathways. Mouse models of CRC bear many similarities to human CRC. As mentioned above, APC is one of the earliest and most frequent genetic mutations found in human CRC and several mouse models of intestinal tumorigenesis have shown that genetic deletion or truncation of murine *Apc* causes multiple intestinal polyps. Carcinogen induced CRC in mice can also be used to model human disease, including administration of the carcinogen azoxymethane (AOM). When deletion of *COX-2* expression is combined with an *APC* truncation, mice exhibit fewer, smaller polyps in a gene-dose dependent manner [13,14]. Similar results are observed when an *EP2* deletion is added to the *APC* mutant mouse background, or when *EP1* or *EP4* KO mice are treated with AOM, suggesting that EP1, EP2, and EP4 are important mediators of PGE_2 signaling in CRC [15-17]. Conversely, the addition of PGE_2 treatment to *APC* mutant mice, or mice treated with AOM, increases both the multiplicity and size of intestinal polyps [18,19]. As mentioned above, 15-PGDH is a known prostaglandin degrading enzyme whose expression is often diminished in CRC [20,21] *15-PGDH* null mice have increased intestinal tumor burden compared to WT mice after AOM carcinogen treatment [22]. These murine studies have led to a greater appreciation of the pathways regulated by COX-2 expression and PGE_2 production in tumorigenesis.

The most common COX inhibitors are nonsteroidal anti-inflammatory drugs (NSAIDs). NSAIDs fall into two main classes; those that inhibit both COX-

1 and COX-2 ('non-specific' i.e. aspirin, Sulindac, Indomethacin, Piroxicam) and those that are specific for COX-2 ('coxibs' i.e. celecoxib, NS398). NSAIDs have been shown to provide both a prophylactic and therapeutic benefit in both hereditary and sporadic human CRC [23-30]. Mouse models also support the role of NSAIDs in diminishing tumor burden. For example, celecoxib treated mice show reduced tumor burden in AOM treated animals; an effect that is reversed in *15-PGDH* null animals [31]. Piroxicam and sulindac treatment of *APC* min mice also decreased tumor burden, but these effects were reversed upon the addition of EP receptor agonists, supporting the importance of blocking COX-2 mediated PGE_2 signaling [32] . The therapeutic benefits of NSAIDs are dependent on both dose and duration of use [23]; however there are unwanted side effects to consider that also correlate with increased NSAID use. Non-specific NSAIDs (excluding aspirin) cause gastrointestinal (GI) harm including increased risk of ulceration, bleeding and related complications [23]. It was hypothesized that these effects were due to inhibition of COX-1 which is important to epithelial survival and functional integrity in the GI tract. These observations factored into the rationale behind the development of COX-2 specific drugs. Unfortunately, despite having reduced GI side effects, use of COX-2 specific inhibitors was associated with a significantly increased risk of adverse cardiovascular events, such as stroke and heart attack [24,33]. Therefore the identification of more selective therapeutic targets downstream of COX-2 signaling has become an important area of ongoing research.

Targeting the blood vessels that feed tumors has also become a priority in

8

cancer therapy. Angiogenesis is the process of recruiting and restructuring blood vessels from pre-existing vasculature, and is essential for tumor growth beyond 1-2 mm in diameter. Early in tumor development an 'angiogenic switch' occurs tipping the balance in favor of pro-angiogenic factors in contrast to angiogenesis inhibitors [34]. In addition to being required for enlargement of the primary tumor, increased tumor vascularization also provides a metastatic path for dissemination to other areas of the body.   Metastatic disease is thus reliant on vascular routes, and increased tumor angiogenesis often correlates with poor patient outcomes in a variety of carcinomas. Indeed studies have shown that microvessel counts from CRC patient tissues increased in concordance with tumor size, local invasion, and lymph node metastasis and is itself a prognostic factor [35,36].

Secreted angiogenic factors are often overexpressed by tumor cells and provide cues that affect endothelial cell proliferation, migration, and invasion. One of the most widely studied pro-angiogenic molecules is vascular endothelial growth factor (VEGF). Increased expressed of VEGF has been observed in colorectal tumors as compared to normal tissue, and associated with increased tumor vessel density and poor patient prognosis [37,38] . While VEGF may be the best studied regulator of angiogenesis, there are a number of other secreted molecules that also regulate this process, including transforming growth factor α (TGFα), epidermal growth factor (EGF), platelet derived growth factor (PDGF), and fibroblast growth factor (FGF) [39]. COX-2 has been linked to angiogenesis through production of some of these factors. *In vitro*, expression of *COX-2* in CACO-2 CRC cells induces autonomous production of both VEGF and FGF, and

9

non-autonomous increases in endothelial cell motility and invasion [40].

Conversely, *COX-2* null fibroblasts secrete less VEGF in culture as compared to wild-type cells [41]. *In vivo*, growth of Lewis lung carcinoma (LLC) cells as xenografts in *COX-2* KO mice exhibit smaller tumor formation correlated with decreased tumor vascularization as compared to xenografts grown in wild-type mice [41]. Similarly, celecoxib treatment of LLC cells grown in wild-type mice also resulted in attenuated tumor formation [41]. Finally, celecoxib treatment in the rat corneal model of angiogenesis resulted in shorter, more interspersed capillary formation, indicating a block in angiogenesis [42,43]. Taken together, the blockage of COX-2 function, either genetically or pharmacologically, has been shown to reduce tumor formation, in part, due to a decrease in angiogenesis.

Another important mediator of tumor biology that has been linked to COX-2 and VEGF signaling is *hypoxia inducible factor 1, alpha subunit (HIF1A). HIF1A* is widely expressed across various cell types, and increased *HIF1A* expression has been observed in multiple cancers, including CRC [44]. HIF1-α is highly regulated by oxygen levels in the cell, and together with HIF1-β serves to regulate genes containing hypoxia response elements (HREs). HIF1-α has been reported to regulate over 60 genes important to cellular processes including angiogenesis, glucose metabolism, survival factors, and invasion factors [45,46]. Both *VEGF* and *COX-2* are included in the list of HIF1-*α* gene targets [47,48]. Forced expression of *HIF1A* in HCT116 colon cancer cells results in increased xenograft tumor formation that is associated with an increase in VEGF levels and

tumor vascularization [49]. Kaidi et al identified several HREs in the *COX-2* promoter, and demonstrated that *COX-2* mRNA is increased during hypoxia through binding of HIF1-α to the *COX-2* promoter in colorectal cancer cells *in vitro* [48]. Further studies have shown that there is reciprocal regulation between COX-2, PGE$_2$, and HIF1-α. *In vitro*, treating HCT116 cells with PGE$_2$ increases HIF1-α protein and subsequent *VEGF* mRNA, which was blocked with inhibitors of EP1, MEK-ERK, and PI3K-AKT [50]. Thus *in vitro* data suggests a complicated signaling interaction among COX-2, HIF1-α and angiogenic factors like VEGF.

Summary

As the third leading cause of cancer related morbidity and deaths, there is a need to find better targeted therapies for CRC. Although a great deal is known about the contribution of inflammation and genetic alterations to disease progression, a detailed understanding of key regulatory pathways is needed for clinical translation of this knowledge. There are complex interactions between inflammation, cyclooxygenase enzymes, angiogenesis, and HIF1-α that play a vital role in tumor formation and advancement. The benefit of anti-inflammatory drugs has proven to be extremely effective in both CRC prevention and treatment. However, like most drugs, unwanted complications of extended use of such drugs exist. Non-selective anti-inflammatory drugs burden the gastric and intestinal compartments, while more selective inhibitors can pose severe cardiovascular risk, especially in certain populations. In this context, we sought to understand the biological responses of tumors *in vivo* to the selective COX-2

drug, celecoxib. Herein we describe changes in gene expression in human rectal

tumors that occur in response to celecoxib treatment and characterize one such

identified novel target. Through this work, we have a clearer understanding of the

COX/HIF1-α/angiogenesis pathway.

CHAPTER II.

CHARACTERIZATION OF GENE EXPRESSION CHANGES IN RESPONSE TO CELECOXIB TREATMENT *IN VIVO,* AND THE IDENTIFICATION OF FOUR JOINTED BOX 1.

Introduction

A large body of data indicates the role of inflammation in cancer formation and progression, including CRC. *COX-2* is a well-described target of inflammation, whose expression is increased in CRC and is associated with poor patient prognosis [4,6,12]. Non-steroidal anti-inflammatory drugs (NSAIDs), including the coxib series that specifically inhibit COX-2 activity, are very efficient in preventing both tumor formation and disease progression. However, the use of COX-2-specific NSAIDs been associated with adverse cardiovascular side effects, including heart attack and stroke. Aside from the effects of coxibs on inhibition of COX-2 activity and associated effects *in vitro*, little is known about actual biological responses to therapies *in vivo*. Understanding biological responses in tumors that might be different from responses in other tissues may identify better targets for the treatment of CRC. With this goal in mind we sought to identify novel therapeutic targets that are altered in response to celecoxib treatment in primary human rectal tumors *in vivo*. Through this screen we have identified gene expression changes previously undescribed in colorectal tumor biology. Importantly, we found a novel potentially COX-2 regulated gene, *Four*

jointed box 1, that was down-regulated after celecoxib treatment, and that contributes to tumor angiogenesis.

Materials and Methods

Ethics statement

Human tissues used for microarray analysis were collected and annotated according to established protocols and approved by the appropriate Institutional Review Boards (IRB) at the Moffitt Cancer Center (MCC) and Vanderbilt University (VUMC) (GSE17536 and GSE17537). Written informed consent was obtained from all patients prior to inclusion in the studies. De-identified human rectal tumor tissue for immunohistochemistry was obtained with VUMC IRB approval. All murine experiments were approved by the Vanderbilt Institutional Animal Care and Use Committee and performed in accordance with the standards of the Association of Assessment and Accreditation of Laboratory Care (AAALAC).

Analysis of human-expression profiling

Tissue preparation, quality control, RNA isolation, and hybridization were performed as previously described [51]. The raw .CEL files of platform Affy 133 plus 2 from MCC and VUMC were combined and pre-processed using the robust multi-array average (RMA) expression measure with quantile normalization method. The Bioconductor package *Affy* (http://www.bioconductor.org/packages/release/bioc/html/affy.html) was employed. Affyprobeset 219522_at was used to compare gene expression

14

levels of *FJX1* between different stages of colon cancer with Wilcoxon rank-sum

test. Kaplan-Meier estimates for disease free and overall survival from 191 stage

I-III colon cancer patients were generated using R software (http://www.r-

project.org). Patients were classified as *FJX1* high and low expression groups

based on a median expression value cut-off using probeset 219522_at and the

log rank test was applied to determine significance.

Celecoxib sub-group statistical analysis

The celecoxib treatment protocol was previously described [10]. Raw

gene expression data (.CEL files, Affymetrix 133 plus 2 array platform) from 16

patient biopsies taken pre- and post- celecoxib treatment (32 tissue samples

total), were preprocessed and normalized, as above, and expressed in $\log_2$

format. The bioconductor limma package was employed for array data analysis

(http://www.bioconductor.org/packages/release/bioc/html/limma.html). A

moderated paired t-test was used to select one hundred fifty-nine probes based

on a cutoff p-value $\leq$0.01 (un-adjusted). The 159 probes were next imported into

Ingenuity Pathway Analysis (IPA®, www.ingenuity.com) and analyzed for

network enrichment by mapping to the IPA global molecular network by

knowledge-based connectivity.

 RNA extraction and qRT-PCR

RNA was extracted using the Qiagen RNeasy Kit (Qiagen) per

manufacturer's instructions. qRT-PCR reactions analyzing *FJX1* in human

tumors were performed using superscript III reverse transcriptase (Invitrogen),

SYBR Green (SA Biosciences) and analyzed on an iCycler (Bio-Rad, Inc.).

Primers used : *FJX1*: 5'-CGTGCTGGCACAGTAAAGAA-3' and 5'-

TTCAAAGTTCTGGGAGGACG-3' or 5'-AGCTGGTGGACCTAGTACAATGGA-3'

and 5'-ACTGCAGGCTGAAGAGGTTGCTTA-3' (Integrated DNA technologies

(IDT)); 18S (SAbiosciences). Relative fold change of expression was calculated

by $2^{-\Delta Ct}$.

Immunohistochemistry

Eleven de-identified formalin fixed and paraffin embedded human

colorectal tumor tissues were obtained from the Vanderbilt Ingram Cancer Center

Tissue Acquisition and Pathology Core. Slides were sectioned at 5µm thickness

and processed as described [52] except slides were heated in 10 mM sodium

citrate, pH6.0 instead of in 100 mM Tris. Partially purified anti-FJX1 antibody

(rabbit polyclonal, 209) was applied at a dilution of 1:2000 and incubated

overnight at 4°C. Slides were washed, incubated in 1:500 goat anti-rabbit

antibody for 30 min., washed and incubated in avidin biotin complex (Vector Labs

Elite ABC kit) for 30 min and washed. Color was developed in 3, 3'

diaminobenzidine (Vector Labs) and nuclei were stained with Gill's #3

hematoxylin (Sigma). Images were taken on an Axioskop 40 upright light

microscope (Carl Zeiss, Inc.).

Results

Gene expression responses in human rectal tumors treated with celecoxib

Inhibition of COX-2 activity in colon cancer patients by the selective inhibitor celecoxib showed early promise in prevention of disease progression until clinical trials were suspended in light of new evidence that use of the agent was associated with a high incidence of cardiac arrests [24,53]. We wanted to identify downstream therapeutic targets of COX-2 in CRC that might be used to bypass side effects associated with selective COX-2 inhibitors. To accomplish this, we extracted RNA from paired rectal tumor biopsies taken before and after 5 day treatment with celecoxib (400mg taken twice daily; n=32 total biopsies; 16 pre and 16 post-treatment) [10]. Efficacy of COX-2 inhibition was confirmed by demonstrating a significant decrease in patient urinary PGE-M levels post-treatment [10]. Differential microarray analysis revealed 159 expression elements mapping to 136 human genes that were significantly altered after celecoxib treatment (Raw P value <0.01, Tables 1 and 2). We conducted pathway enrichment analysis on the 136 known genes using a commercially available knowledge-based database. The collection of genes differentially expressed in the tumors before and after celecoxib treatment was significantly enriched in a network known to regulate hematological system development and function, cell death, and cellular growth and proliferation, (P < 0.005, Table 3). The analysis was supported by the presence of central nodes (defined as genes/complexes having at least four direct or indirect interactions with celecoxib regulated genes) within the network that are known regulators of inflammation

17

and cancer progression. These nodes included nuclear factor kappa B (NFkB), interleukin 1 (IL-1), and p38 mitogen-activated protein kinase (p38 MAPK).

<u>*FJX1* mRNA and protein expression is increased in CRC and is associated with poor patient prognosis.</u>

One of the genes that exhibited decreased expression after celecoxib treatment and was present in the top network was *four jointed box one (FJX1),* a unique gene with no known function in tumor biology. *In silico* analysis of *FJX1* mRNA expression in clinically annotated samples collected at Vanderbilt Medical Center (VUMC) and the H. Lee Moffitt Cancer Center (MCC) (Clinical information, Table 4) revealed that *FJX1* mRNA is significantly increased across all stages of CRC as compared to normal colorectal tissue and colorectal adenomas (Figure 3A, stage 1, $P < 0.02$; stages 2, 3 and 4, $P < 0.00001$). There was also a significant difference between *FJX1* mRNA expression when stages 1 and 2 were compared to stages 3 and 4 ($P < 0.02$), indicating that *FJX1* expression is further increased in more advanced stages of colon cancer.

To validate our microarray findings, we conducted quantitative RT-PCR analysis for *FJX1* mRNA and found *FJX1* mRNA expression levels were between five- and seventy-fold higher in colon cancer tissues than in normal adjacent tissue from the same patient (Figure 3B, one-sided t-test $P < 0.0004$). Next, we examined if *FJX1* expression correlated with patient survival in a subset of stage I-III CRC patient samples from the VUMC and MCC colorectal cancer gene expression array datasets (n=191). Samples were stratified into two groups

18

based on lower (n=95) and higher (n=96) than median expression of *FJX1* and the relationship between sample *FJX1* mRNA expression and patient survival was determined by Kaplan-Meier analysis. In this retrospective analysis, patients with higher than median *FJX1* mRNA expression had significantly worse disease-free and overall survival as compared to those with lower *FJX1* expression (Figure 3, C and D). These data show that *FJX1* mRNA expression is increased in human colorectal cancer and that higher expression in tumors is associated with worse patient outcomes.

By immunohistochemical analysis of colorectal tumors and adjacent normal tissues, we found that FJX1 was expressed in eight of eleven tumors at moderate to high levels that varied across the tumor in most cases, while little to no FJX1 was detected in normal mucosa (Figure 4 and data not shown). In more differentiated tumors, FJX1 was primarily located in apical cytoplasm of the epithelial cells but was also found in basal cytoplasm in less well differentiated tumors and those with greater intensity of FJX1 immunoreactivity. These data support that FJX1 protein levels are elevated in CRC tissue as compared to normal in concordance with elevated mRNA levels observed via microarray and qPCR data.

TABLE 3: The top network from Ingenuity Pathway analysis of celecoxib regulated genes includes known inflammatory targets and FJX1.
Gene symbol and name of the genes found in the top network after IPA analysis of celecoxib regulated genes.   * Indicates central nodes.

Gene Symbol	Gene Name
BCL11A	B-cell CLL/lymphoma 11A (zinc finger protein)
COL24A1	collagen, type XXIV, alpha 1
COL5A1	collagen, type V, alpha 1
CSNK2A1	casein kinase 2, alpha 1 polypeptide
CXCL6	chemokine (C-X-C motif) ligand 6 (granulocyte chemotactic protein 2)
ENO1	enolase 1, (alpha)
ENPP1	ectonucleotide pyrophosphatase/phosphodiesterase 1
ERCC1	excision repair cross-complementing rodent repair deficiency, complementation group 1 (includes overlapping antisense sequence)
FJX1	four jointed box 1 (Drosophila)
FKBP10	FK506 binding protein 10, 65 kDa
FKBP1A	FK506 binding protein 1A, 12kDa
FRZB	frizzled-related protein
GJB2	gap junction protein, beta 2, 26kDa
HYOU1	hypoxia up-regulated 1
ITCH	itchy E3 ubiquitin protein ligase homolog (mouse)
JUN	jun proto-oncogene
MAP2K5	mitogen-activated protein kinase kinase 5
OSBPL2	oxysterol binding protein-like 2
PCBP2	poly(rC) binding protein 2
PPME1	protein phosphatase methylesterase 1
UNC5B	unc-5 homolog B (C. elegans)
WNT5A	wingless-type MMTV integration site family, member 5A
YPEL1	yippee-like 1 (Drosophila)
CN*	Calcineurin proteins
hCG*	Chorionic Gonadotropin
IL1*	Interleukin 1
LDL*	Beta Lipoprotein, Low density lipoprotein, Oxidised LDL
NFkB*	nuclear factor kappa beta
P38 MAPK*	P38 Mitogen-activated protein kinase
PDGF BB*	Platelet-Derived Growth Factor

Table 4. **Patient Sample Demographics, Pathology and Clinical Follow-up data.** The numbers of patient samples used in this study are broken down by demographic, pathologic and clinical follow up characteristics. The celecoxib treatment cohort consists of 16 matched pairs of samples (pre-treatment and post-treatment) and was used to identify *FJX1* as a celecoxib responsive gene element. VUMC and MCC are publicly available datasets of fresh tumor biopsies from newly diagnosed CRC cases which had received no prior treatment and were used for establishing the association between FJX1 expression and AJCC stage and clinical outcome. Pre-treatment celecoxib samples were included in the VUMC dataset. The proportion of patient samples correlated with each demographic, pathologic and clinical characteristic is given in parenthesis. N/A = Not Applicable.

	Celecoxib Treatment	VUMC + MCC
Total number of patients	N=16	N=250
Mean age +/- SD	60.0 +/- 10.00	65.0 +/- 13.26
Male	8 (50.0%)	132 (52.8%)
Stage I	4 (25.0%)	33 (13.2%)
Stage II	4 (25.0%)	76 (30.4%)
Stage III	8 (50.0%)	82 (32.8%)
Stage IV	0 (0.0%)	59 (23.6%)
Median follow-up (months)	N/A	42.7
Deaths	N/A	84 (33.6%)
Caucasian	14 (88.0%)	215 (86.0%)
African-American	2 (12.0%)	15 (6.0%)
Unknown/Other	0	20 (8.0%)
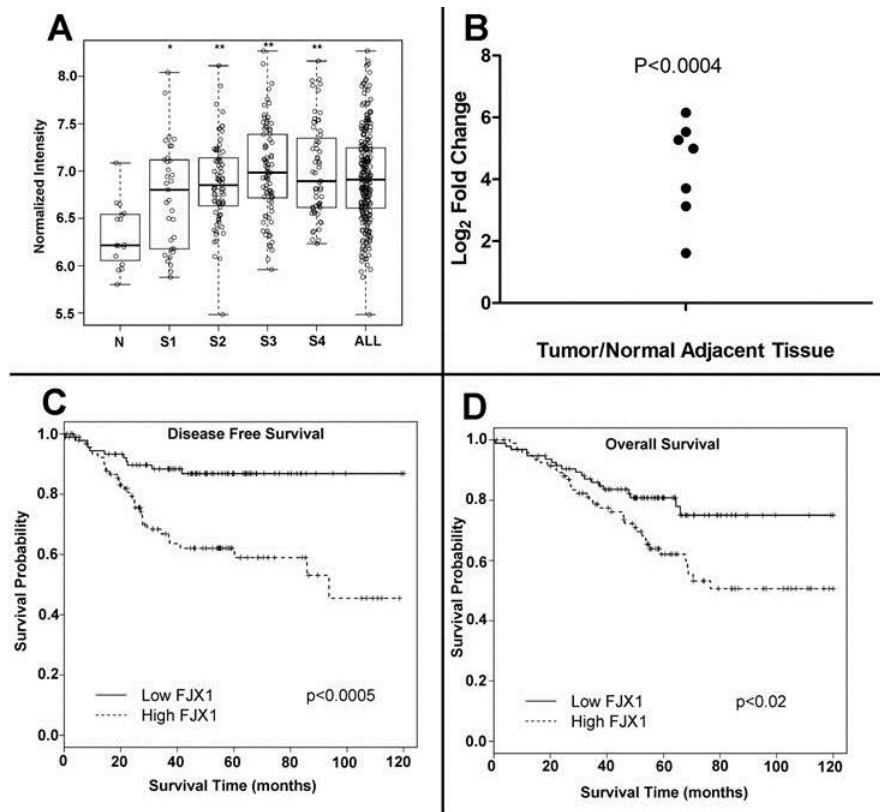
Figure 3. *FJX1* **mRNA expression is upregulated in CRC and is associated with poor patient prognosis.** **(A)** Normalized microarray-based signal intensity from *FJX1*-specific mRNA across 250 carcinoma and 16 normal CRC tissues. Significance was determined by Wilcoxon rank sum test as compared to normal. *P < 0.02; **P < 0.00001. N = normal; S1, S2, S3, and S4 = stage 1, 2, 3, and 4 respectively; all = stages 1-4. **(B)** Log_2 fold change of *FJX1* specific mRNA in tumor tissue as compared to matched normal adjacent tissue as determined by qPCR. Datapoints represent the mean calculated values of four technical replicates/patient. Significance was determined using a one sample t-test. **(C/D)** Kaplan-Meier estimates relative to **(C)** disease free survival (c index 0.75) and to **(D)** overall survival (c index 0.57) for CRC patients (stages 1-3, n=191) separated into lower than median (solid line, n=95) and higher than median (dashed line, n=96) *FJX1* mRNA expression groups. Significance was determined by Log-rank test.
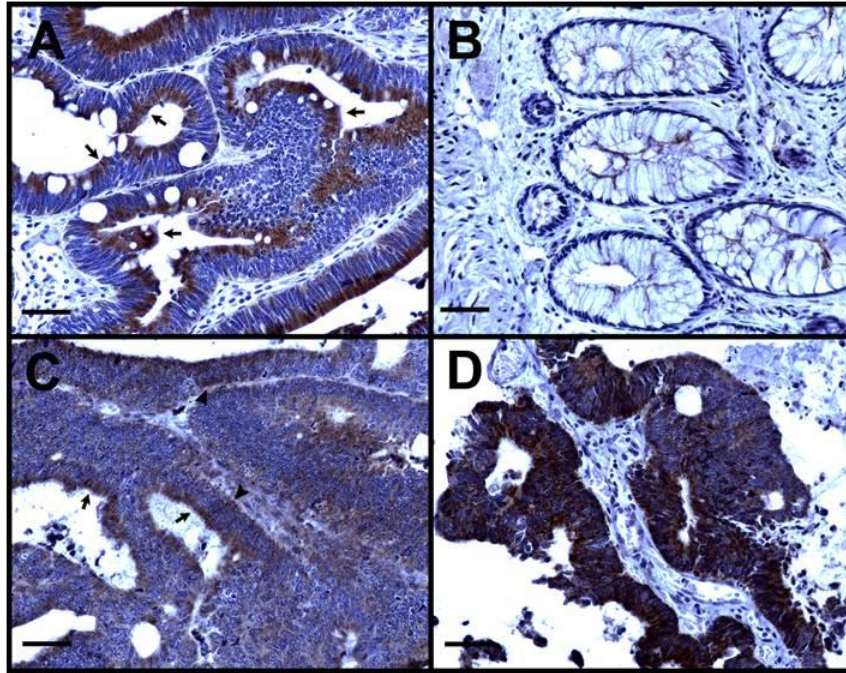
Figure 4. FJX1 protein expression is elevated in rectal tumors. (A) FJX1 (brown) is detected at a high level in apical cytoplasm of a well-differentiated rectal tumor. (B) Nearby adjacent normal epithelium is negative for FJX1. (C) A rectal tumor with low to moderate expression has FJX1 present mostly apically but occasionally basally. (D) In a rectal tumor showing loss of cellular polarity, FJX1 is located throughout the cytoplasm of most cells. Nuclei are counterstained in blue. Arrows indicate apical FJX1 localization; arrowheads indicate basal FJX1 localization. Scale bar = 50 μm.

Discussion

FJX1 expression is increased in CRC and associated with poor patient prognosis

       NSAIDs, which inhibit COX activity, are one of the most widely used classes of drugs, and numerous studies have shown their efficacy in limiting both tumor formation and progression. COX-2 selective NSAIDs were developed in the hopes of bypassing gastrointestinal side effects commonly associated with the extended use of non-selective NSAIDs. However, the discovery that selective COX-2 inhibitors pose severe cardiovascular risk has driven the field to look for alternative solutions. To address this problem we performed microarray analysis on human rectal tumors before and after treatment with the selective COX-2 inhibitor, celecoxib. Pathway analysis of the genes altered after treatment revealed a network involved in regulation of hematological system development and function, cell death, and cellular growth and proliferation. Included in this network were genes that are known regulators of inflammation and cancer progression, including genes encoding nuclear factor kappa B (NFkB), interleukin 1 (IL-1), and p38 mitogen-activated protein kinase (p38 MAPK). To our knowledge, this is the first experiment analyzing the biological mechanism of COX-2 inhibition in actual human tumors *in vivo*. These gene changes provide a basis for further exploration not only into relevant alternative therapeutic targets *in vivo*, but also to the alterations of genes potentially involved in cardiovascular homeostasis that are altered upon COX-2 inhibition.

Of those genes present in the top network was *FJX1*, a unique gene that was previously uncharacterized in cancer biology. In a large CRC microarray dataset, we found *FJX1* mRNA levels increased in concordance with the progression from normal tissue through later stages of cancer. In freshly prepared samples we confirmed that *FJX1* mRNA and protein was increased in tumor tissue compared to normal adjacent. The association between high *FJX1* expression and poor patient prognosis supports the hypothesis that *FJX1* is an oncogene in CRC. Further, the identification of *FJX1* as a putative COX-2 regulated gene suggests it could be a relevant therapeutic target. A biological basis for these observations will be further discussed in the next chapters.

CHAPTER III.

DEVELOPMENT OF FJX1 SPECIFIC VECTORS, ANTIBODIES AND CHARACTERIZATION OF RECOMBINANT FJX1 *IN VITRO.*

Introduction

We identified *Four jointed box 1 (FJX1)* as a candidate oncogene in CRC as it was inhibited in rectal tumors in response to celecoxib treatment, and its expression is increased in CRC compared to normal tissue. *FJX1* is the human ortholog of *four jointed (fj)* in *Drosophila*. In the fly, *fj* is a Golgi-associated kinase that contributes to planar cell polarity (PCP), limb development, and wing development [54-58]. Wingless, Jak/Stat, Notch, and Fat signaling have been shown to influence *fj* expression, and *fj* in turn can regulate expression of notch ligands, wingless, and fat [54,58,59]. Phenotypes observed upon abnormal expression of *fj* have been largely attributed to the ability of fj to phosphorylate specific cadherin residues on two large atypical cadherins, dachsous (ds) and fat (ft) [57,60,61]. Initial experiments identified amino acids 490-492 (DNE) as being required for fj kinase activity, while later experiments demonstrated mutation of amino acid 490 (D) alone was sufficient to lose kinase function [57,61]. Together, ft, ds, and fj influence growth through the Hippo-warts pathway, and PCP through a pathway which likely lies in parallel to frizzled/starry night signaling [62].

Mammalian *FJX1* has been far less studied that *fj*. Murine *FJX1* is highly expressed throughout the central nervous system and in several epithelial

26

structures during development, including the gut [63,64]. *FJX1* knockout mice are viable and fertile. However, they display a neuronal defect characterized by an increase in dendrite length or a decrease in dendrite arborization [65]. One report has suggested that *FJX1* is influenced by Notch signaling, citing the observation of increased *FJX1* promoter activity after transfection with Notch1, 2, or 3 [63] but we have failed to reproduced these results in our laboratory (data not shown).

As noted above*, Drosophila fj* is a kinase that phosphorylates specific cadherin residues on the large atypical cadherins ft and ds [57,61]. Sequence alignment of *fj* and various species, including mouse, rat, and human show complete conservation of all three residues (Figure 5). Further, McNeill and colleagues have provided some data that the ft/ds/fj cassette may be conserved in mammals [66]. Sequence analysis of the mammalian *ft* and *ds* homologues show highest conservation between *Fat4* and *ft*, and between *Dachsous* (*Dchs1*) and *ds* [66]. Upon genetic deletion of *Fat4* various PCP defects are observed, as well as an increase in *FJX1* mRNA [66] . Further, the combined deletion of *FJX1* and *Fat4* has an additive cystic kidney phenotype that is more severe than defects observed in either single mutant animal [66].

At the onset of these studies, there were no commercially available *FJX1* expression vectors or FJX1-specific antibodies. Here we describe our recombinant versions of *FJX1*, *Fat4*, and *Dchs1* and their transient or stable expression in various cell lines. We also describe the generation of multiple FJX1 specific antibodies and their characterization in enzyme-linked

27

immunoassays (ELISA), immunoblotting, and immunofluorescence.

```
Human       309  LFSLQWDPRVMQRATSNLHRG-PGGALVFLDNEAGLVHGYRV  349
Mouse       309  LFSLQWDPRVMHRATSNLHRG-PGGALVFLDNEAGLVHGYRV  349
Rat         419  LFSLQWDPRVMHRATSNLHRG-PGGALVFLDNEAGLVHGYRV  459
Drosophila  460  LYNFQWNADIMAAPAHNLARQSASQLLVFLDNESGLLHGYRL  501
```

Figure 5. Sequence alignment of *human, mouse,* and *rat FJX1* with

***Drosophila fj.* Residues identified in *Drosophila* as being essential for kinase

activity, which are conserved in mammals, are highlighted in yellow.

Materials and Methods

Plasmid construction and generation of stable lines.

Full length human *FJX1* cDNA (*hFJX1)* was obtained from the Vanderbilt University Genome Science Shared Resource (clone id 5482332). *hFJX1* was MYC tagged *(hFJX1MYC*) at the C terminus using the primers 5'-GATCGAATTCGGGAGCATGGGCAGGAGGATG-3' and 5'-CTAATGCAGATCCTCTTCTGAGATGAGTTTTTGTTCAGTCCCAGACCGGCGG CCGTAC-3' , cloned into the EcoRV site of pIRES-EGFP (Clontech), and subcloned into the EcoRI site of pcDNA3.1 zeo (Invitrogen). HEK293T cells were transfected with pcDNA3.1 or pcDNA3.1 *hFJX1MYC* using Effectene (Qiagen) per manufacturer's instructions and stable polyclonal populations HEK293T[PC] and HEK293T[PCFJX1] were selected using 200 ug/mL zeocin (Invitrogen). *hFJX1* cDNA was FLAG tagged (*hFJX1FLAG*) at the C terminus by PCR amplification with the primers 5'-GATCGAATTCGGGAGCATGGGCAGGAGGATG-3' and 5'-GATCCTCGAGAGTCCCAGACCGGCGGCCGTAC-3' and cloned into the EcoR1 and Xho1 sites of pCMV4a (Stratagene). *hFJX1* cDNA was also mutated at amino acids 338 (aspartate, D) and 340 (glutamate, E) to alanine and FLAG tagged at the C terminus (*hFJX1DEFLAG*). Two separate PCR reactions were performed on *hFJX1* cDNA using the primers: A) 5'-TAT ACT CGA GAG TCC CAG ACC GGC GGC CG-3' and 5'-CTG GTC TTT CTG GCC AAT GCG GCG GGC TTG GTG-3' or B) 5': 5'-GAT CGA ATT CGG GAG CAT GGG CAG GAG GAT G-3 and 5'-CAC CAA GCC CGC CGC ATT GGC CAG AAA GAC CAG-3'.

The products of reactions A and B were then set up in another PCR reaction

using primers 5'-GAT CGA ATT CGG GAG CAT GGG CAG GAG GAT G-3' and

5'-TAT ACT CGA GAG TCC AGA CCG GC GGC CG-3' to engineer 5' EcoRI

and 3' XhoI sites. Purified PCR products were cloned into the EcoRI and XhoI

sites of pCMV4a. *hFJX1MYC*, *hFJX1FLAG,* and *hFJX1DEFLAG* were

subcloned into the EcoRI site, EcoR1/Sgf1 sites, and EcoR1/Sgf1 sites

respectively of LZRS-MS-GFP (gift of Dr. Al Reynolds). HEK293T Phoenix cells

were transfected with LZRS-MS-GFP, LZRS-MS-GFP *hFJX1MYC*, LZRS-MS-

GFP *hFJX1FLAG* or LZRS-MS-GFP *hFJX1DEFLAG* using effectene. At 48 and

72hrs post transfection, viral supernatant containing 5 ug/mL hexadimethrine

bromide (Sigma Aldrich) was filtered (0.45 micron) and added to target cells

(LZRS-MS-GFP, LZRS-MS-GFP *hFJX1MYC* to CACO2, KM12C, SW480; LZRS-

MS-GFP, LZRS-MS-GFP *hFJX1FLAG,* or LZRS-MS-GFP *hFJX1DEFLAG* to

SW480, HMEC-1 and HEK293T) for 4-8hrs. Stable polyclonal populations were

obtained via flow cytometry. Nucleotides 1-1170 of *Dachsous1* (represents

cadherins 1-3, amino acids 1-390) were amplified from HEK293T RNA using the

primer 5' CGT ACT CGA GCT GGG CAC TTA TAC TGG CAG C 3', purified,

then re-amplified with 5'- GCA TGA ATT CAT GCA GAA GGA GCT GGG CAT

TG -3' and 5'- CGT ACT CGA GCA CAG AGA TGC GAG CAA CGA GC- 3' to

engineer EcoR1 and XhoI sites at the 5' and 3' termini respectively. The purified

PCR product was cloned into the EcoR1 and XhoI sites of pCMV4a to create a C

terminal FLAG tag, *hDachsousFLAG*. Nucleotides 1-1075 of *FAT4* (represents

cadherins 1-3, amino acids 1-358) were amplified from HEK293T RNA using the

primer 5' CGT ACT CGA GGG ACC GGG TAG AAG ACA GGG C-3', purified,

then re-amplified with GCA TGA GCT CAT GGA CTT AGC ACC AGA CAG G-3'

and 5'-CGT ACT CGA GGG AAG TAG CGG AAC TTC ACT ACC G-3' to

engineer SacI and XhoI sites at the 5' and 3' termini respectively. The purified

PCR product was cloned into the SalI site of pCMV4C to create a C terminal

FLAG tag, *hFAT4FLAG*.

Cell culture

HEK293T, HEK293T Phoenix, HCT116, HCT8, CACO2, LS174T, HCA7

and SW480 (ATCC) were cultured in RPMI 1640 (Gibco) with 10% FBS (Atlanta

Biologicals), 100U/mL pen/strep (Gibco), and 100U/mL L-glutamine (Gibco) at 37

^{o}C with 5% CO_2. HMEC-1 cells (F. Candl, Center for Disease Control) were

cultured in MCDB131 (Gibco), supplemented with 10% FBS, 10ng/mL epidermal

growth factor (Becton-Dickson), 100U/mL L-glutamine (Gibco), and 1µm/mL

hydrocortisone (Sigma Chemical). KM12C (Gift of Dr. Isiah Fidler) [67] were

cultured in MEM (Gibco) with 10% FBS (Atlanta Biologicals), 100U/mL pen/strep

(Gibco), 100U/mL L-glutamine (Gibco), sodium pyruvate (Gibco), non-essential

amino acids (Gibco) and MEM vitamins (Gibco). YAMC cells (Gift of Bob

Whitehead) were cultured in RPMI supplemented with 5% FBS (Atlanta

Biologicals), 100U/mL pen/strep (Gibco), 100U/mL L-glutamine (Gibco), ITS

(Gibco) and 5U/mL gamma interferon (Roche) at 33 ^{o}C with 5% CO_2.

Immunological detection methods and reagents

Generation of FJX1*-specific antibodies:*

FJX1 peptide antibody (Covance, rabbit peptide). The peptide sequence Ac-CVFRERTARRVLE-amide (corresponding to amino acids 364-376) was used for immunization of 4 rabbits (156, 157, 158, 159), in collaboration with Covance. Antibody from 158 serum was affinity purified using an affinity purification column made from the immunization peptide (Thermo Scientific, 44999)

FJX1 recombinant protein antibody (*Covance rabbit polyclonal*). Nucleotides 352-1314 of human *FJX1* were amplified by PCR (5'-GATCGAATTCGTGCACGGGGGCGTCTTCTGG-3' and 5'-GATCGTCGACCTCCCGGTGACACTAAGTCCCAGAC-3'), cloned into the EcoRI and SalI sites of pET44A (Novagen) and transformed into BL21-codon plus (DE3)-RIL (Stratagene). Transformed cells were treated with isopropyl β-D-1-thiogalactopyranoside to produce recombinant HIS tagged FJX1 protein. Recombinant HIS-FJX1 was purified using Ni-NTA beads (Invitrogen) under denaturing conditions, eluted with 2M pH = 3.0 glycine buffer, and dialyzed before immunization in rabbits (208, 209) in collaboration with Covance, Inc. 208 and 209 sera have been effective in western blotting, ELISA and immunofluorescence. Partial purification of 209 serum using G protein coupled column (Pierce) enabled its use in immunohistochemistry.

ELISA: Sub-confluent cell lines were cultured in serum-free conditioned media for 24 hours before collection (5mL/60cm^2). Conditioned media was spun at 300 x g for five minutes to pellet debris, and then transferred to a fresh tube. 100uL of conditioned media/well of a 96 well plate (COSTAR 3590) was incubated overnight at 4°C. Plates were washed four times with PBST (PBS+1.0%

33

TWEEN). Plates were blocked with 5% milk-PBST for one hour at room temperature and FJX1 antibody (208 or 209) diluted 1:1000 – 1:5000 in 5% milk was incubated overnight at 4°C. Plates were washed four times with PBST. Anti-rabbit secondary (Jackson Immunoresearch) was diluted 1:2500 in 5% milk-PBST and incubated for 30 minutes at room temperature. Plates were washed four times with PBST. Reagent A and B (R and D systems, DY999) were mixed 1:1 and 100uL was added per well for 20 min at room temperature. The reaction was terminated by adding 50uL of $2NH_2SO_4$ and plates were read at 450 nm with the reference set at 562 nm.

Immunoblotting: Cells were lysed in radio-immunoprecipitation assay (RIPA) buffer (150Mm sodium chloride, 1% Igepal, 0.5% sodium deoxycholate, 1% sodium dodecyl sulfate, 50mM Tris-Cl) supplemented with aprotinin, leupeptin, sodium orthovanadate, sodium fluoride, and phenylmethylsulfonyl fluoride before resolution by SDS-polyacrylamide gel electrophoresis (SDS-PAGE). FJX1 peptide antibody: Affinity purified 159 was diluted 1:1000 in 5% milk-PBST overnight at 4°C. FJX1 polyclonal antibodies: Whole serum from 208 and 209 was diluted 1:3000 in 5% milk-PBST overnight at 4°C. Commercial antibodies: β-actin (Sigma Chemical, 5% milk-PBST 1:10,000), MYC 9E10 (Vanderbilt Monoclonal Antibody Core, mouse monoclonal, 5% milk-PBST 1:1000); Abcam FJX1 (5% milk-PBST 1:1000); Sigma FJX1 (5% milk-PBST 1:1000). Anti-rabbit HRP and Anti-mouse HRP were diluted 1:5000 in 5% milk-PBST and incubated for 30 minutes at room temperature. For de-glycosylation and de-phosphorylation reactions, cells were lysed in RIPA without additional inhibitors.

Peptide N-Glycosidase F and Antarctic phosphatase (New England Biolabs) were used according to manufacturer's protocols.

Immunofluorescence: Cells were fixed in 4% paraformaldehyde for 15 minutes, blocked with 3% BSA-PBS , and incubated with primary antibodies: MYC 9E10 (Vanderbilt Monoclonal Antibody Core, 1:100); GM130 (BD Biosciences, 1:300); FJX1 (Abcam, 1:200). Secondary antibodies were: anti-rabbit DyLight 488 and anti-mouse DyLight 594 (Jackson ImmunoResearch Laboratories, 1:100). Nuclei were stained with 4',6-diamidino-2-phenylindole (DAPI) (Sigma-Aldrich). Images were captured on an Axioplan 2 upright fluorescent microscope (Carl Zeiss).

Cell proliferation

Cell proliferation was determined from at least 3 biological replicates performed in triplicate at each time point using the Quick Cell Proliferation Assay Kit (Biovision) per the manufacturer's instructions.

Results

Characterization of FJX1 specific antibodies.

Since there is a paucity of published information on FJX1 function in mammalian systems, we determined the cellular and biological effects of *FJX1* expression in human cell lines. In collaboration with Covance, we derived 6 rabbit polyclonal antibodies; 4 from immunization with a peptide (156-159) and 2 from immunization with recombinant human *FJX1* (208 and 209). We stably expressed a C-terminally MYC tagged version of human *FJX1* in human embryonic kidney cells, HEK93T, (HEK293T[PCFJX1]) for use in characterization of our antibodies as well as the vector alone for use as a control (HEK293T[PC]). Based on amino acid composition, the full-length human FJX1 protein (protein ID, NP_055159) has a predicted size of 48.5 kDa. There is a potential signal sequence cleavage site after amino acid 24, that would predict a processed form of approximately 46 kDa (Figure 6A). In whole cell lysates from MYC-tagged *FJX1* transfected HEK293T[PCFJX1] cells, we consistently detect four FJX1 specific protein bands of approximately 48kDa, 46kDa, 40kDa, and 37 kDa sizes using the 208 polyclonal FJX1 antibody (Figure 6B, lane 2) and these bands matched the bands recognized by the commercially available anti-MYC antibody (Figure 6C, lane 2). Conditioned media from HEK293T[PCFJX1] cells also contained 40kDa and 37 kDa FJX1-specific bands (Figure 6, B and C, lane 4) which is consistent with observations that both *D. melanogaster* four-jointed (FJ) and *M. musculus* FJX1 proteins are secreted [59,63].
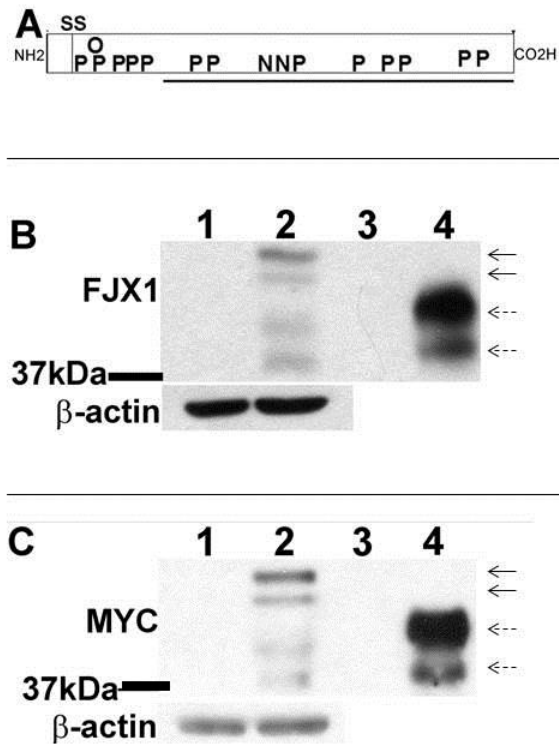
Figure 6. Stably expressed recombinant MYC-tagged *FJX1* increases FJX1 protein. (A) Schematic diagram of human FJX1 protein, with N-terminus (NH2) and C-terminus (CO2H) indicated. SS indicates predicted signal sequence site after amino acid 24. Approximate locations of predicted phosphorylation (P), N-linked (N) and O-linked (O) glycosylation sites are shown. Antigenic region (solid line, amino acids 118-437) used to generate recombinant *FJX1* sequence is underlined. **(B, C)** Matched immunoblots of HEK293T whole cell lysate (lanes 1, 2) or conditioned media (lanes 3, 4) stably expressing vector (lanes 1,3) or MYC-tagged *FJX1* (lanes 2,4) probed with **(B)** Anti FJX1 or **(C)** Anti MYC. β-actin served as the loading control.
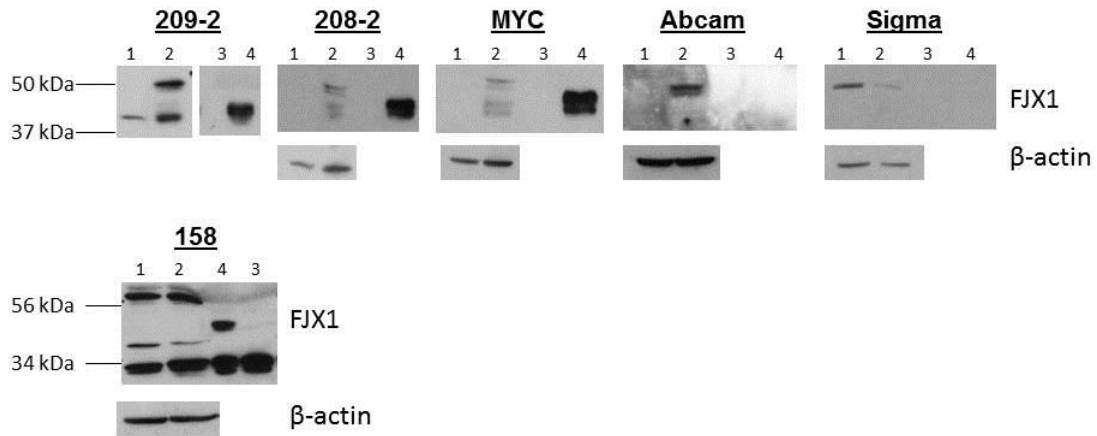
Figure 7. FJX1 antibodies in immunoblotting. For all panels lane 1 =

HEK293T^{VEC} whole cell lysate, 2 = HEK293T^{PCFJX1} whole cell lysate, 3 =

HEK293T^{VEC} conditioned media, and 4 = HEK293T^{PCFJX1} conditioned media.

Immunoblots were probed with FJX1 antibodies as notes. β-actin served as the

loading control**.**

Similar to the polyclonal 208 antibody, the polyclonal 209 antibody detected the same bands in HEK293T^{PCFJX1} whole cell lysate and conditioned media, while the peptide antibodies only recognized secreted FJX1 (Figure 7 and data not shown). More recently, several commercially available FJX1 antibodies were developed, and we tested one from Abcam and one from Sigma. Interestingly, the Abcam antibody only detected intracellular FJX1, and neither the Abcam nor the Sigma antibodies detected secreted FJX1 (Figure 7).

Both polyclonal FJX1 antibodies (208 and 209) were able to detect secreted FJX1 from HEK293T^{PCFJX1} conditioned media in an ELISA (Figure 8). The increase in signal intensity nicely correlated with the amount of conditioned media (Figure 8). Serum from animal 208 gave the best signal to noise ratio, and was used for subsequent experiments.

Finally, we tested the ability of the polyclonal antibodies in immunofluorescence. Patterns of FJX1 expression in the HEK293T^{PCFJX1} cells were similar using 208, 209, MYC and Abcam-FJX1 antibodies (Figure 9). The Abcam FJX1 antibody gave the most robust signal. We confirmed the specificity of FJX1 staining by showing co-localization with MYC staining in HEK293T^{PCFJX1} cells (Figure 10, panels i-iii).
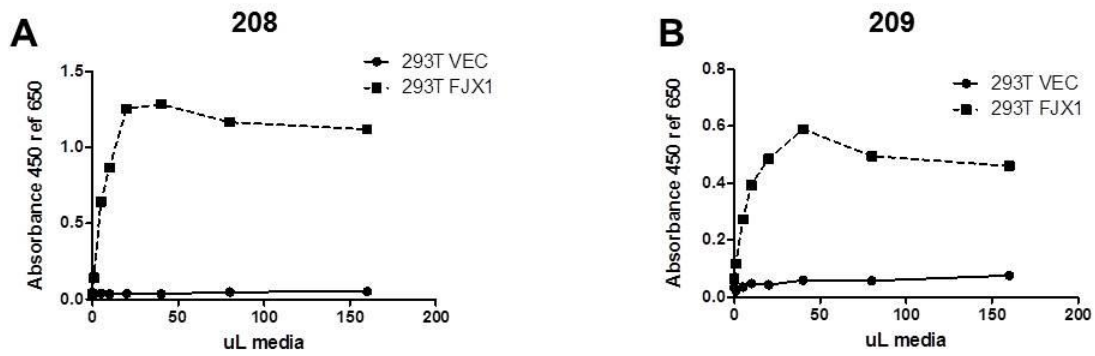
Figure 8. FJX1 antibodies detect secreted recombinant FJX1 in ELISA. Absorbance representing detection of secreted FJX1 in conditioned media from vector (VEC) or FJX1 MYC (FJX1) stably transduced HEK293T cells using antibodies from rabbits 208 **(A)** and 209 **(B)**.
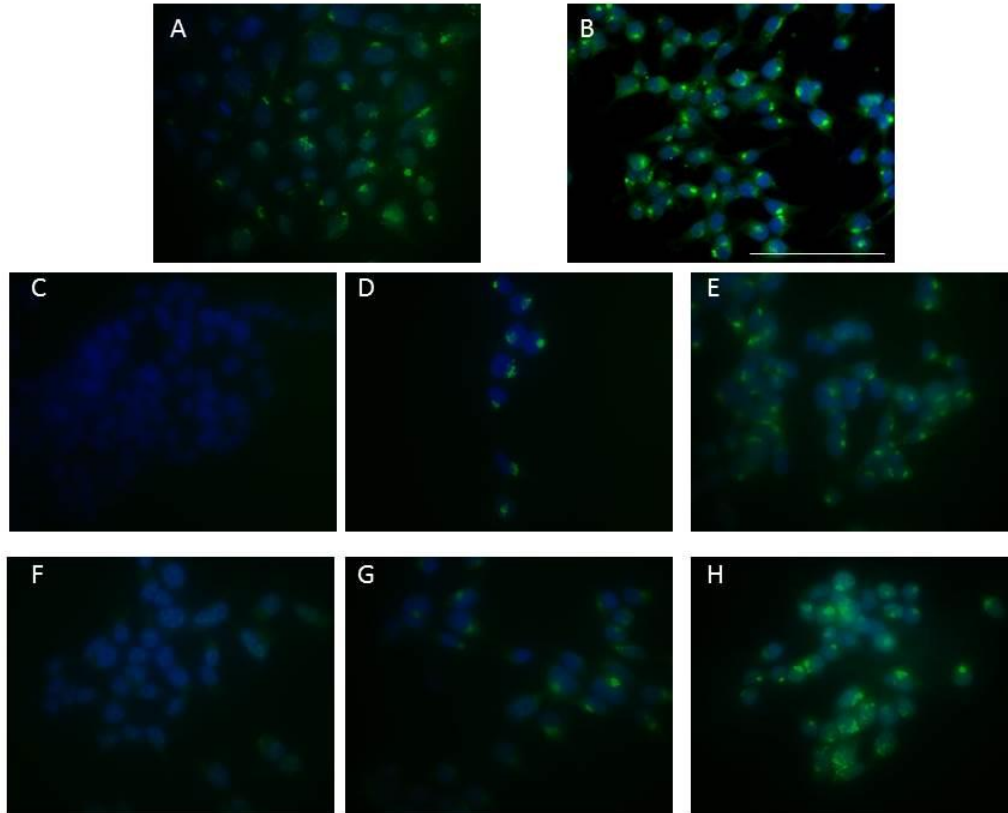
Figure 9. FJX1 antibodies in immunofluorescence. Representative FJX1 staining in HEK293T^{PCFJX1} cells using the following antibodies: (A) MYC (B) Abcam FJX1 (C) 208 pre bleed (D) 208 bleed 1 (E) 208 bleed 2 (F) 209 pre bleed (G) 209 bleed 1 (H) 209 bleed 2. Pre-bleeds (animal bleeds before antigen immunization, C and F) served as negative controls.

Recombinant FJX1 localizes to the Golgi apparatus and is glycosylated and
phosphorylated in both the cellular and the secreted form.

Studies by Strutt and colleagues have shown that *D. melanogaster* fj
protein localizes to the Golgi apparatus [56]. Using the Abcam FJX1 antibody to
track the intracellular pool of FJX1 in HEK293T[PCFJX1] we found it co-localized with
the Golgi marker GM130 (Figure 10, panels iv-vi). Based upon amino acid
sequence, various post-translational modifications are predicted for FJX1 protein,
including two putative N-glycosylation (amino acids 248 and 277), one O-
glycosylation (amino acid 53), and thirteen potential phosphorylation sites (Figure
6A). It was previously reported that the majority of exogenously expressed
mouse Fjx1 in HEK293T cells is a secreted protein that is sensitive to digestion
with endoglycosidase H [63]. We extended this analysis by treating whole cell
lysate and conditioned media from HEK293T[PCFJX1] cells with peptide N-
glycosidase F (PNGaseF), which cleaves all polysaccharide moieties; and
antarctic phosphatase, which removes phosphorylation groups. Treatment with
PNGaseF resulted in a relatively uniform increase in gel electrophoresis mobility,
corresponding to an approximate 5kDa decrease in size, with the upper double
band collapsing into a single species (46-48kDa to 41kDa; 40kDa to 35kDa;
37kDa to 32kDa) suggesting that all forms of recombinant, MYC-tagged FJX1
are N-glycosylated (Figure 10, B and C, lane 1 vs. lane 3). Phosphatase
treatment alone failed to significantly alter mobility of FJX1, possibly due to
masking of any subtle shift by the larger effect of protein glycosylation (Figure 10,
B and C, lane 1 vs. lane 2). Treatment of lysates and conditioned media with

both PNGase F and phosphatase resulted in the 40kDa and 37 kDa bands collapsing into one band, suggesting that FJX1 is phosphorylated (Figure 10, B and C, lane 1 vs. lane 4). Thus, recombinant MYC-tagged FJX1 behaves similarly to recombinant forms of the protein that have been described in both *D. melanogaster* and in *M. musculus*.

After determining the accuracy of the FJX1 antibodies we next screened various cell lines for endogenous FJX1 expression. Surprisingly, we failed to detect secreted endogenous FJX1 in either normal (HEK293T, YAMC, HMEC-1, HUVEC, MCF10A, RAW264.7, MCT, HT-22) or cancerous lines (SW480, SW620, HT29, HCT116, HCA7, KM12C, HCT8, DKO1, DLD1, MCF7, MDMB468, CAD, HL60, BXPC3, PANC1) (Figure 11 and 12 and data not shown), even when conditioned media was concentrated at least 30 fold (Figure 11C). Conversely, we were able to detect endogenous FJX1 in conditioned media from primary rat hippocampal neurons by both ELISA (Figure 11, A and B) and immunoblot (Figure 12). We did occasionally observe bands that migrated similarly to the smaller secreted forms of recombinant FJX1 in whole cell lysate from some CRC cell lines (Figure 12). However these bands were very faint and RNA levels as determined by qPCR were very low (data not shown). Further, although we confirmed *FJX1* specific siRNA inhibited *FJX1* at the mRNA level, we observed no changes in FJX1 protein banding pattern in whole cell lysates in one such cell line, SW480 (Figure 13 and data not shown).
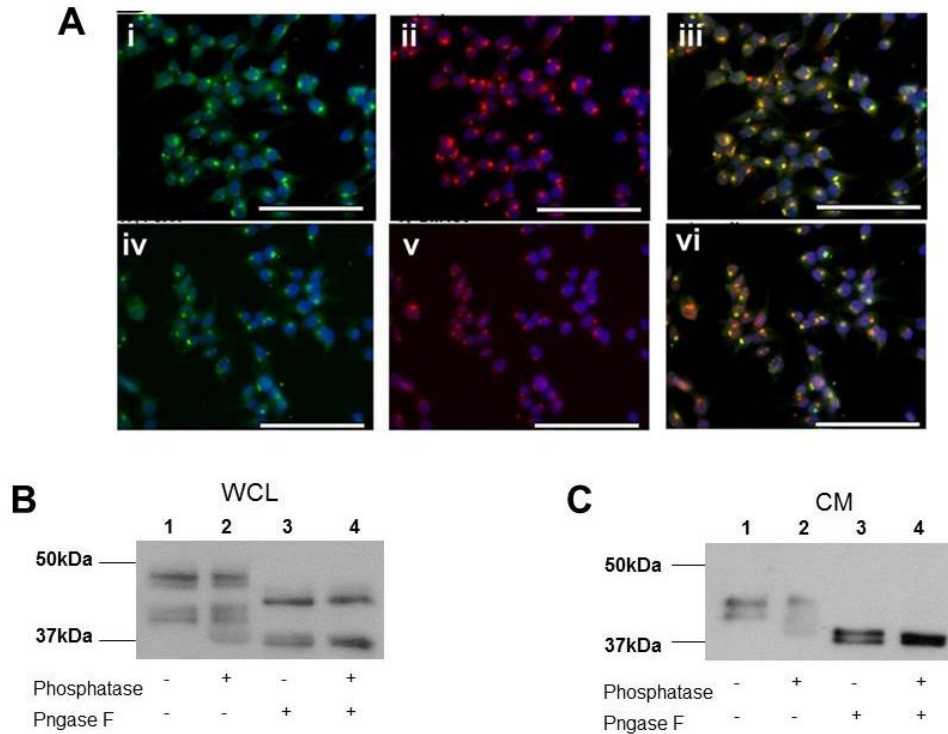
Figure 10. Recombinant FJX1 is glycosylated, phosphorylated, and localizes to the Golgi apparatus in HEK293T cells. (A) Representative fluorescent images of HEK293T FJX1 cells dual stained for FJX1 (i, green) and MYC (ii, red) or FJX1 (iv, green) and the Golgi marker, GM130 (v, red). Nuclei were stained with DAPI (blue). Respective merged images are shown (iii, vi). Scale bar = 100 mm. FJX1-specific immunoblots using **(B)** whole cell lysate (WCL) or **(C)** conditioned media (CM) from HEK293T FJX1 cells with (+) and without (-) treatment with PNGaseF and/or antarctic phosphatase.
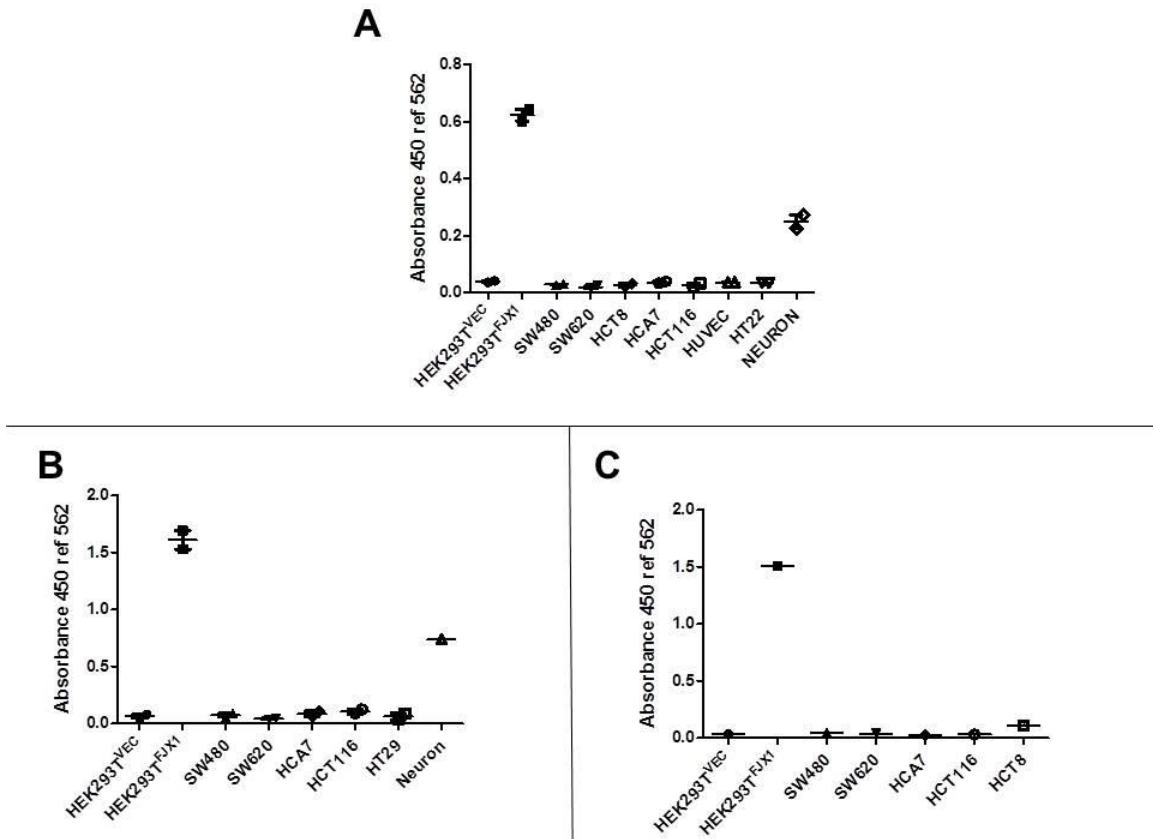
Figure 11. FJX1 ELISA detects recombinant human FJX1 and endogenous rat FJX1. (A-C). Absorbance representing FJX1 specific signal in conditioned media from cell cultures as labeled. Each data point represents a technical replicate. Samples in **(C)** were concentrated ~30X.
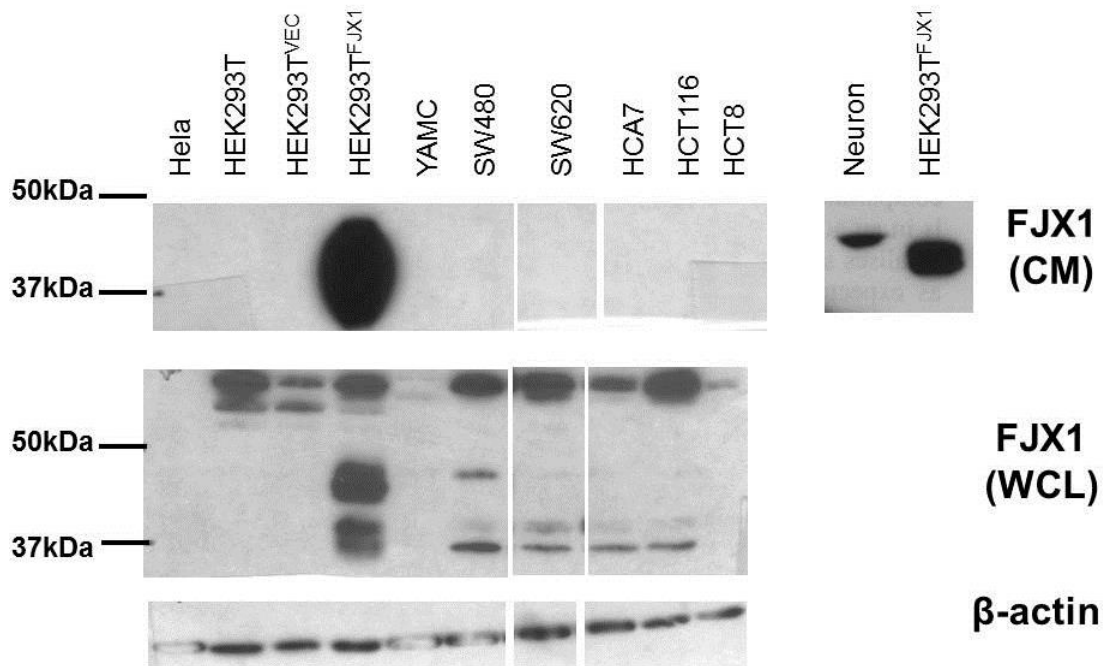
Figure 12. Endogenous and recombinant expression of FJX1 in various cell lines. Representative FJX1 protein immunoblots of conditioned media (CM) or whole cell lysate (WCL) from various cell cultures. Note, all WCL were run on the same gel but cropped for ordering purposes. VEC = vector and FJX1 = FJX1 stable transduction respectively. Anti-β-actin served as loading controls for WCL.

Because FJX1 expression was lost when CRC cells were established as cell lines, we used expression vectors to test the biological function of FJX1 in cancerous cells. We expressed the C-terminal MYC-tagged version of human *FJX1* in the CRC lines SW480, KM12C, and CACO2. Similar to what we observed in the HEK293T^{PCFJX1} cells, SW480^{FJX1MYC} whole cell lysates exhibited FJX1-specific bands of approximately 46kDa, 40kDa, and 37kDa, with additional bands migrating at 80kDa and 75kDa; again proteins corresponding to the smallest two peptides were secreted (Figure13, A and B). All of these forms detected in SW480^{FJX1MYC} whole cell lysate and conditioned media were ablated upon treatment with siRNA specific to *FJX1*. Since no alteration in banding pattern was observed in SW480^{VEC} whole cell lysate after *FJX1* siRNA treatment, we conclude that endogenous levels of FJX1 are either absent, or low enough to preclude detection by immunoblotting in these cells. Expression of FJX1 protein in both whole cell lysate and conditioned media from CACO2^{FJX1MYC} and KM12C^{FJX1MYC} was also confirmed (Figure 14). Estimations of cellular proliferation in the presence or absence of serum showed no significant difference between vector and MYC-tagged *FJX1*-transduced cell lines *in vitro* (Figure 15, A and B, and data not shown).
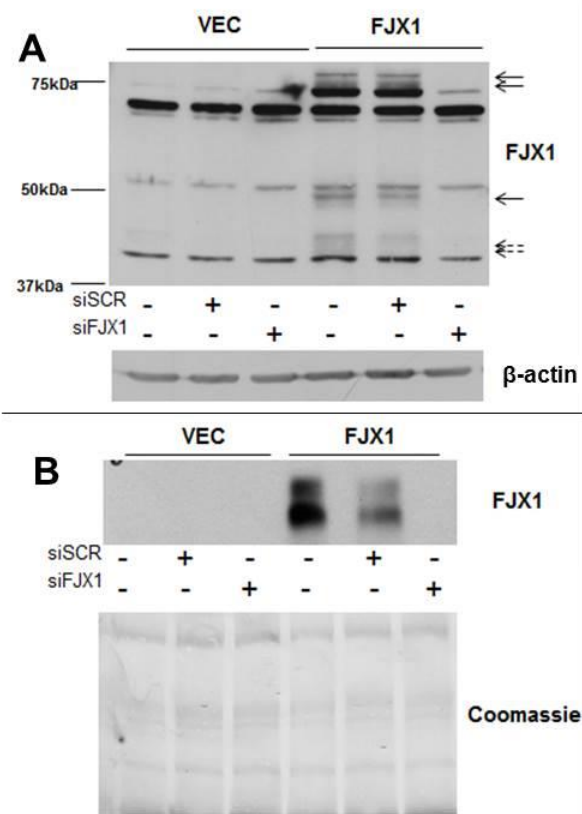
Figure 13. Stably expressed recombinant MYC-tagged *FJX1* increases FJX1 protein in SW480 colon cancer cells. VEC = SW480^{VEC}. FJX1 = SW480^{FJX1MYC}. **(A)** Whole cell lysate or **(B)** conditioned media from cells treated with scrambled control oligonucleotide (siSCR) or *FJX1* targeted (siFJX1) RNAi. Anti-β-actin and Coomassie stain served as loading controls for **A, and B** respectively. Solid arrow indicates FJX1 species detected only in whole cell lysate, dashed arrows indicate FJX1 specific secreted forms.
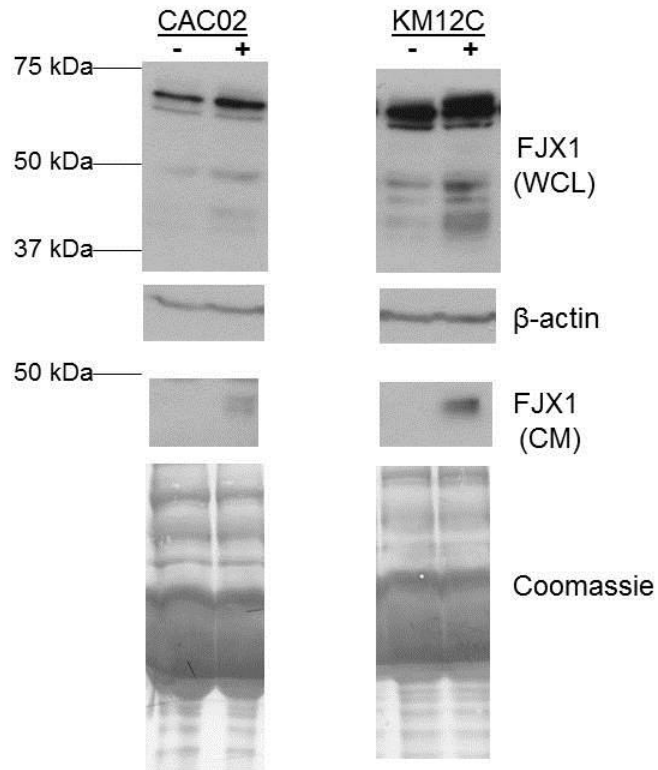
Figure 14. Stably expressed recombinant MYC-tagged *FJX1* increases FJX1 protein in colon cancer cells. Representative FJX1 protein immunoblot of whole cell lysate (WCL) and conditioned media (CM) from vector (-) or FJX1 (+) transfected CACO2 and KM12C cell lines. Anti-β-actin and Coomassie stain served as loading controls for WCL and CM respectively.
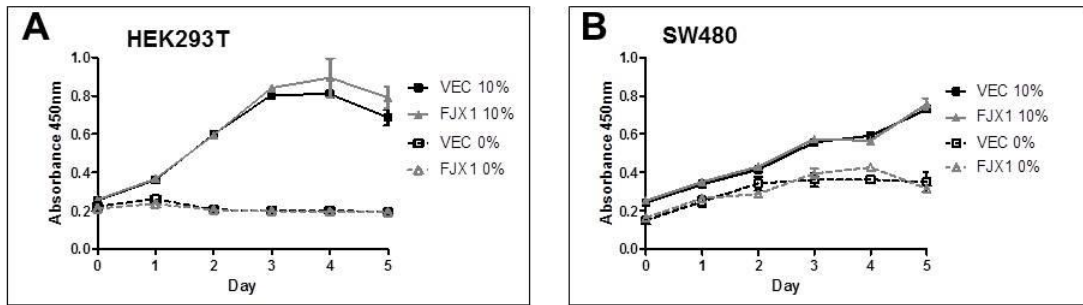
Figure 15. Stably expressed recombinant MYC-tagged *FJX1* does not affect cellular proliferation *in vitro*. (A, B) Representative experiments of metabolized WST-1 reflecting an estimation of cellular proliferation over 5 days in **(A)** HEK293T and **(B)** SW480 cells stably expressing either empty vector (VEC) or MYC-tagged FJX1 (FJX1) grown in 0% or 10% serum as indicated. The mean values of replicates are graphed with bars indicating the standard deviation.

Construction of Fat4, Dchs1 cadherin constructs and mutant FJX1.

Drosophila fj is a kinase that phosphorylates specific cadherin residues on the large atypical cadherins, ft and ds [57,61]. In mammals there are two *ds* homologues, (*Dchs1* and *Dchs2*) and four *ft* homologues (*Fat1-4*), with *Dchs1* and *Fat4* exhibiting the most sequence homology to their respective *Drosophila* counterparts. We aligned the cadherin domains between Dchs1 and ds and found that cadherin domain 3 of human Dchs1 has a conserved serine residue that has been identified as a fj target [57]. Similarly, comparison of Fat4 and ft revealed that cadherin domains 3 and 13 both have a conserved serine residue. In the fly, subtle but distinct mobility shifts are observed when *ft* and *fj* or *ds* and *fj* are co-expressed. We thus generated FLAG-tagged versions of each protein that contained the first 3 cadherin domains *(Fat4^{cad1-3} or Dchs1^{cad1-3})* and transiently expressed them in HEK293T^{VEC} and HEK293T^{PCFJX1} cells. Since these constructs represent extracellular portions of Fat4 and Dchs1 that lack the transmembrane region, they were readily detectable in conditioned media using the anti-FLAG antibody (Figure 16). We detected no altered mobility of either Fat4^{cad1-3} or Dchs1^{cad1-3} in the presence of FJX1 (Figure 16). Co-expression of *FJX1* and *Dchs1^{cad1-3}* may have caused a slight decrease in Dchs1^{cad1-3} expression, however further experimentation will be required to determine if Dchs1^{cad1-3} levels are actually altered in the presence of FJX1.

In *Drosophila*, mutation of all three amino acids 490-492 (DNE) or single mutation of amino acid 490 completely abolished fj kinase activity [57,61]. Sequence alignment of *fj* and various species, including mouse, rat, and human

show complete conservation of these residues (Figure 5). To test if mutation of these conserved residues altered FJX1 function in our assays, we engineered a recombinant C terminally FLAG- tagged version of human *FJX1* with the conserved D and E amino acids mutated to A (*FJX1^{FLAGDE}*) and expressed it in HEK293T, SW480, and HMEC-1 cells. Immunoblot analysis showed similar expression levels between the mutant and wild-type versions of FJX1, however we noticed that mutant FJX1 was migrating slightly faster (Figure 17). We hypothesized that the altered mobility could be due to a potential auto-phosphorylation event, which has been observed in the fly [57], and would be lost upon mutation of a putative kinase sequence. We treated conditioned media from the *FJX1* and *FJX1DE* transduced HEK293T and SW480 cell lines with peptide N-glycosidase F (PNGaseF) and/or antarctic phosphatase. Treatment with PNGaseF resulted in a relatively uniform increase in gel electrophoresis mobility for both wild-type and mutant FJX1, with an approximately 5kDa decrease in size suggesting that mutant FJX1 is N-glycosylated similarly to wild-type (Figure 17). Phosphatase treatment alone failed to alter mobility of both versions of FJX1 significantly, possibly due to masking of any subtle shift by the larger effect of protein glycosylation (Figure 17). Treatment with both PNGase F and phosphatase resulted in wild-type FJX1 collapsing into one band, while mutant FJX1 remained a distinct doublet, suggesting that wild-type but not mutant FJX1 is phosphorylated (Figure 17).The relevance of this mutant to FJX1 biological function *in vitro* will be discussed further in chapter IV.
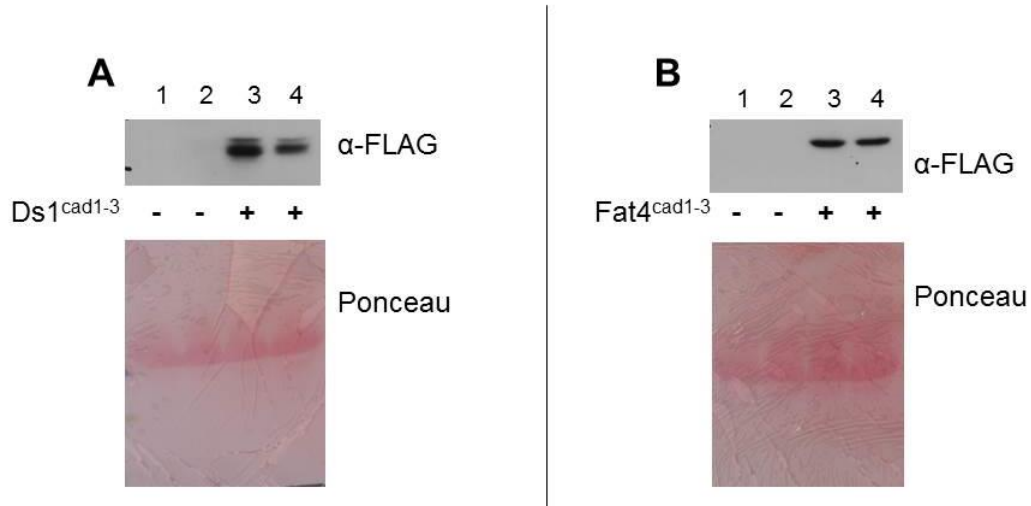
Figure 16. FJX1 does not alter Dchs1 or Fat4 cadherin constructs mobility in immunoblotting. Representative FLAG immunoblot of conditioned media from HEK293T^{VEC} (lanes 1 and 3) or HEK293T^{PCFJX1} (lanes 2 and 4) cells with (+) or without (-) transient transfection of **(A)** *Dchs1^{cad1-3}* or **(B)** *Fat4^{cad1-3}*. Ponceau staining served as a loading control.
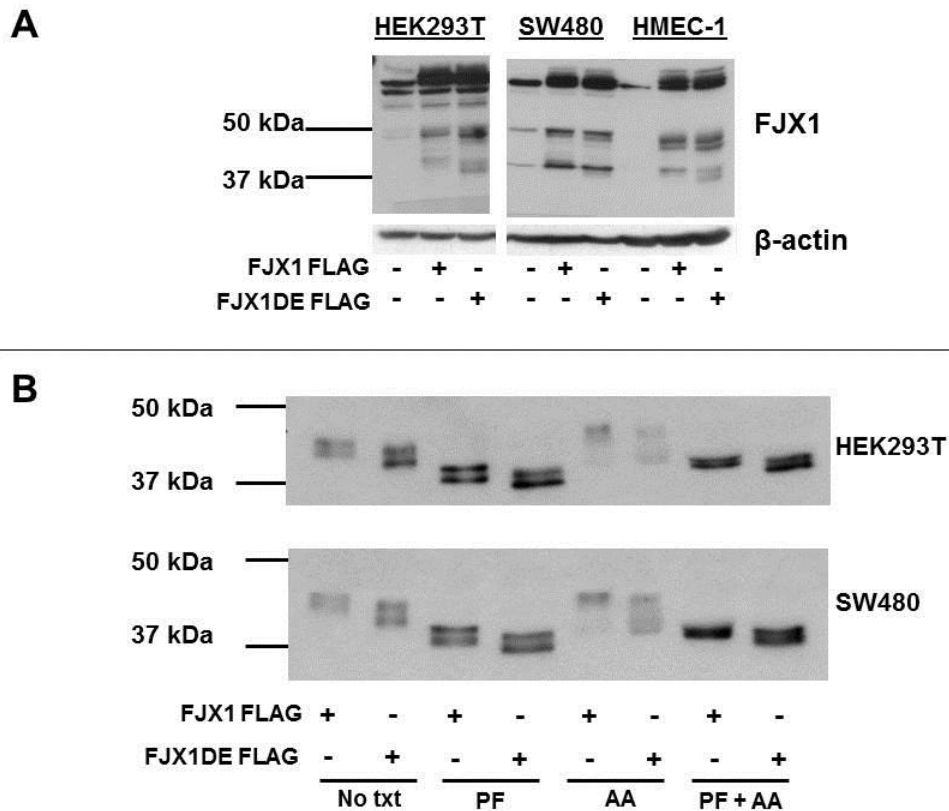
Figure 17. Expression of mutant FJX1 in various cell lines. (A)
Representative FJX1 immunoblot of whole cell lysates from indicated cell lines
stably transfected with vector control, wild-type *FJX1* (FJX1 FLAG) or mutant
FJX1 (FJX1DEFLAG). β–actin served as the loading control. **(B)** Representative
FJX1 immunoblot of HEK293T[FJX1FLAG], HEK293T[FJX1FLAGDE], SW480[FJX1FLAG] and
SW480[FJX1FLAGDE] conditioned media with (+) and without (-) treatment with
PNGaseF (PF) and/or antarctic phosphatase (AA).

Discussion

FJX1 is the mammalian homologue of *drosophila fj*, a kinase involved in body patterning and limb development. Mouse studies have described the normal physiological expression pattern of *FJX1* and its role in neuron formation; however little else is known about FJX1. Despite microarray data demonstrating that *FJX1* mRNA expression is increased in a variety of cancers, ours is the first to characterize expression of human *FJX1 in vitro.* Due to the paucity of *FJX1* specific reagents, we developed several rabbit polyclonal antibodies using either a peptide sequence or a recombinant version of human *FJX1* as the antigen. Of the peptide antibodies (156-159) 159 proved to be useful in detecting secreted FJX1 via immunoblot. The polyclonal antibodies (208 and 209) generated against recombinant FJX1 were by far superior, and were effective in ELISA, immunoblotting, and immunofluorescence. These FJX1-specific antibodies allowed us to screen for endogenous *FJX1* expression as well as characterize recombinant FJX1 localization and processing. Surprisingly we failed to detect endogenous FJX1 in conditioned media from immortalized normal or cancerous cell lines, including those derived from breast, lung, colon, enodothelial, and neuronal tissue. Conversely we were able to detect endogenous secreted FJX1 from primary rat hippocampal neurons. Loss of *FJX1* expression in extensively cultured cells *in vitro* may be caused by a lack of paracrine interactions that are supported *in vivo*.

We used our antibodies to characterize recombinant *FJX1* expression and processing *in vitro.* Like *Drosophila* fj [56], the intracellular pool of human FJX1

protein is found to localize to the Golgi apparatus. We detected four to five distinct bands in cells transduced with recombinant *FJX1*, with the smaller two species also being detected in conditioned media. In HEK293T^{PCFJX1} cells we showed that all four forms of FJX1 are glycosylated, while the secreted doublet collapses into a single species when both glycosylation and phosphorylation groups are removed. The secreted forms of FJX1 likely occur from a cleavage event subsequent to the normal processing that removes the signal sequence, due to their size. Additionally, a commercially available antibody from Abcam only detects the intracellular forms of FJX1. Although the exact sequence used for rabbit immunization is proprietary (personal communication) it was confirmed that the region lies somewhere after the signal sequence but before amino acid 80. It will be interesting to determine where exactly FJX1 is cleaved, and which proteins are responsible for this processing.

Drosophila fj is a kinase that phosphorylates specific cadherin residues on two large atypical cadherins fat and dachsous [57,61]. The three key residues of fj involved in kinase function (DNE) are completely conserved across multiple species, including mouse and human. Mutation of the conserved aspartic acid within this region was sufficient to inhibit the biological function of *fj* [61]. Additionally, the serine residues that fj phosphorylates on ft and ds [57] are also conserved in mammalian Fat4 and Dchs1. Since Fat4 and Dchs1 are extremely large proteins (~5147 and 3298 amino acids respectively) we expressed smaller, recombinant versions that only contained domains surrounding the first conserved serine residue (*Fat4*$^{cad1-3}$ or *Dchs1*$^{cad1-3}$). We were unable to observe

an obvious change in immunoblot mobility upon expression of *Fat4*[cad1-3] in

HEK293T[PCFJX1] cells, however it appeared that there was some alteration in

Dchs1[cad1-3] abundance. Further experiments will be needed to determine if the

alteration in Dchs1[cad1-3] is only at the level of protein expression, or if it is due to a

change in post translational modification. The addition of phosphatase treatment

may help to clarify this point, but a more direct test will be to use fully

recombinant versions in an *in vitro* kinase assay.

Alternatively, we created a FLAG-tagged version of *FJX1* in which the

aspartic acid and glutamic acid residues in the putative kinase domain were

mutated to alanine. Interestingly, the smaller secreted forms of FJX1 differed in

gel mobility upon mutation of these D and E residues. It has been suggested

that fj undergoes autophosphorylation *in vitro [57]*, and thus we tested whether

mutant FJX1 was phosphorylated or otherwise modified. Both wild-type and

mutant FJX1 were altered by glycosidase treatment, suggesting both forms

undergo glycosylation. While phosphatase treatment in combination with

PNGase treatment of wild-type FJX1 results in the collapsing of FJX1 into a

single band, mutant FJX1 did not show a mobility shift, suggesting mutant FJX1

is not phosphorylated. Unfortunately, due to the similarity in size of recombinant

mutant FJX1, Fat4[cad1-3] and Dchs1[cad1-3] , and the fact that they are all FLAG-

tagged we were unable to test whether protein levels of Fat4[cad1-3] or Dchs1[cad1-3]

were altered in the presence of FJX1 wild-type as compared to the FJX1 DE

mutant. However, using MYC-tagged *FJX1* expression in HEK293T cell, we

found no evidence that specific domains of Ft and Dchs were phosphorylated. It

may be that these cadherins require the full-length protein for correct regulation or it may be that they are not phosphorylated by FJX1 in all cells or species. Whichever the case may be, this negative result indicated that other studies were needed to understand FJX1 function in mammalian cells, particularly in CRC cells.

CHAPTER IV.

FJX1 PROMOTES TUMORIGENESIS THROUGH INCREASED

ANGIOGENESIS IN COLORECTAL CARCINOMA

Introduction

We identified *FJX1* as a gene regulated by celecoxib inhibition in CRC. As discussed above, *FJX1* is elevated at both the mRNA and protein levels in human CRC tissue, and high expression of *FJX1* is associated with poor patient prognosis. Therefore, understanding its biological role in CRC may identify pathways and targets for more effective treatment of this disease. The role of human FJX1 has not been biologically tested to date, however tumor gene expression analysis data have suggested a potential oncogenic role in a variety of cancers. *FJX1* gene amplification and increased mRNA expression have been observed in oral squamous carcinomas and in derived squamous carcinoma cell lines [68,69]. *FJX1* mRNA expression is upregulated in ovarian tumor endothelial cells as compared to normal ovarian endothelial cells [70,71] and thus has been suggested as a candidate tumor vasculature marker in ovarian cancer [72]. Despite these observations of altered *FJX1* mRNA expression in other cancers, the biological function of FJX1 and its effects on tumor progression are unknown. Here we describe FJX1 as tumor promoter through its ability to enhance tumor angiogenesis.

Material and Methods

<u>Cell culture</u>

HEK293T, CACO2, and SW480 (ATCC) cells were cultured in RPMI 1640 (Gibco) with 10% FBS (Atlanta Biologicals), 100U/mL pen/strep (Gibco), and 100U/mL L-glutamine (Gibco) at 37 ^{o}C with 5% CO_2. HMEC-1 cells (F. Candl, Center for Disease Control) were cultured in MCDB131 (Gibco), supplemented with 10% FBS, 10ng/mL epidermal growth factor (Becton-Dickson), 100U/mL L-glutamine (Gibco), and 1µm/mL hydrocortisone (Sigma Chemical). KM12C (Gift of Dr. Isiah Fidler) [67] were cultured in MEM (Gibco) with 10% FBS (Atlanta Biologicals), 100U/mL pen/strep (Gibco), 100U/mL L-glutamine (Gibco), sodium pyruvate (Gibco), non-essential amino acids (Gibco) and MEM vitamins (Gibco).

<u>Immunological detection methods and reagents</u>

Immunoblotting: Cells were lysed in radio-immunoprecipitation assay (RIPA) buffer (150Mm sodium chloride, 1% Igepal, 0.5% sodium deoxycholate, 1% sodium dodecyl sulfate, 50mM Tris-Cl) supplemented with aprotinin, leupeptin, sodium orthovanadate, sodium fluoride, and phenylmethylsulfonyl fluoride before resolution by SDS-polyacrylamide gel electrophoresis (SDS-PAGE). Whole serum from rabbit 208 was diluted 1:3000 in 5% milk-PBST overnight at 4°C. Commercial antibodies: β-actin (Sigma Chemical, 5% milk-PBST 1:10,000). Anti-rabbit HRP and Anti-mouse HRP were diluted 1:5000 in 5% milk-PBST and incubated for 30 minutes at room temperature.

Immunohistochemistry: Immunohistochemistry was performed by the

Vanderbilt Immunohistochemistry Core Shared Resource for Ki-67 (Vector Laboratories), Cleaved caspase 3, and CD34 (Santa Cruz Biotechnology). Staining was quantified using the Ariol SL-50 automated slide scanner (Applied Imaging) as previously described [74]. Cross sections of CD34 stained tissue were used to determine the number of vessels per mm^2 tissue (including perivasculature for xenograft tumors). Significance was determined using Mann-Whitney and t test.

Partially purified anti-FJX1 antibody (rabbit 209 polyclonal) was applied at a dilution of 1:2000 and incubated overnight at 4°C. Slides were washed, incubated in 1:500 goat anti-rabbit antibody for 30 min., washed and incubated in avidin biotin complex (Vector Labs Elite ABC kit) for 30 min and washed. Color was developed in 3, 3' diaminobenzidine (Vector Labs) and nuclei were stained with Gill's #3 hematoxylin (Sigma). Images were taken on an Axioskop 40 upright light microscope (Carl Zeiss, Inc.).

Collection of conditioned medium and siRNA

Epithelial cell lines (HEK293T, SW480, KM12C, CACO2) were allowed to grow to ~60% confluence (typically 24 hrs) before media was refreshed (5mL/10cm; containing 0% FBS). After 16-24 hours, conditioned media were collected, spun at 300 g for 5 minutes, and supernatant transferred to a fresh tube. For fractionation experiments, 4mL of conditioned media was spun at 4000 g for 30 minutes at 4°C in an Amicon ultra 30K membrane tube (Millipore). Serum free medium was added to the fraction that was retained on the column to

equal the volume that flowed through the column. Conditioned media was used for endothelial tube assays within one hour of collection. SW480^{VEC} or SW480^{FJX1} cells were transfected with 100nM pooled siRNA specific to FJX1 (Qiagen) or non-targeting scrambled siRNA (Dharmacon) replated at 48 hours post transfection, and re-fed with serum free media after 72 hours. After 96 hours, media was collected and processed as above.

Endothelial tube formation

Phenol red free growth factor reduced matrigel (BD biosciences) was allowed to solidify in 96 well plates (50uL/well) for 30 minutes at 37°C. HMEC1 (30,000 cells) in complete media were plated on top of the matrix and an equal volume of conditioned media containing 0% FBS or 10% FBS from epithelial cell lines (HEK293T, SW480, KM12C, CACO2) was added. For autonomous experiments, 20,000 HMEC1^{VEC} or HMEC1^{FJX1} cells were plated on top of the matrix. Images were taken 16-18 hours after HMEC-1 cells were plated for tube formation, with three images taken per well. Experiments were performed in triplicate at least three times, with each data point being the average of three images of three technical replicates. Significance was determined by Mann-Whitney, ANOVA, or Student's t test as noted.

Xenograft and mouse carcinogenesis models

One million SW480^{VEC} or SW480^{FJX1} cells were injected subcutaneously onto single flanks of athymic female nu/nu mice (Harlan Sprague Dawley). For KM12C^{VEC} and KM12C^{FJX1} cell lines, a single female nu/nu mouse received

1×10^6 cells on one flank, and 2×10^6 cells on the opposite flank with the same cell line injected subcutaneously per mouse. Tumor growth was monitored by taking external measurements on the animal and at the time of sacrifice (volume = $4/3 \pi r^3$).

FJX1 -/- (KO) mice on a C57BL/6 genetic background were obtained from H. McNeil [66]. Azoxymethane (AOM, Sigma) was given intraperitoneally at 12.5 ug/g. Dextran sodium sulfate (DSS, MP Biomedicals, formula weight 36,000-50,000) was prepared in drinking water at 3%. At eight weeks of age the mice were randomized into one of four treatment groups; no treatment (KO n=8; WT; n=6), AOM alone (KO; n=3; WT n=1), DSS alone (KO n=8; WT n=8), or AOM and DSS (KO n=8; WT n=8). Mice were injected with AOM (day 1), given three cycles of DSS (days 6-10, 27-31, and 48-51) and allowed a four week recovery period [75,76]. After experimental completion, mice were euthanized and analyzed for the number of colonic polyps. Formalin fixed paraffin embedded colonic tissue sections were then subjected to histological analysis by M.K. Washington as previously described [77] by Dieleman and colleagues. Briefly, intensity, location (mucosal, submucosal, transmural), and extent of involvement of the inflammatory infiltrate was assessed, as well as severity and extent of crypt injury.

Results

FJX1 expression promotes tumor growth *in vivo*

To determine whether *FJX1* expression alters xenograft tumor formation *in vivo,* we injected vector and *FJX1* transduced cells (SW480 or KM12C) on the flanks of athymic nude mice. One million SW480 cells were injected onto a single flank of each mouse with 10 mice in each group. At 26 days post injection, both groups of mice exhibited 100% tumor incidence; however, SW480^{FJX1MYC} tumors were larger than SW480^{VEC} tumors so tumors were excised for histological examination (Figure 18A). After excision, the SW480^{FJX1MYC} derived tumors were approximately twice the size (Figure 18B; average volume: 58.0 +/- 5.8 mm^3 vs 27.1 +/- 2.9 mm^3, P < 0.0005) and with a mass 1.5 times greater than the SW480^{VEC} tumors (Figure 18C; average weight: 71.0 +/- 6.75 mg vs 45.1 +/- 5.8 mg, P < 0.05). SW480^{VEC} cells produced tumors with no detectable FJX1 protein while SW480^{FJX1MYC} cells continued to produce FJX1 protein *in vivo* (Figure 18D).

We next examined whether this change in tumor size was determined by differences in rates of proliferation or apoptosis. SW480^{FJX1MYC} tumors had significantly more Ki67-positive nuclei compared to SW480^{VEC} tumors (P < 0.05), indicating an increase in the number of actively proliferating cells (Figure 19A). There was no significant difference in levels of cleaved caspase 3 (Figure 19B). Thus, overexpression of *FJX1* affected xenograft tumor size due primarily to differences in the rate of tumor cell proliferation.
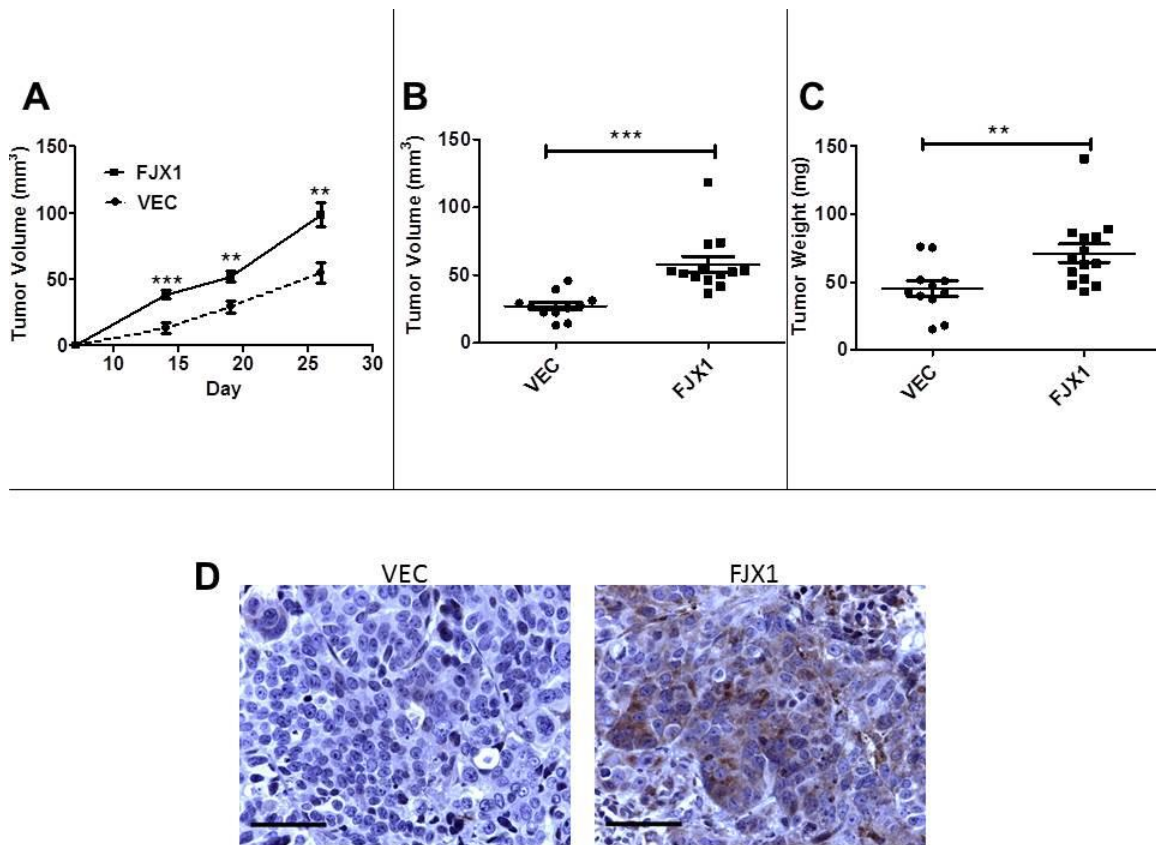
Figure 18. Overexpression of MYC-tagged *FJX1* in SW480 colon cancer cells promotes tumor growth *in vivo*. For all panels, VEC = SW480[VEC] (n=11); FJX1 = SW480[FJX1MYC] (n=14). **(A)** Estimation of tumor volume (mm^3) measured *in vivo* over time. **(B)** Final tumor volume measured following removal from animal. **(C)** Final tumor weight (mg) measured following removal from animal. **(D)** Representative FJX1 immunohistochemistry on SW480 xenograft tumors. Scale bar = 50 µm.

Since *FJX1* enhanced tumor cell proliferation *in vivo* but it had no direct effect on cell proliferation *in vitro* (Figure 15), we postulated that factors associated with the tumor microenvironment such as angiogenesis contributed to this discrepancy. To test this hypothesis, tumor vasculature was measured using the endothelial marker CD34. Total CD34 staining showed a slight increase in SW480^{FJX1MYC} tumors as compared to SW480^{VEC} (data not shown). Focusing on the presence of larger vessels, that is CD34+ vessels with an area of at least 50 μm^2, showed SW480^{FJX1MYC} tumors contained approximately twice as many of these larger vessels than SW480^{VEC} tumors per mm^2 of tumor section (5.84 +/- .56 vs 3.18 +/- .44 .respectively, $P < 0.005$, Figure 19C, representative images in 19D). These data suggest that FJX1 overexpression promotes xenograft tumor growth *in vivo* by non-cell-autonomous effects, increasing recruitment of vasculature, thereby allowing increased tumor cell proliferation.

For KM12C transduced cells, one million cells were injected subcutaneously into the right flank and two million cells were injected subcutaneously into the left flank of each athymic nude mouse, with ten mice per group. KM12C transduced cells grew rapidly and tumors were excised on day 7 due to size of left flank tumors. Tumors grown from a million cells had no significant difference between KM12C^{VEC} and KM12C^{FJX1} tumor weight or volume (data not shown). However, KM12C^{FJX1} tumors grown from two million cells were significantly larger than KM12C^{VEC} tumors (Figure 20).
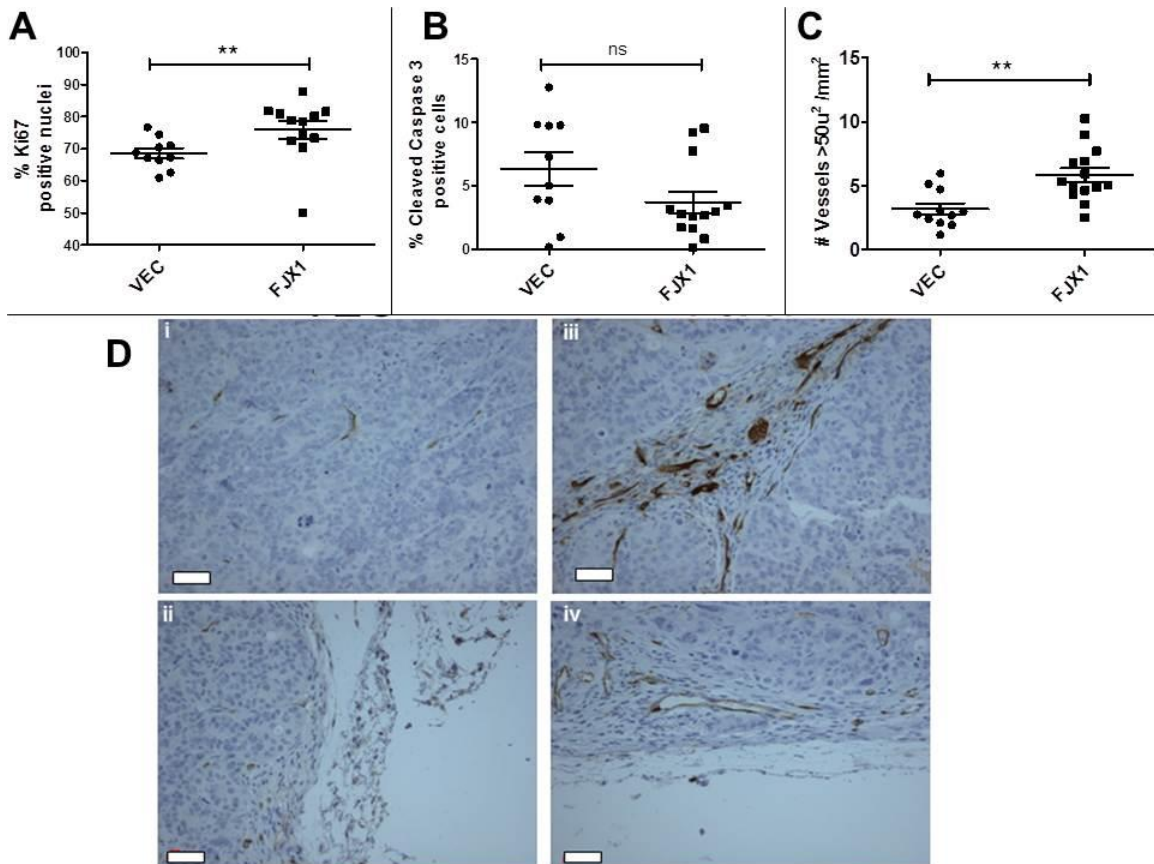
Figure 19. Overexpression of MYC-tagged *FJX1* in SW480 colon cancer cells promotes tumor growth *in vivo*. For all panels, VEC = SW480[VEC] (n=11); FJX1 = SW480[FJX1MYC] (n=14). **(A)** Percent of Ki67 positively stained nuclei. **(B)** Percent of cleaved caspase positively stained cells. **(C)** Number of blood vessels larger than 50 μm^2 per mm^2 per tumor section. **A/B/C** Each data point represents quantification of an entire cross section of tumor. Significance was determined by the Mann-Whitney test; ns= not significant *P < 0.05, **P < 0.005. Bars and whiskers represent mean and standard error of the mean respectively. **(D)** Representative light images from CD34 stained SW480[VEC] (i-ii) or SW480[FJX1MYC] (iii-iv) tumor sections. Scale bar = 20 microns.
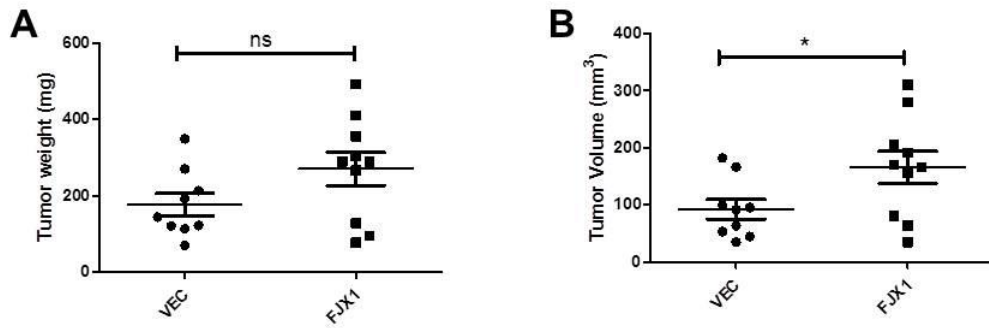
Figure 20. Overexpression of MYC-tagged *FJX1* in KM12C colon cancer cells promotes tumor growth *in vivo*. For all panels, VEC = KM12C^{VEC} (n=10); FJX1 = KM12C^{FJX1MYC} (n=10). Final tumor weight **(A)** and volume **(B)** after removal from animal. Significance was determined by the Mann-Whitney test; ns= not significant, *P < 0.05. Bars and whiskers represent mean and standard error of the mean respectively.

In order to determine whether endogenous expression of FJX1 has an influence on tumorigenesis, we employed a well-characterized model of inflammation/carcinogenesis using azoxymethane (AOM) and dextran sodium sulfate (DSS) to induce colonic tumors in mice [75,76]. For this experiment we used C57BL/6 mice that were homozygous null for *FJX1* (KO, n=8) and compared them with wild-type C57BL/6 littermates (WT, n=8). The mice were given an initial dose of AOM followed by three cycles of DSS as described in Methods. Upon gross examination, *FJX1* null mice had significantly fewer colonic polyps than the wild-type control mice (Figure 21A). We assessed the inflammation and crypt damage of formalin fixed paraffin embedded colonic sections from the *FJX1* null and WT mice as described by Dieleman et al. This method takes into account both the inflammation severity/crypt damage and the percentage of tissue affected. There was no significant difference between *FJX1* null and WT mice when assessing the inflammation score, extent of inflammation, and crypt damage, which combined is known as the total histological score (Figure 21B). We then assessed the vasculature associated with *FJX1* null and WT colonic sections by quantifying CD34 stained colonic tissue sections. We found that *FJX1* null colonic sections had significantly fewer blood vessels per mm^2 than WT mice (Figure 21C). Thus, genetic deletion of endogenous *FJX1* in mice results in inhibition of colonic tumorigenesis in association with reduced tissue angiogenesis, consistent with the increase in tumor vasculature observed in SW480[FJX1MYC] cells grown as xenografts.
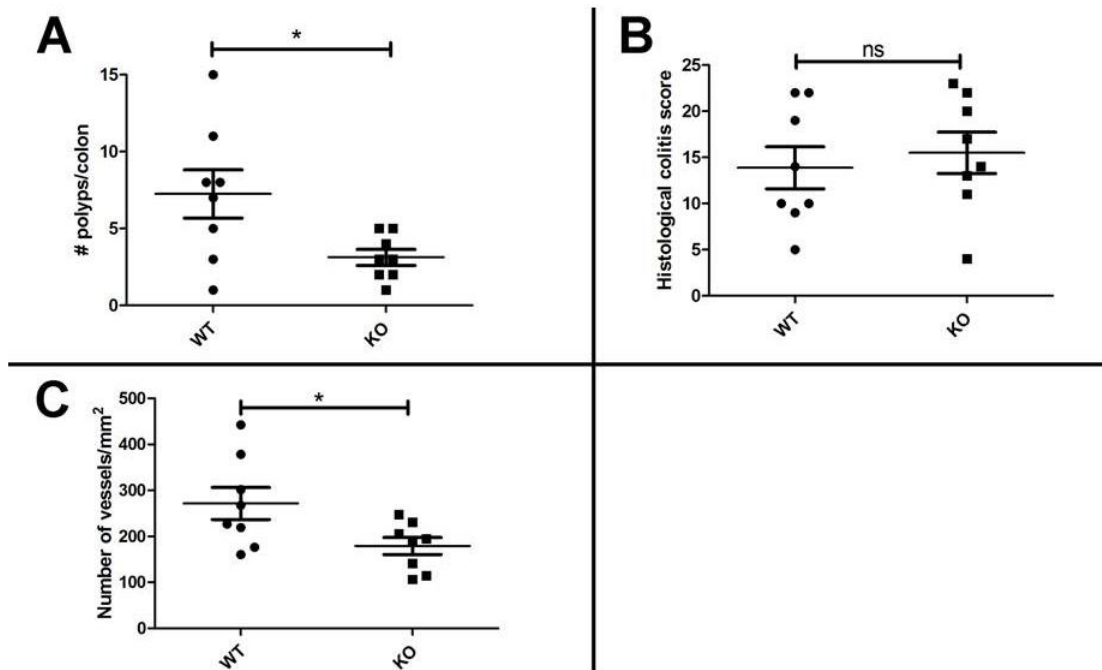
Figure 21. *FJX1* **null mice have fewer polyps than wild-type littermates in a**
mouse model of tumorigenesis. For all graphs WT = wild-type (n=8); KO =
FJX1 null (n=8). **(A)** Number of colonic polyps counted in mice after treatment
with AOM/DSS. **(B)** Histological colitis score as determined on hematoxylin and
eosin stained colonic sections after treatment with AOM/DSS. **(C)** Number of
blood vessels per mm^2 of tissue section as determined on CD34 stained colonic
sections after treatment with AOM/DSS. * = p<0.05. ns = not significant.

Conditioned media from FJX1-overexpressing tumor cells increases endothelial cell tube formation *in vitro.*

Since overexpression of *FJX1* in the SW480 xenograft tumors resulted in increased angiogenesis, we used the widely accepted endothelial tube assay [78,79] to test whether FJX1-conditioned media affected HMEC-1 endothelial cells *in vitro.* We found that conditioned media from *FJX1* transduced HEK293T, SW480, and KM12C cells significantly increased the number of endothelial tubes formed by HMEC-1 cells on Matrigel as compared to conditioned media from vector transduced control cells (Figure 22). Interestingly, autonomous expression of FLAG-tagged *FJX1* in HMEC-1 cells also promoted tube formation *in vitro* (Figure 22, note for the autonomous experiment 20,000 cells were used as opposed to 30,000 cells for non-autonomous). We failed to observe a difference in endothelial tube formation when cells were treated with conditioned media from *FJX1* transduced CACO2 cell lines as compared to VEC transduced control cells (Figure 22). It is interesting to note that conditioned media from CACO2^{VEC} cell lines greatly stimulated endothelial tube formation as compared with conditioned media from other cell lines, perhaps accounting for why the addition of *FJX1* did not further enhance tube formation.

To demonstrate that increased tube formation by SW480^{FJX1MYC} conditioned media is specifically a result of increased *FJX1* expression, we used oligonucleotides specific for *FJX1* (siFJX1) to inhibit *FJX1* expression. Inhibition of FJX1 protein expression was confirmed by immunoblotting of both whole cell lysate and conditioned media (Figure 23). Although conditioned media from

71

SW480^{FJX1MYC} cells untreated (UT) or transfected with scrambled siRNA (siSCR) maintained the ability to promote HMEC1 tube formation as compared to SW480^{VEC}, SW480^{FJX1MYC} cells transfected with *siFJX1* failed to augment tube formation (Figure 23).

To determine if secreted FJX1 protein (approximately 40 and 37 kDa) is directly responsible for the non-autonomous increase in capillary tube formation, conditioned medium was fractionated using a 30,000 nominal molecular weight cut-off filter. Elimination of FJX1 protein from the flow-through fraction was confirmed by immunoblotting (Figure 23). Interestingly, the flow-through fraction of media maintained the ability to promote HMEC-1 tube formation (Figure 23). Thus, our data indicate that overexpression of *FJX1* by tumor cells is associated with increased secretion of other pro-angiogenic factors contained within the flow-through fraction.

Figure 22. Autonomous and non-autonomous expression of *FJX1* selectively enhances endothelial capillary tube formation *in vitro*. Data represent the number of HMEC-1 tube structures formed on Matrigel following treatment with FJX1 conditioned media as compared with VEC conditioned media for the cell lines indicated (293T, SW480, CACO2, KM12C). No CM = no conditioned media treatment. For HMEC1 cell lines, data represent the number of tube structures formed in Matrigel after stable expression of vector (VEC) or FJX1 (FJX1).
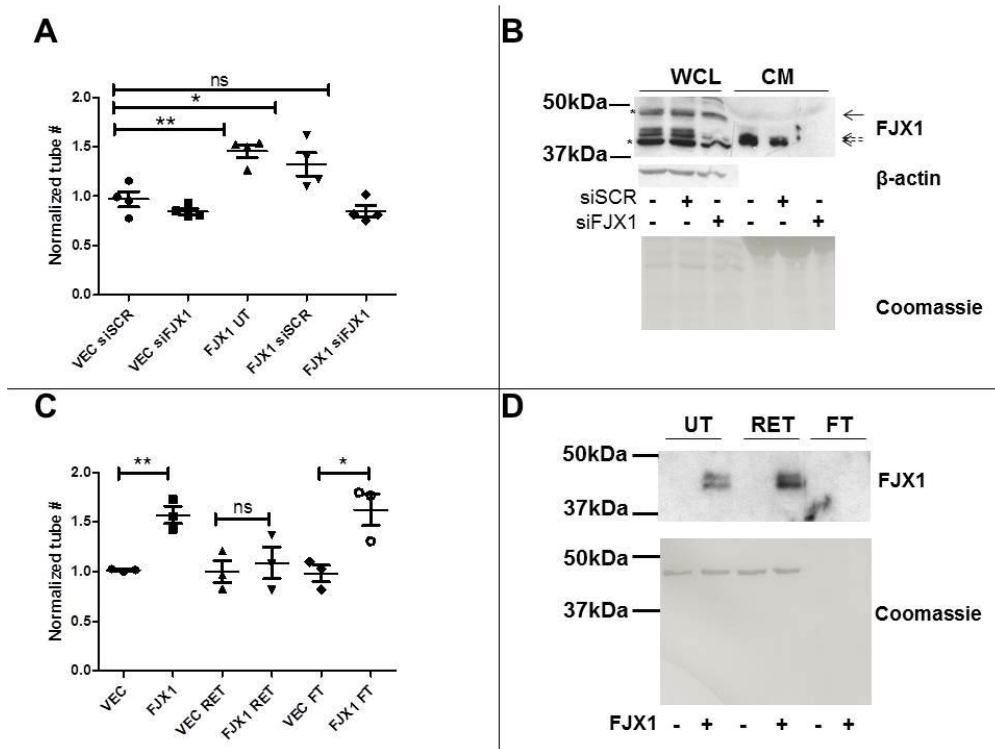
Figure 23. Conditioned media from SW480^FJX1 cells enhances endothelial capillary tube formation *in vitro*. (A) Relative number of HMEC-1 tube structures formed in the presence of conditioned media from SW480 cells treated as noted as compared to VEC untreated. **(B)** Representative FJX1 immunoblot of whole cell lysate from SW480^FJX1MYC cells treated as noted. (**A/B)** siFJX1 and siSCR denotes treatment with *FJX1* specific siRNA and scrambled siRNA respectively. β-actin and Coomassie stain served as loading controls for whole cell lysate (WCL) and conditioned media (CM), respectively. Asterisks (*) = non-specific band. **(C)** Relative number of HMEC-1 tube structures as compared with VEC after fractionation of the conditioned media. **(D)** Representative FJX1 immunoblot of conditioned media from SW480 cells after fractionation. RET = retained on column; FT = flow through. **(A/C)** Each data point represents the value of a biological replicate and bars and whiskers represent the mean and standard error of the replicates, respectively. Significance was determined by Student's t-test; *P < 0.05; **P < 0.005; ns=not significant.

Discussion

In chapter II we described our discovery of _FJX1_ through an _in vivo_ screen to identify celecoxib regulated genes. We demonstrated that _FJX1_ mRNA and protein are increased in CRC tissue as compared with normal, and that patients with high _FJX1_ have significantly worse prognosis. We postulated that our observation that patients with higher _FJX1_ mRNA expression have worse survival outcomes is related to the functional effects of _FJX1_ on tumor formation. This hypothesis is supported by our experimental observations. First, mice lacking endogenous _FJX1_ had fewer colonic polyps after AOM/DSS treatment as compared to wild-type littermates, suggesting that _FJX1_ expression enhances tumor formation _in vivo_. Second, when we performed xenograft experiments in athymic mice, we found that tumors from SW480 and KM12C cells transduced with _FJX1_ exhibited increased size and proliferation as compared to vector transduced controls. In both the _FJX1_ KO mice, and the SW480 xenograft models we found an association between vascularization and _FJX1_ expression; colonic sections and tumor xenografts lacking _FJX1_ had fewer blood vessels. It will be of interest to determine if the KM12C^{FJX1} xenografts also exhibit increased tumor angiogenesis. It is well recognized that without angiogenesis, tumors remain limited in both size and location, thus posing limited threat to the overall health of the individual [80]. It is likely that the correlation between high expression of _FJX1_ and poor patient survival can be attributed to the pro-angiogenic effects of increased _FJX1_ expression and its downstream targets.

We demonstrated that conditioned media from HEK293T, SW480, and KM12C cells with augmented *FJX1* expression promoted endothelial capillary tube formation. This non-autonomous phenotype was maintained even upon exclusion of secreted FJX1 protein, suggesting that enhanced expression of *FJX1* is associated with increased secretion of other factors that are pro-angiogenic. It was also interesting that autonomous expression of *FJX1* in the endothelial cell lines promotes capillary tube formation, indicating that angiogenic effects of FJX1 are not specific to a single cell type. It is unclear why CACO2 cells transduced with *FJX1* did not promote capillary tube formation, but may reflect tumor-specific variation and/or more subtle differences that were not measurable in these assays. Since three of the cell lines in our studies, SW480, KM12C and HEK293T, do not express detectable levels of COX-2, results from these experiments argue that the effect is FJX1 specific and not due to previously described angiogenic effects of COX-2 [40]. Furthermore, this supports our gene expression data from human tumor samples indicating that *FJX1* expression is downstream of COX-2 function.

CHAPTER V.

FJX1 PROMOTES ANGIOGENESIS THROUGH REGULATION OF

HIF1-α.

Introduction

We have found that FJX1 is upregulated in colorectal cancer (chapter II), and that FJX1 can promote tumor formation by increasing tumor vasculature (chapter IV). Prior to our work, human FJX1 had only been described in terms of microarray expression data. By microarray analysis, alteration in *FJX1* mRNA expression occurs in various cell types treated with different cytokines, including tumor necrosis factor α (TNF-α) treatment of HMEC-1 cells [81]; interleukin 1 (IL-1) treatment of HUVEC cells [82]; lipopolysaccharide (LPS) treatment of human monocytes [83]; and human chorionic gonadotropin (hCG) treatment of fibroblasts from endometriosis patients [84]. There are no reports concerning what signaling molecules may be downstream of FJX1. Since the non-autonomous effect of *FJX1* expression is not a direct effect of secreted FJX1, we wanted to identify both the secreted pro-angiogenic factor found in conditioned media from *FJX1* transduced cells, as well as identify potential signaling pathways that were altered intracellularly by *FJX1* expression.   We began by analyzing microarray data from two independent human CRC databases to look for genes that were concordantly regulated with *FJX1*. We also specifically tested the association between *FJX1* expression and known angiogenesis related genes. Finally we used a proteomic approach to analyze conditioned

media from SW480^{VEC} and SW480^{FJX1} cells. Here we describe our identification

of HIF1-α as an important mediator of the FJX1 pro-angiogenic program.

Materials and Methods

<u>*FJX1* angiogenesis correlation analysis</u>

WebGestalt [85] was used to identify biological processes that are

significantly associated with *FJX1* expression and gene set enrichment analysis

(GSEA) [86] was used to specifically test the association between *FJX1*

expression and expression of other angiogenesis related genes. Two human

CRC datasets GSE17536 and GSE17537 were normalized using the RMA

algorithm and pairwise absolute Pearson's correlation coefficient was calculated

between the *FJX1* probe set 219522_at and all other probe sets. The probe sets

were ranked based on their correlation with *FJX1*. The top 500 probe sets for

each dataset were subjected to the Gene Ontology biological process enrichment

analysis respectively using WebGestalt. The ranked lists were analyzed using

GSEA to test whether known angiogenesis genes (Gene Ontology annotation

GO:0001525) were enriched at the top of the lists, identify the leading edge

subset, and determine the gene set's enrichment signal [86].

<u>RNA extraction and qRT-PCR</u>

RNA was extracted using the Qiagen RNeasy Kit (Qiagen) per

manufacturer's instructions. qRT-PCR reactions analyzing *HIF1A*, *PMM1*, *18S*

and *VEGF-A* mRNA levels in cell lines were performed using the Roche

transcriptor universal cDNA master and analyzed on the Lightcycler 480 II

(Roche). Primers used; *HIF1A*: 5'-GGTTCACTTTTTCAAGCAGTAGG-3' and 5'-GTGGTAATCCACTTTCATCCATT-3' (IDT) with probe #3 (Roche); *18S*: 5'-GCAATTATTCCCCATGAACG-3' and 5-GGGACTTAATCAACGCAAGC-3' (IDT) with probe #48 (Roche); *VEGF-A*: 5'-CCTTGCTGCTCTACCTCCAC-3' and 5'-CCACTTCGTGATGATTCTGC-3' (IDT) with probe #29 (Roche); *PMM1*: 5'-TTCTCCGAACTGGACAAGAAA-3' and 5'-CTCTGTTTTCAGGGCTTCCA-3' (IDT) with probe #7 (Roche).   Relative fold change of expression was calculated by $2^{-\Delta Ct}$.

Cell culture

HEK293T, CACO2, and SW480 (ATCC) were cultured in RPMI 1640 (Gibco) with 10% FBS (Atlanta Biologicals), 100U/mL pen/strep (Gibco), and 100U/mL L-glutamine (Gibco) at 37 ^{o}C with 5% CO_2. HMEC-1 cells (F. Candl, Center for Disease Control) were cultured in MCDB131 (Gibco), supplemented with 10% FBS, 10ng/mL epidermal growth factor (Becton-Dickson), 100U/mL L-glutamine (Gibco), and 1μm/mL hydrocortisone (Sigma Chemical). KM12C (Gift of Dr. Isiah Fidler) [67] were cultured in MEM (Gibco) with 10% FBS (Atlanta Biologicals), 100U/mL pen/strep (Gibco), 100U/mL L-glutamine (Gibco), sodium pyruvate (Gibco), non-essential amino acids (Gibco) and MEM vitamins (Gibco). Hypoxic conditions were achieved using a hypoxia chamber equilibrated with 1% O_2, 5% CO_2 and 94% N_2. MG132 (Enzo life sciences) and cycloheximide (Sigma) were used at 50uM and 100uM.

Immunoblotting

Cells were lysed in radio-immunoprecipitation assay (RIPA) buffer (150Mm sodium chloride, 1% Igepal, 0.5% sodium deoxycholate, 1% sodium dodecyl sulfate, 50mM Tris-Cl) supplemented with aprotinin, leupeptin, sodium orthovanadate, sodium fluoride, and phenylmethylsulfonyl fluoride before resolution by SDS-polyacrylamide gel electrophoresis (SDS-PAGE). Whole serum from 208 was diluted 1:3000 in 5% milk-PBST overnight at 4°C. Commercial antibodies: β-actin (Sigma Chemical, 5% milk-PBST 1:10,000), HA (Cell signaling, rabbit polyclonal, 5% milk-PBST 1:1000), HIF1-α (Novus, rabbit polyclonal, 5% milk-PBST 1:1000), and Annexin I (Invitrogen, Rabbit polyclonal, 5% milk-PBST 1:2000) Anti-rabbit HRP and Anti-mouse HRP were diluted 1:5000 in 5% milk-PBST and incubated for 30 minutes at room temperature.

Collection of conditioned medium and siRNA

SW480^{VEC} or SW480^{FJX1} cells were transfected with 100nM pooled siRNA specific to HIF1-α (Dharmacon) or non-targeting scrambled siRNA (Dharmacon), and HEK293T cells were transfected with pcDNA3.1, HA-HIF1-α or pcDNA3.1 hFJX1, replated at 48 hours post transfection, and re-fed with serum free media after 72 hours. After 96 hours, media was collected, spun at 300g for 5 minutes and transferred to a fresh tube and directly used in endothelial tube assays. For fractionation experiments, 4mL of 5mL total conditioned media was spun at 4000 g for 30 minutes at 4°C in an Amicon ultra 30K membrane tube (Millipore). Serum free medium was added to the fraction that was retained on the column to

equal the volume that flowed through the column. Conditioned medium from

sub-confluent SW480^{VEC} and SW480^{FJX1} cells was analyzed using the VEGF

ELISA (R&D Systems) per manufacturer's instructions. ELISA data was derived

from three biological replicates performed in duplicate and significance was

determined using Student's t-test.

<u>Proteomic sample preparation</u>

Conditioned media from SW480^{VEC} or SW480^{FJX1} cells was spun at 4000 g

for 30 minutes at 4°C in an amicon ultra 30K membrane tube (Millipore) from six

10cM plates. The flow through fraction from each biological replicate was

MEOH/CHCl3 precipitated. An equal volume of methanol and .25% of

chloroform was added and the samples were spun at 13,000 RPM for 15

minutes. The supernatant was removed and the samples werer washed with

1mL of 100% methanol and spun for an additional 10 minutes. The protein pellet

was then dried with a SpeedVac (Thermo Fisher) and then was suspended in

200 uL of 50% 2,2,2-trifluoroethanol (Acros Organics), 50% 50 mM ammonium

bicarbonate (Fisher Scientific) (v/v). Protein concentration was measured using

the BCA protein assay (Pierce Biotechnology). A total of 200ug of protein from

the conditioned media was reduced with 100uL of 100mM dithiothreitol (Pierce

DTT, No-Weigh Format) an incubated at 60°C for 30 minutes with shaking. After

cooling down the tubes, 100 uL of 200 mM iodoacetamide was added and

incubated 20 min at room temperature in the dark. Samples were diluted with

600 uL of 50 mM ammonium bicarbonate. In order to generate peptides suitable

for MS-MS analysis, the samples were digested by adding trypsin (20g,

81

trypsin/protein ratio of 1:50 (w/w), Promega) and digestion was carried out at 37°C overnight. After lyophilizing the resulting peptide mixture, samples were reconstituted by distilled water and applied to Sep-Pak C18 cartridges (Waters). After washing the column with 1 ml of distilled water, digested peptides were eluted from the column with 1 ml of 80% acetonitrile. Eluted peptides were evaporated to dryness in a SpeedVac (Thermo-Fisher) and reconstituted with 2.5 ml of 6 M urea for isoelectric focusing (IEF) of peptides.

IEF Fractionation of Peptide Digests and LC-MS/MS Analyses

Four independent IEF peptide separations were performed on each 200 ug sample. Immobilized pH gradient (IPG) strips, 24 cm, pI 3.5– 4.5 (IPGphor, GE Health Care), were rehydrated overnight, then loaded and focused using an Ettan IPGphor 3 IEF system (GE Health Care) for 25 hours. Immediately after focusing, IPG strips were cut into 20 pieces and peptides were extracted, the extracts were dried down, desalted, dried down again and then reconstituted in 0.1 ml of 0.1% formic acid for LC-MS/MS analysis LC-MS/MS analysis were performed on an LTQ-Velos mass spectrometer (Thermo Fisher).

Endothelial tube formation

Phenol red free growth factor reduced matrigel (BD biosciences) was allowed to solidify in 96 well plates (50uL/well) for 30 minutes at 37°C. HMEC1 (30,000 cells) in complete media were plated on top of the matrix and an equal volume of conditioned media containing 0% FBS from epithelial cell lines (HEK293T, SW480) was added. Images were taken 16-18 hours after HMEC-1

cells were plated for tube formation, with three images taken per well. Experiments were performed in triplicate at least three times, with each data point being the average of three images of three technical replicates. Significance was determined by Mann-Whitney, ANOVA, or Student's t test as noted.

*Result*s

FJX1 expression is associated with expression of known angiogenesis genes.

In order to identify the mechanism by which FJX1 elicits pro-angiogenic activity in tumor cells, we analyzed the top 500 genes that are most highly correlated with *FJX1* expression in two human colorectal cancer datasets from VUMC and MCC. Gene Ontology enrichment analysis by WebGestalt revealed significant enrichment of angiogenesis genes in both tumor datasets. This observation was further confirmed by gene set enrichment analysis (GSEA) that directly compares the correlations between *FJX1* expression and 186 predefined angiogenic factors (GO:0001525) to those between *FJX1* expression and all other genes (Figure 24, P < 0.001). This GSEA analysis identified 43 angiogenic factors with strong and consistent association with *FJX1* expression in both datasets, representing the core genes that account for the enrichment signal (the leading edge subset). These genes, including *HIF1A*, VEGF receptors *Flt1* and *KDR*, and *VEGFC* (Table 5), suggest an association of *FJX1* and angiogenic gene expression in human colorectal cancer tumor samples.

Of the significant genes from the GSEA, HIF1-α is a well-characterized transcription factor that regulates the expression of many pro-angiogenic molecules. Furthermore, at least ten of the 43 genes found in the leading edge subset have been shown to be regulated by HIF1-α (Table 5) [87-92] [93-96]. We observed no changes in *HIF1A* mRNA comparing vector transfected controls and *FJX1* expressing cells (Figure 25 A-C). However, we found increased HIF1-

α expression in *FJX1* transduced cells (Figure 25D). To test if enhanced HIF1-α

protein expression contributed to the increased capillary tube-stimulating activity

in SW480^{FJX1MYC} conditioned media, we suppressed *HIF1A* expression with

siRNA specific to *HIF1A*.   Inhibition of *HIF1A* was confirmed at both the mRNA

(Figure 26A) and protein levels (Figure 26B). While conditioned media from

SW480^{FJX1MYC} cells that were untreated or were transfected with scrambled

siRNA (siSCR) maintained the ability to promote increased HMEC1 tube

formation as compared to conditioned medium from SW480^{VEC} cells,

SW480^{FJX1MYC} cells transfected with *HIF1A* specific siRNA failed to do so (Figure

26C P < 0.0001). Further, inhibition of *HIF1A* did not affect secreted levels of

FJX1 protein (Figure 26D), supporting the conclusion that secreted FJX1 is not

the direct effector of endothelial cell capillary tube formation. Rather, *FJX1*

expression causes secretion of other pro-angiogenic proteins in a HIF1-α

dependent manner.
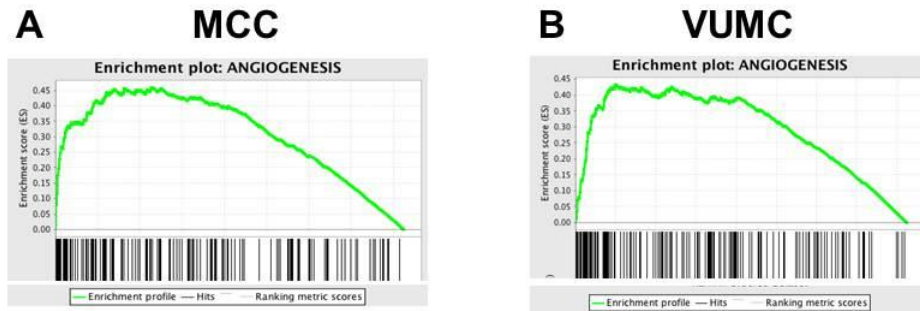
Figure 24. *FJX1* **mRNA expression in human colorectal cancers correlates with expression of known angiogenic factors.** Gene-set enrichment analysis of 186 defined angiogenic factors (GO:0001525) ranked by correlation from left (highest rank) to right (lowest rank) with *FJX1* expression in independent publicly available colon cancer microarray datasets **(A)** MCC and **(B)** VUMC. The enrichment score is shown by the green curve. Vertical black lines indicate the position of known angiogenic genes in the ranked list, with the density of these genes (and corresponding enrichment score) decreasing with declining correlation to *FJX1*.

Table 5. Gene symbol, gene name, and literature citation for association

with HIF1-α for the top 43 genes found in the leading edge subset of both

VUMC and MCC datasets after GSEA analysis

Gene Symbol	Gene name	Reference for regulation by HIF1-α
ANGPT1	angiopoietin 1	
ANGPT2	angiopoietin 2	Simon et al., J Cell Phys 2008
ANGPTL3	angiopoietin-like 3	
ANPEP	alanyl (membrane) aminopeptidase	
CDH13	cadherin 13, H-cadherin (heart)	
COL15A1	collagen, type XV, alpha 1	
COL18A1	collagen, type XVIII, alpha 1	
COL4A2	collagen, type IV, alpha 2	
COL4A3	collagen, type IV, alpha 3 (Goodpasture antigen)	
CTGF	connective tissue growth factor	
CYR61	cysteine-rich, angiogenic inducer, 61	Wolf et al., Endocrinology 2010; Wan et al., J. Exp Clin Can Res 2011
DDAH1	dimethylarginine dimethylaminohydrolase 1	
EDNRA	endothelin receptor type A	
ELK3	ETS-domain protein (SRF accessory protein 2)	
ENG	endoglin	Sanchez-Elsner et al., JBC 2002
ENPEP	glutamyl aminopeptidase (aminopeptidase A)	
FLT1 (VEGFR1)	fms-related tyrosine kinase 1 (vascular endothelial growth factor/vascular permeability factor receptor	Okuyama et al., JBC 2006
HDAC5	histone deacetylase 5	
HIF1A	hypoxia inducible factor 1, alpha subunit (basic helix-loop-helix transcription factor)	
JAG1	jagged 1	
KDR (VEGFR2)	kinase insert domain receptor (a type III receptor tyrosine kinase)	
KLK3	kallikrein-related peptidase 3	
MMP14	matrix metallopeptidase 14 (membrane-inserted)	Wan et al., J. Exp Clin Can Res 2011

Table 5 Continued.

Gene Symbol	Gene name	Reference for regulation by HIF1-α
MYH9	myosin, heavy chain 9, non-muscle	
NRP1	neuropilin 1	
PLAU	plasminogen activator, urokinase	
PLXDC1	plexin domain containing 1	
PLXND1	plexin D1	
PTEN	phosphatase and tensin homolog	
PTPRM	protein tyrosine phosphatase, receptor type, M	
RHOB	ras homolog gene family, member B	
ROBO1	roundabout, axon guidance receptor, homolog 1	
SERPINE1	serpin peptidase inhibitor, clade E (nexin, plasminogen activator inhibitor type1), member 1	Elvidge et al., JBC 2006
SERPINF1	serpin peptidase inhibitor, clade F (alpha-2 antiplasmin, pigment epithelium derived factor) member 1	
SLIT2	slit homolog 2	
SOX18	SRY (sex determining region Y)-box 18	
SPHK1	sphingosine kinase 1	Anelli et al, JBC 2008
TEK	tyrosine kinase, endothelial	Lai et al., J Mol Med 2012
TGFB2	transforming growth factor, beta 2	
THBS1	thrombospondin 1	Osada-Oka et al., J Cell Biochem 2008
THY1	Thy-1 cell surface antigen	
TIE1	tyrosine kinase with immunoglobulin-like and EGF-like domains 1	
VEGFC	vascular endothelial growth factor C	Spinella et al, Can Res. 2009
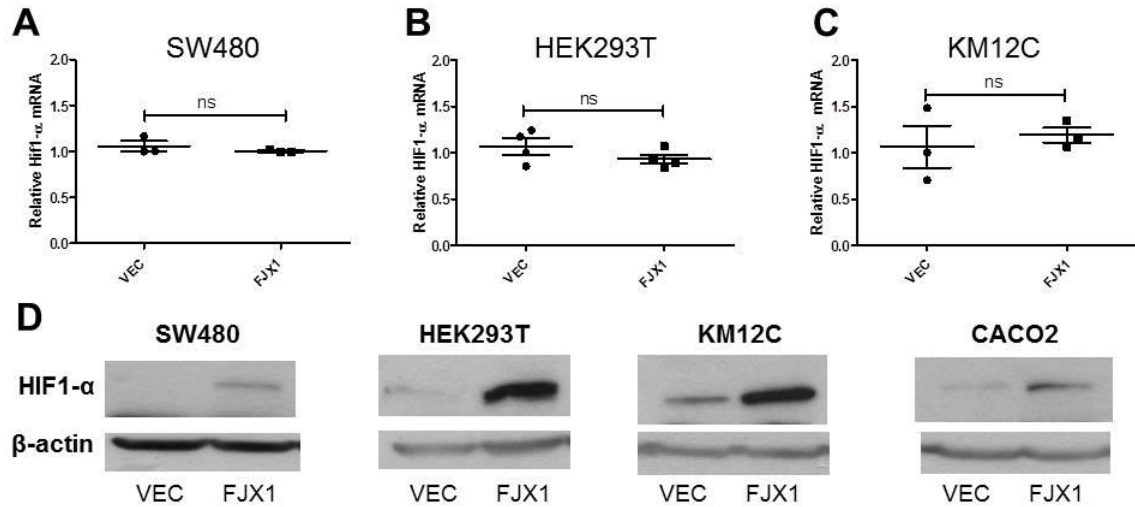
Figure 25. *FJX1* expression does not alter *HIF1-α* mRNA expression but increase HIF1-α protein. Relative fold change in *HIF1-α* mRNA expression in **(A)** SW480**, (B)** HEK293T and **(C)** KM12C transfected with vector (VEC) or *FJX1* (FJX1). Each data point is the mean of a biological replicate. Bars and whiskers represent mean and standard error of the mean respectively. Significance was determined by a Student's t-test. ns = not significant. **(D)** Representative HIF1-α protein levels as determined by immunoblot of whole cell lysates from VEC and *FJX1* transduced cell lines. β-actin served as the loading control.
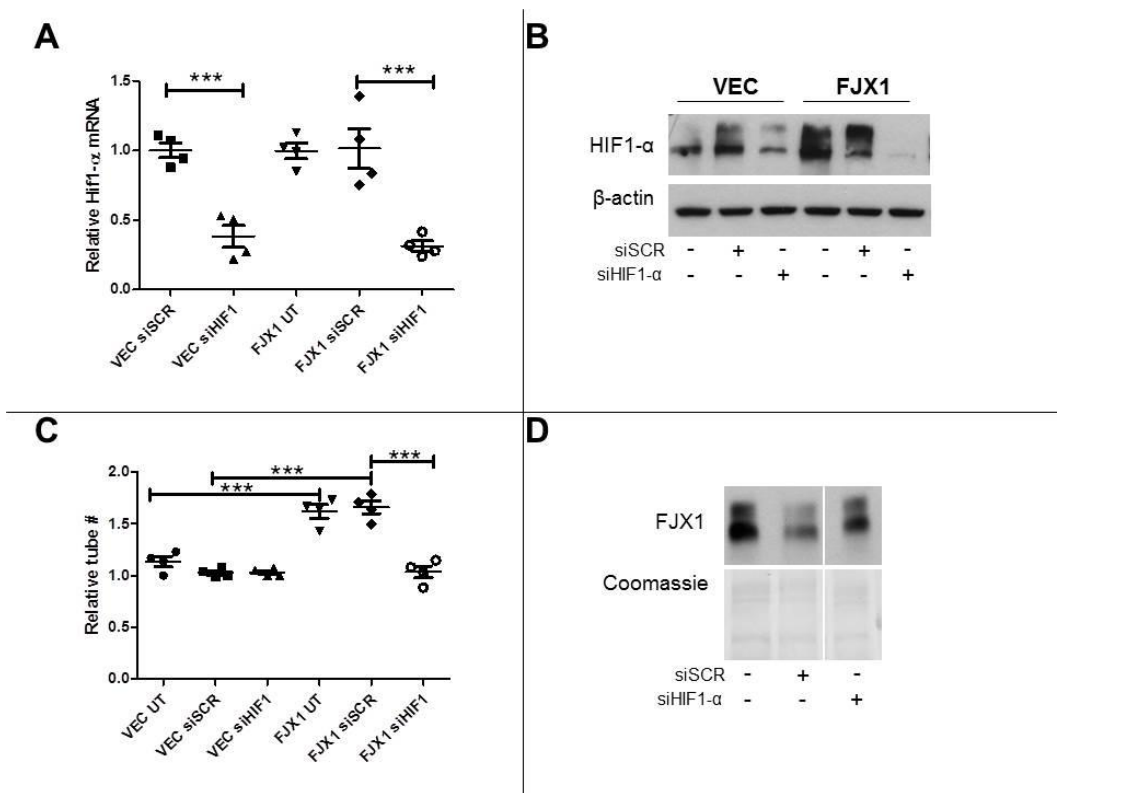
Figure 26. Increased HIF1-α contributes to FJX1-induced increase in endothelial tube formation (A) Relative fold change in *HIF1-α* mRNA expression in SW480^{FJX1MYC} (FJX1) as compared to SW480^{VEC} (VEC). **(B)** Representative HIF1-α immunoblot of whole cell lysates. β-actin served as the loading control. **(C)** Relative number of HMEC-1 tube structures as compared with SW480^{VEC} (VEC) UT after treatment with conditioned media from SW480 cell derivatives as noted. **(D)** Representative immunoblot of FJX1 in conditioned media from SW480^{FJX1MYC} cells. Coomassie stain represents loading control. UT= untreated. siSCR = treated with scrambled siRNA. siHIF1 = treated with *HIF1A* siRNA. Each data point is the mean of a biological replicate. Bars and whiskers represent mean and standard error of the mean respectively. Significance was determined by ANOVA. *** = p<0.0001.

Next we analyzed whether expression of a mutated version of *FJX1*
affected endothelial tube formation and *HIF1A* expression. This mutation was
based upon sequence homology with *Drosophila fj*: residues essential for fj
kinase activity that were conserved in FJX1 were mutated from aspartic acid and
glutamine to alanine (*FJX1*^{DEFLAG}). We found that conditioned media from
HEK293T and SW480 cells expressing *FJX1*^{DEFLAG} promoted tube formation
similarly to conditioned media from wild-type *FJX1* expressing cells (Figure 27, A
and B). Similarly, expression of either wild-type or mutant *FJX1* in HMEC-1 cells
promoted autonomous capillary tube formation as compared to vector expressing
control cells (Figure 27C). Finally, we observed a similar increase in HIF1-α
protein levels regardless of whether wild-type or mutant *FJX1* was expressed in
cell lines (Figure 27D). Taken together, we found that mutation of the putative
kinase domain of FJX1 has no effect on capillary tube formation.

<u>HIF1-α is sufficient to promote endothelial capillary tube formation *in vitro.*</u>

We then determined whether transient *HIF1A* expression alone in the
HEK293T cells was sufficient to induce release of the angiogenic factor into the
conditioned medium. Upon transient transfection of either *FJX1-MYC* or *HA-
HIF1A,* HIF1-α protein expression was increased compared to vector transduced
cells (Figure 28B) whereas *HIF1A* mRNA was only increased when *HA-HIF1A*
was transfected (Figure 28A). Conditioned media from HEK293T cells
transiently transfected with either *HA-HIF1A* or *FJX1-MYC* stimulated HMEC-1
tube formation as compared to conditioned media from vector

91
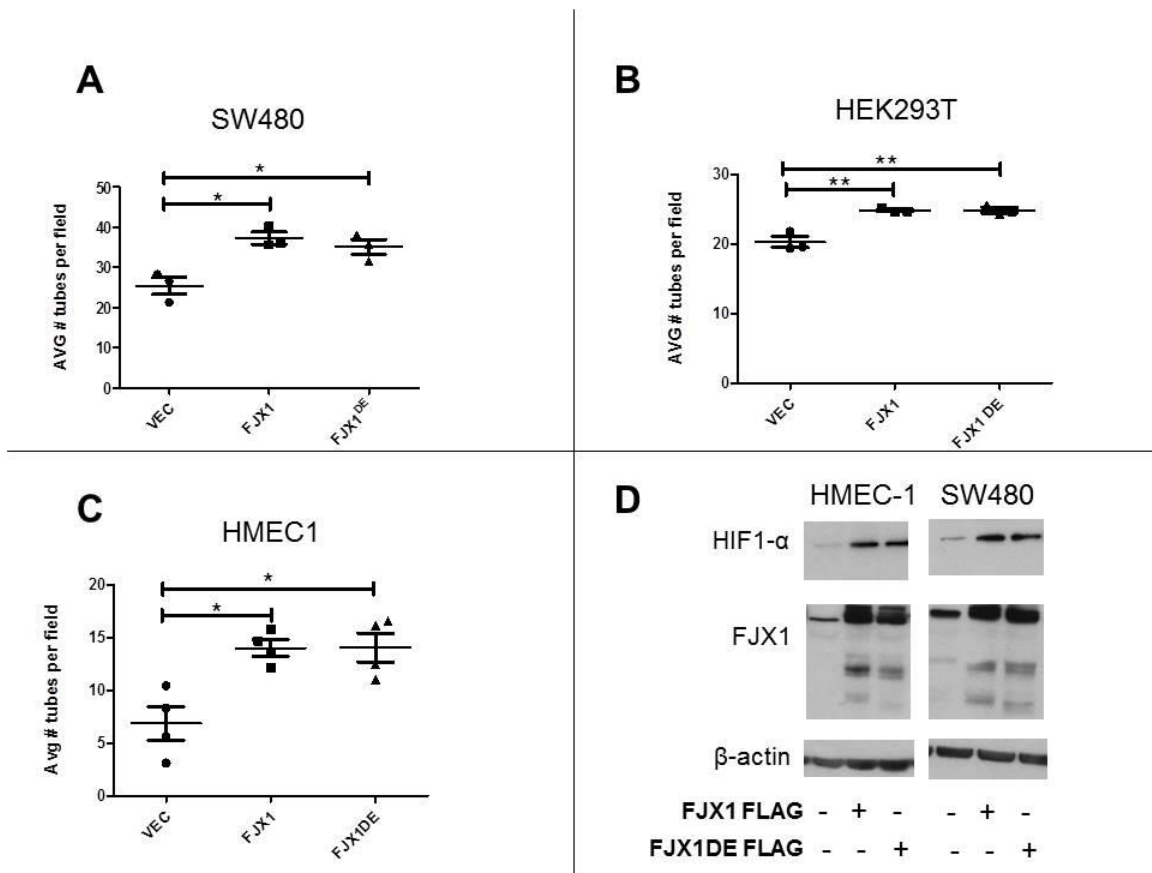
Figure 27. Autonomous and non-autonomous expression of *FJX1^FLAG* and *FJX1^DEFLAG* enhances endothelial capillary tube formation *in vitro*. (A/B) Data represent the number of HMEC-1 tube structures formed on matrigel following treatment with FJX1, or FJX1^DE conditioned media as compared with VEC conditioned media for **(A)** HEK293T and **(B)** SW480. **(C)** For HMEC1 cell lines, data represent the number of tube structures formed in matrigel after stable expression of vector (VEC), FJX1, or FJX1^DE. **(D)** Representative immunoblot of HIF1-α in whole cell lysates from SW480 and HMEC-1 cell lines stably expressing VEC, FJX1, or FJX1DE.
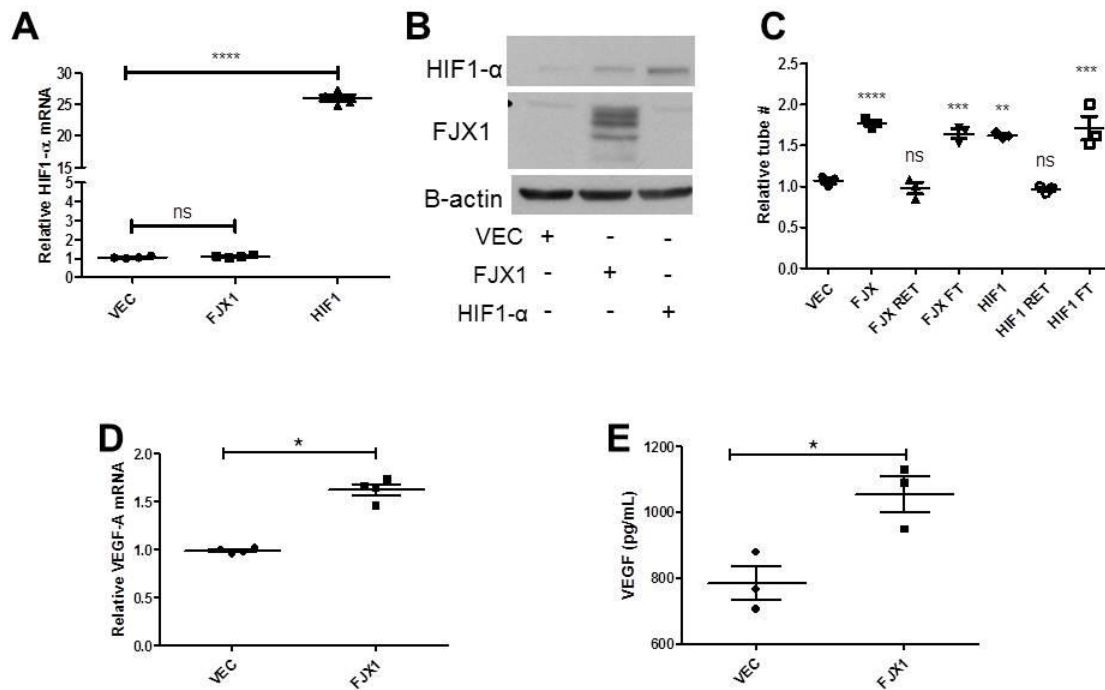
Figure 28. Increased HIF1-α expression is sufficient to promote endothelial tube formation *in vitro*. (A) Relative fold change in *HIF1A* mRNA expression in HEK293T transiently transfected with vector (VEC), *FJX1* (FJX1) or *HIF1A* (HIF1). Each data point is the mean of a technical replicate. β-actin served as the loading control. **(B)** Representative western blot of HIF1-α and FJX1 protein in HEK293T cells transiently transfected with VEC, *FJX1*, or *HA-HIF1A* **(C)** Relative number of HMEC-1 tube structures after treatment with conditioned media from vector, *FJX1* or *HIF1A* transduced HEK293T cells including fractionation of the media. RET = retained on column; FT = flow through.

transduced controls (Figure 28C). Furthermore, fractionation of conditioned

media using a 30,000 nominal molecular weight cut-off filter revealed that the

pro-angiogenic factor was found in the flow through (Figure 28C), similar to what

we observed with the SW480^{FJX1MYC} cells (Figure 23C).

VEGF-A is a transcriptional target of HIF1-α [47] and has been well

characterized as an angiogenic stimulus. *VEGF-A* mRNA was upregulated in

SW480^{FJX1} cells as compared with SW480^{VEC} (Figure 28D) and VEGF-A protein

was increased in total SW480^{FJX1MYC} conditioned media as compared with

SW480^{VEC} by ELISA (Figure 28E). However, species of VEGF-A detected by

commercially available antibodies was excluded from the flow through fraction

that contained the pro-angiogenic factor that promoted HMEC-1 tube formation

(data not shown).

FJX1 post-transcriptionally regulates HIF1-α protein levels.

To determine how HIF1-α protein levels were regulated by FJX1 we

transiently expressed HA-tagged *HIF1A* with and without *FJX1* in HEK293T cells.

When co-expressed with *FJX1*, HIF1-α protein levels were increased under both

normoxic and hypoxic conditions (Figure 29A). Addition of the proteasome

inhibitor MG132 equalized HIF1-α protein levels whether or not FJX1 was

present, suggesting elevated HIF1-α protein levels were a reflection of reduced

degradation rather than increased translation (Figure 29A). The addition of

cycloheximide, which halts new protein translation, showed that HIF1-α protein

was stabilized in the presence of FJX1 (Figure 29B). Our data therefore support

a model whereby FJX1 expression can increase HIF1-α protein stability and promote secretion or release of pro-angiogenic molecules.

Proteomic analysis of conditioned media from SW480 cell lines.

Our data thus far have shown that conditioned media from SW480[FJX1] cells contains pro-angiogenic factors. These factors are found in the flow through compartment after fractionation based on a 30,000 nominal molecular weight cut off. To identify this secreted pro-angiogenic factor we performed proteomics on the flow through fraction of conditioned media from SW480[VEC] and SW480[FJX1] cells. The top 16 peptides identified as being increased in SW480[FJX1] conditioned media mapped to Annexin A1; Ina-D like protein and Ina-D like protein isoforms 2,4,5; tenascin C and tenascin C isoforms 2,3,4,5,6,1414AD1/16. Of the three proteins and related isoforms, annexin A1 was smallest in size and known to be secreted from cells. We confirmed by immunoblot that annexin A1 was indeed increased in conditioned media from SW480[FJX1] as compared to SW480[VEC] cells. However, we were unable to detect annexin A1 in the flow through fraction (Figure 30). This may be due to a failure of the antibody to detect smaller peptides (Figure 30). Further analysis will be required to see if annexin A1 is cleaved into smaller active fragments that account for the pro-angiogenic factor in SW480[FJX1] conditioned media.
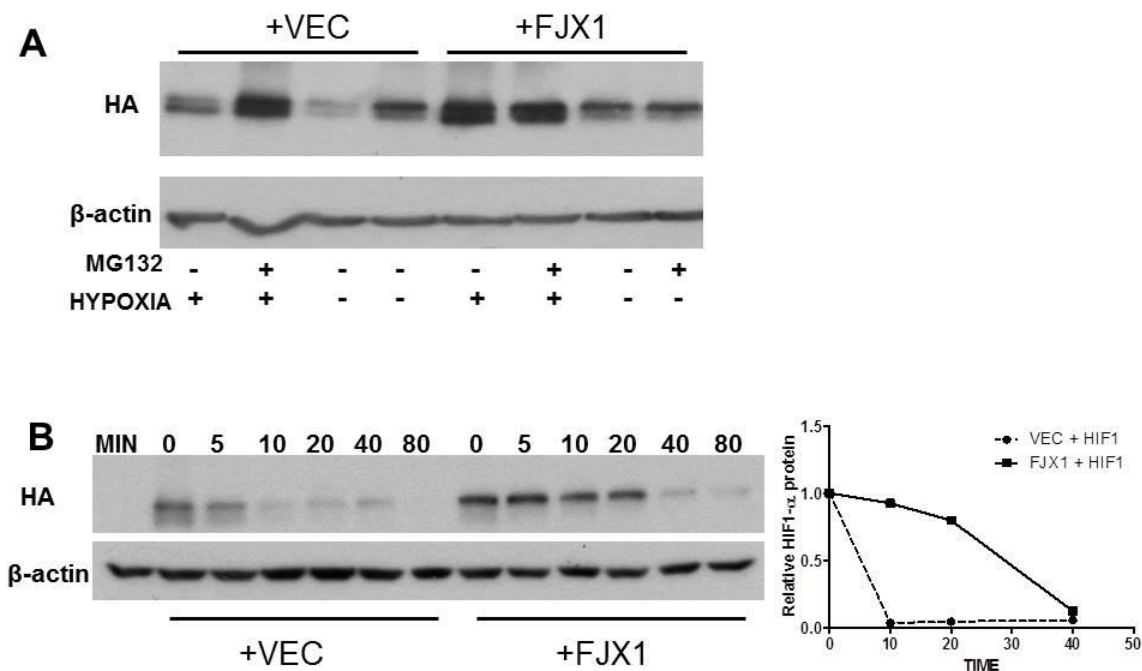
Figure 29. FJX1 enhances HIF1-α protein stability by enhancing HIF1-α half-life. (A) Representative HA immunoblot of whole cell lysates from HEK293T cells transfected with *HA-HIF1A* and VEC or *FJX1* cultured in normoxia or hypoxia (4 hours) with or without treatment of MG132 (50uM 2hrs). **(B)** Representative HA immunoblot of whole cell lysates from HEK293T cells transfected with *HA-HIF1A* and VEC or *FJX1* pre-cultured in hypoxia (2hrs) and treated with cycloheximide (100uM) for the indicated time in minutes. Quantification is graphed on the right.
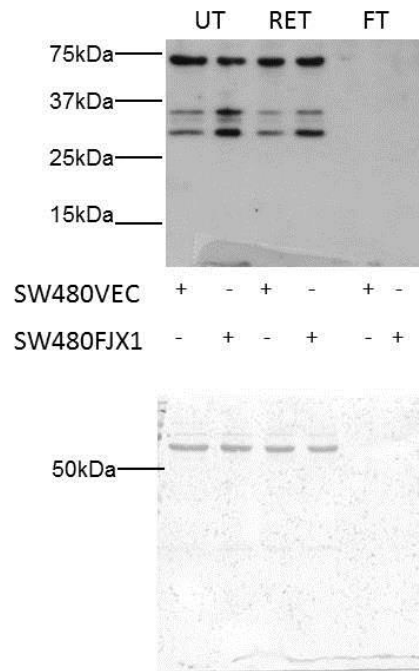
Figure 30. Conditioned media from SW480^{FJX1} cells has increased levels of Annexin A1 as compared to SW480^{VEC} cells. Representative Annexin A1 immunoblot of conditioned media from SW480 cells after fractionation. RET = retained on column; FT = flow through.

Discussion

We identified FJX1 as a protein that is overexpressed in CRC and demonstrated a pro-tumorigenic role for FJX1 through its ability to promote angiogenesis. To correlate our observations linking increased angiogenesis with enhanced *FJX1* expression (either *in vivo* or *in vitro*) we queried two human colorectal cancer datasets for association between expression of *FJX1* and known angiogenesis factors. Indeed, we found strong correlations between *FJX1* expression and expression of pro-angiogenic genes such as *HIF1A*, *VEGF-C*, and *angiopoietin 1* and *2*.

We detected increased HIF1-α protein in *FJX1* transduced HEK293T, SW480, KM12C, and CACO2 cells and experimentally linked HIF1-α levels to increased capillary tube formation. HIF1-α has been shown to induce pro-angiogenic programs through modulation of a variety of molecules including but not limited to VEGF, FLT1, ANGPT2, THBS1 and CYR61 [87-89,91,95,96]. The ability of several known targets to either promote or hinder endothelial cell function is complex and context dependent. For example, ANGPT2 promotes endothelial sprouting in the presence of VEGF, but promotes endothelial regression in the absence of VEGF [97,98]. Also, proteins may undergo proteolytic processing into smaller peptides that are functionally distinct from the full length form, i.e. VEGF and COL18A1 [99,100]   Although we detected increased expression of the HIF1-α-regulated VEGF-A in *FJX1* expressing cells, VEGF-A was excluded from the flow through fraction of conditioned media that contained the angiogenic stimulus associated with *FJX1* expression. This

molecule may represent a smaller VEGF related fragment or peptide not detectable by available reagents, or indeed a novel HIF1-α regulated modulator of angiogenesis

Expression of *FJX1* caused increased levels of HIF1-α through an increase in HIF1-α protein stability. Although we initially identified a concordant relationship between *FJX1* mRNA and *HIF1-α* mRNA expression in human colonic tumors, we were only able to attribute a post-translational role of FJX1 on HIF1-α regulation *in vitro*. This discrepancy may be due to the complex interactions within the tumor microenvironment that are not supported by our *in vitro* model. Alternatively, it is possible that a common co-regulatory factor influences both *FJX1* and *HIF1-α* mRNA expression *in vivo*. Under normoxic conditions, HIF1-α protein is hydroxylated at proline residues by prolyl hydroxylases (PHD) allowing for ubiquitin mediated proteasomal degradation involving von Hippel-Lindau [101,102]. Since PHD enzymes have an absolute requirement for molecular oxygen, hypoxic conditions inhibit PHD function and allow for HIF1-α protein stabilization. Altered mitochondrial function has also been linked to PHD activity with prevailing hypotheses being 1, that reactive oxygen species (ROS) from complex III inhibit the PHD enzymes[103,104], or 2, that oxygen being shunted through the complex limits the availability of oxygen which is required by the PHD enzymes independently of ROS production [105,106]. It will be interesting to determine whether FJX1 is interfering with PHD activity, perhaps by altering mitochondrial function or affecting more downstream targets that are part of the degradation complex.

Drosophila fj is a kinase that phosphorylates specific cadherin residues on two large cadherins fat and dachsous [57,61]. The three key residues of the fj putative kinase domain (DNE) are completely conserved across multiple species, including mouse and human. Mutation of the conserved aspartic acid within this region was sufficient to inhibit the biological function of *fj* [61]. When we mutated the aspartic acid and glutamic acid residues, we found no functional change in our *in vitro* assays. Specifically, expression of either wild-type or mutant *FJX1* promoted both autonomous and non-autonomous endothelial capillary tube formation as compared to vector expressing control cells. Similarly, increased HIF1-α protein was observed in both cells that express wild-type or mutant *FJX1* as compared to control cells. This may be because FJX1 is not a kinase, or perhaps these specific mutations in FJX1 do not prohibit kinase activity. It would be surprising if FJX1 was not a kinase, as the fj kinase residues are completely conserved among numerous organisms. However, Strutt and colleagues have reported evidence that fj need not be secreted to be functional, while Probst et al. have reported that FJX1 is functional as a secreted protein. Perhaps mammalian homologues have acquired additional function through evolution. Regardless, much more work will be required to determine if FJX1 is indeed a kinase, and if so, what is the biological relevance of its kinase activity.

We also performed proteomic analysis on the flow through fraction of conditioned media from SW480^{VEC} and SW480^{FJX1} cell lines to identify the secreted angiogenic peptide(s) regulated by FJX1 and HIF1-α. We found increased expression of peptides from annexin A1, tenascin C, and InaD-like

proteins. Annexin A1 is a relatively small secreted protein that has been historically thought of as anti-inflammatory. However, the generation of *annexin A1* KO mice revealed an important role in angiogenesis and wound healing [107,108]. We detected higher levels of secreted annexin A1 in conditioned media from *FJX1* transduced cells, but failed to detect species in the flow through fraction that contained the pro-angiogenic stiumulus. Again, it is possible that annexin a1 undergoes a modification into smaller peptides undetectable by the available regents. Tenascin C is a huge glycoprotein that is secreted into the extracelluar space, and is thought to play a role in tissue remodeling. Ina-D like protein is a scaffolding protein found localized to tight junctions. Neither tenascin C or ina-d like proteins have been described as active small peptides in the literature, but it will be of interest to determine if their expression is altered in FJX1 transduced cells. Further we could use siRNA mediated inhibition of all these potential candidates (VEGFA, annexin A1, tenascin C, and Ina-D) in the FJX1 transduced cells to see if capillary tube formation is reliant on their expression.

GENE EXPRESSION ANALYSIS OF SW480 CELL LINES AFTER ALTERED *FJX1* AND *HIF1A* EXPRESSION.

Introduction

Four jointed box 1 (FJX1) is the human orthologue of *four jointed (fj)* in *Drosophila*. Wingless, Jak/Stat, Notch, and Fat signaling have been shown to influence *fj* expression, and *fj* in turn can regulate expression of notch ligands, wingless, and fat [54,58,59]. Fj has also been associated with the hippo tumor suppressor pathway through its effects on fat and dachsous signaling. Studies on the role of mammalian FJX1 in signaling pathways have been extremely limited. One report has suggested that *FJX1* is influenced by Notch signaling, citing the observation of increased *FJX1* promoter activity after transfection with Notch1, 2, or 3 [63] but we have failed to reproduced these results in our laboratory (data not shown). McNeill and colleagues have provided some data that the ft/ds/fj cassette may be conserved in mammals [66] . There have also been a variety of microarray datasets that suggest various cytokines can influence *FJX1* expression including inflammatory stimuli such as TNF-α, IL-1 and LPS [81-83]. We have demonstrated that expression of FJX1 in the SW480 colorectal cancer cell line causes an increase in xenograft tumor formation associated with an increase in tumor vascularization. *In vitro*, the FJX1 specific effect on endothelial cells requires HIF1-α. In order to try to understand how FJX1 regulates HIF1-α protein levels and angiogenesis, we performed

microarray analysis on SW480 cells transduced with vector or *FJX1* and treated

with siRNA specific to *FJX1*, *HIF1A* or scrambled control.

Materials and Methods

<u>SW480 cell line microarray</u>

Microarray analysis was performed on four biological replicates of the

following cells: SW480^{VEC}, SW480^{FJX1}, SW480^{FJX1} treated with scrambled siRNA,

SW480^{FJX1} treated with *HIF1A* specific siRNA, and SW480^{FJX1} treated with *FJX1*

specific siRNA. siRNA treatment lasted a total of 96 hours, and the cells were in

serum free media for the final 24 hours in culture. RNA was extracted using the

Qiagen RNeasy Kit (Qiagen) per manufacturer's instructions. Quality of RNA

samples was assessed using an Agilent Bioanalyzer. Target generation is

performed using the Ambion WT Sense reaction kit from Affymetrix and following

the manufacturer's protocol with 130ng of intact RNA. cDNA target is then

enzymatically fragmented and end-labeled using the Affymetrix labeling reagents

according to manufacturer's protocols. The cRNA, cDNA, and fragmented and

end-labeled targets are assessed using an Agilent bioanalyzer to ensure that the

amplified targets meet the recommended smear range and to also assess

whether fragmentation and end-labeling are complete. For 3' U133 array plate,

the requisite amount of fragmented target (6ug) is then added to the hybridization

cocktail for each array. Fragmented and labeled targets in hybridization cocktail

are heat denatured, centrifuged, and then added on the appropriate Affymerix

array plate and loaded onto the Affymetrix GeneTitan. Multi Channel (MC)

platform and array plate undergo an overnight incubation/hybridization according to manufacturer's protocol. After hybridization, the array plate is washed, and stained per standard Affymetrix GeneTitan automation platform protocol instructions. After washing is complete, the arrays are scanned on the Affymetrix Gene Titan scanner. Resulting data is analyzed by Affymetrix Expression Console v. 1.3 using an RMA normalization algorithm producing log base 2 results.

The differentially expressed probes were imported into Ingenuity Pathway Analysis (IPA®, www.ingenuity.com) and analyzed for network enrichment by mapping to the IPA global molecular network by knowledge-based connectivity.

Results

Microarray analysis of SW480 cell lines.

In order to better understand the signaling pathways altered upon *FJX1* expression and subsequent *HIF1A* silencing, we performed microarray analysis on untreated SW480^{VEC} and SW480^{FJX1} cells, as well as SW480^{FJX1} cells treated with scrambled siRNA, siRNA specific to *FJX1* or siRNA specific to *HIF1A* (summary of gene changes in Table 6). Normalized mRNA levels from the experiment confirmed that the *FJX1* and *HIF1A* siRNA were effective at lowering mRNA from their respective genes (Figure 31, A and B). It should be noted that the microarray probe for *FJX1* lies in the 3' untranslated region, thus accounting for why SW480^{FJX1} mRNA levels, which were achieved by stable transduction of *FJX1* cDNA, are not increased compared to SW480^{VEC} cells (Figure 31A).

We identified 335 expression elements as differentially expressed (minimum 1.5 fold change) between SW480^{VEC} UT and SW480^{FJX1} UT cells (unadjusted p value > 0.05, Table 7).   We then conducted pathway enrichment analysis using a commercially available knowledge-based database. The collection of genes differentially expressed in SW480 cells transduced with *FJX1* were significantly enriched in a network known to regulate RNA Post-Transcriptional Modification, Cell Cycle, and Protein Synthesis (P < 0.005, Figure 32). Central nodes (defined as genes having at least four direct or indirect interactions within the network) included *cluster of differentiation 24 (CD24), extracellular signal related kinase 1/2 (ERK1/2)* and *RNA polymerase II*. When comparing SW480^{FJX1} cells treated with scrambled siRNA or siRNA specific to *FJX1* we identified 819 elements showing a 1.5 fold change between cell lines (unadjusted p value > 0.05, Table 8). Using a cutoff of 2 fold or greater the list was narrowed to 98 genes, and this list was used for pathway analysis. The top network identified was characterized by genes involved in Cardiovascular System Development and Function, Organismal Development, and Organ Morphology (P < 0.005, Figure 33). Central nodes included *cysteine-rich angiogenic inducer 61 (CYR61), p38 mitogen associated protein kinase (p38 MAPK),* and *ERK 1/2*. Finally, we compared SW480^{FJX1} cells treated with scrambled siRNA or siRNA specific to *HIF1A* and found 108 elements showing a 1.5 fold change between cell lines (unadjusted p value > 0.05, Table 9). The top network identified from these 108 was characterized by genes involved in Cellular Movement, Embryonic Development, and Cardiovascular System

Development and Function (P < 0.005, Figure 34). Central nodes included *HIF1-*

α, TGF-β, *p38 MAPK,* and *ERK 1/2*.

Table 6. **Summary of the number of genes altered between the indicated cell lines after microarray analysis**. VEC = SW480^{VEC}. FJX1 = SW480^{FJX1}. FJX1siSCR = SW480^{FJX1} cells treated with scrambled siRNA. FJX1siFJX1 = SW480^{FJX1} cells treated with FJX1 specific siRNA. FJX1siHIF1 = SW480^{FJX1} cells treated with HIF1-α specific siRNA.

CONTROL		1.5 fold change			2.0 fold change		
		UP IN CONTROL	DOWN IN CONTROL	TOTAL	UP IN CONTROL	DOWN IN CONTROL	TOTAL
VEC	FJX1	265	70	335	24	4	28
FJX1siSCR	FJX1siFJX1	342	477	819	28	70	98
FJX1siSCR	FJX1siHIF1	44	64	108	1	5	6
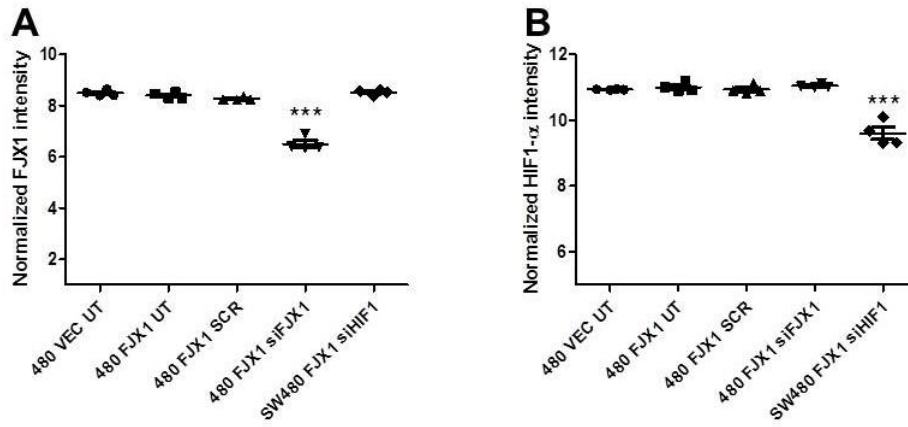
Figure 31. Validation of siRNA in cells used for microarray.

Normalized microarray signal for **(A)** *FJX1* and **(B)** *HIF1A* for cell lines as indicated.   *** = p<0.0001.
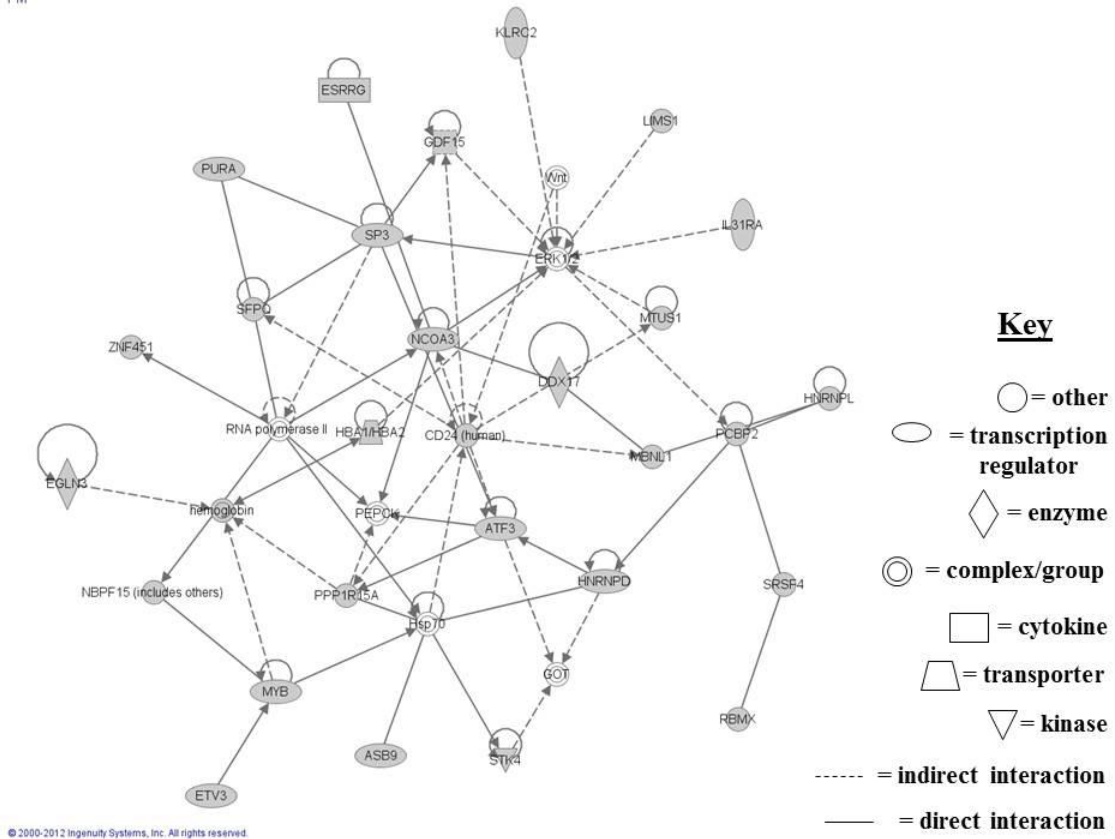
Figure 32. Top network after IPA analysis of the genes differentially expressed between SW480^{VEC} and SW480^{FJX1} cells.
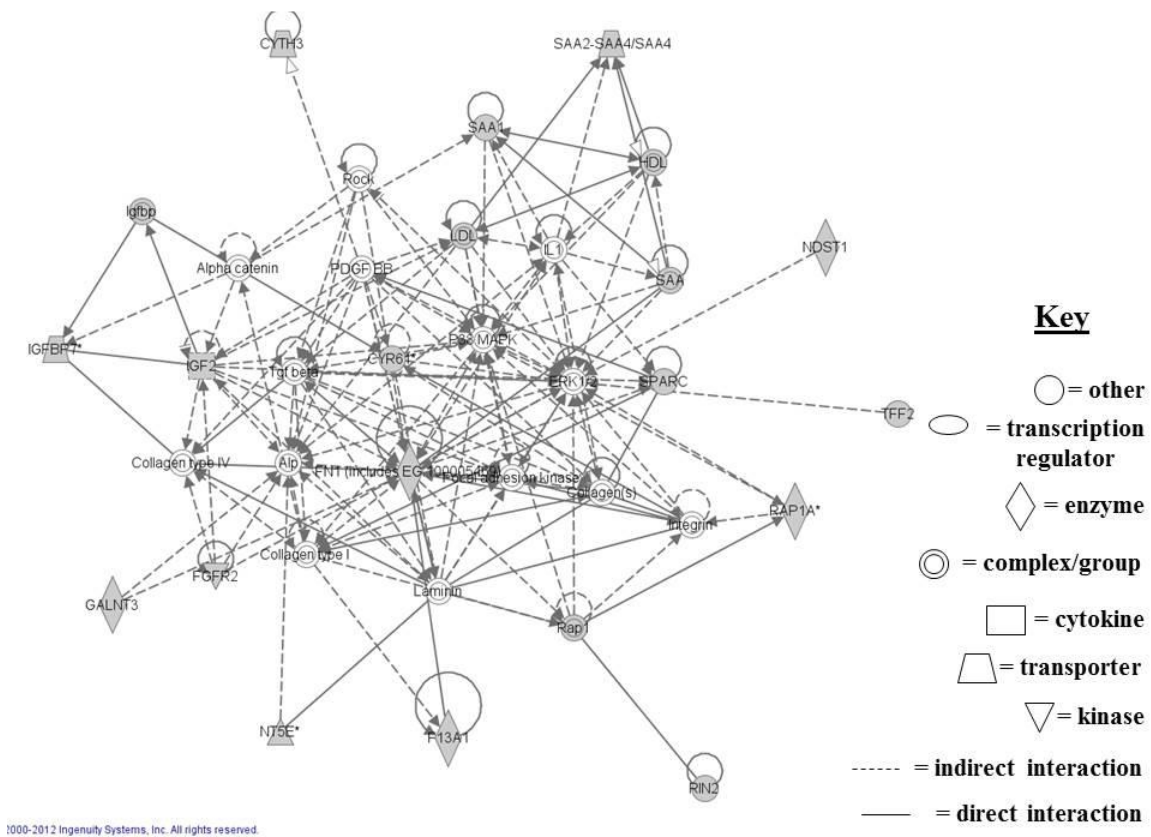
Figure 33. Top network after IPA analysis of the genes differentially expressed between SW480^{FJX1} cells treated with scrambled siRNA and SW480^{FJX1} cells treated with *FJX1* specific siRNA.

Key

◯ = other

⬭ = transcription regulator

◇ = enzyme

◎ = complex/group

▭ = cytokine

⬔ = transporter

▽ = kinase

- - - - = indirect interaction

—— = direct interaction
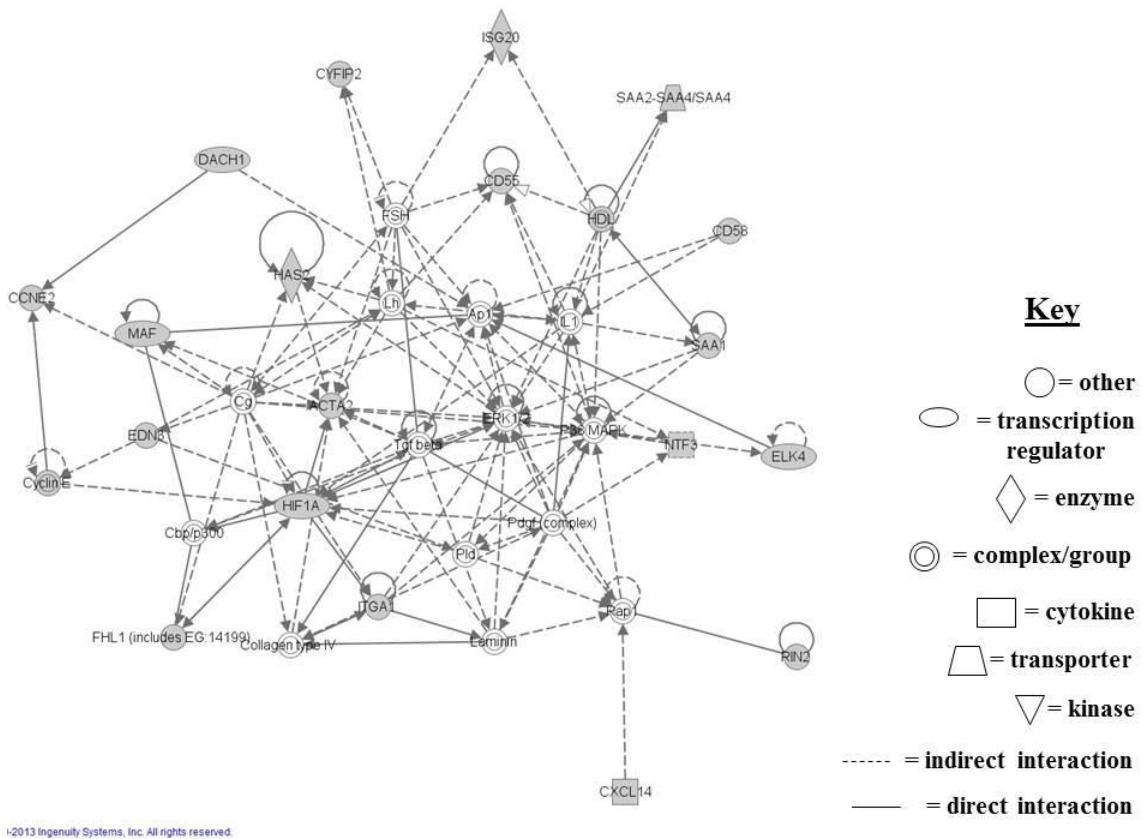
Figure 34. Top network after IPA analysis of the genes differentially expressed between SW480^FJX1 cells treated with scrambled siRNA and SW480^FJX1 cells treated with *HIF1A* specific siRNA.

111

Next, we overlapped the gene lists derived from comparison of SW480^{VEC} UT vs SW480^{FJX1} UT and SW480^{FJX1} siSCR vs SW480^{FJX1} *siFJX1*. This analysis was performed to try to identify molecules that were increased upon *FJX1* expression and subsequently silenced after *FJX1* siRNA treatment or vice versa. We identified 18 elements mapping to 17 unique genes, 6 of which exhibited opposing expression patterns based upon *FJX1* expression or silencing; *inhibin beta e, lethal (3) malignant brain tumor-like protein, CD24, nebulette, proline rich 20, and serine protease 33* (Table 10).

We also overlapped the gene lists derived from comparison of SW480^{VEC} UT vs SW480^{FJX1} UT and SW480^{FJX1} siFSCR vs SW480^{FJX1} *siHIF1A*. Our hypothesis was that genes increased by *FJX1* transduction that subsequently were inhibited after *HIF1A* siRNA would be potential candidates to analyze for their role in the endothelia phenotype. There were six genes that exhibiting significant changes in both gene lists: *CD24; serine palmitoyltransferase, long chain base subunit 3; CD55 molecule, decay accelerating factor for complement (Cromer blood group); Insulin-like growth factor binding protein-like 1; Lix1 homolog (chicken);* and *Vacuolar protein sorting 8 homolog (S. cerevisiae)* (Table 11). Of the six genes, *CD55* was the only molecule shown to be increased after *FJX1* expression and subsequently decreased upon *HIF1-α* silencing. Ongoing experiments will be required to see if *CD55* plays a role in the pro-angiogenic phenotype associated with such gene changes in SW480 cells.

Table 10. Genes found to be significantly altered in both SW480^{VEC} vs SW480^{FJX1} and SW480^{FJX1} siSCR vs SW480^{FJX1} *siFJX1* gene lists. Gene symbol, title and fold change for the 19 elements is shown. Negative and positive values reflect a decrease and increase in gene expression respectively.

Gene Symbol	Gene Title	Fold-Change (FJX1 UT vs. VEC UT)	Fold-Change (FJX1 SIFJX1 vs. FJX1 SCR)
AK5	adenylate kinase 5	1.60558	2.08229
EREG	epiregulin	1.81392	1.61777
FRMD5	FERM domain containing 5	1.57505	2.3398
INHBE	inhibin, beta E	1.93314	-4.16243
L3MBTL3	l(3)mbt-like 3 (Drosophila)	1.60835	-1.52025
OLR1	oxidized low density lipoprotein receptor 1	1.56132	1.93603
PRSS23	Protease, serine, 23	1.75382	1.85366
SPTLC3	serine palmitoyltransferase, long chain base subunit 3	1.58785	1.73475
CBFA2T2	core-binding factor, runt domain, alpha subunit 2; translocated to, 2	-1.67661	-1.52391
CD24	CD24 molecule	-1.55722	1.96449
IGF2 /// INS-IGF2	insulin-like growth factor 2 (somatomedin A) /// INS-IGF2 readthrough transcript	-1.7717	-2.39021
METTL3	methyltransferase like 3	-1.57098	-1.55455
MYH7B	myosin, heavy chain 7B, cardiac muscle, beta	-2.26467	-2.03838
NEBL	nebulette	-1.58306	1.51457
PCP4	Purkinje cell protein 4	-2.24821	-2.37463
PRR20A /// PRR20B /// PRR20C /// PRR20D /// PRR20E	proline rich 20A /// proline rich 20B /// proline rich 20C /// proline rich 20D /// pro	-1.64367	3.3548
PRSS33	protease, serine, 33	-1.61552	3.32338
ROBO1	Roundabout homolog 1 (Drosophila)	-1.52572	-1.61176

Table 11. Genes found to be significantly altered in both SW480^{VEC} vs SW480^{FJX1} and SW480^{FJX1} siSCR vs SW480^{FJX1} *siHIF1A* gene lists. Gene symbol, title and fold change for the 19 elements is shown. Negative and positive values reflect a decrease and increase in gene expression respectively.

Gene Symbol	Gene Title	Fold-Change (FJX1 UT vs. VEC UT)	Fold-Change (FJX1 SIHIF vs. FJX1 SCR)
SPTLC3	serine palmitoyltransferase, long chain base subunit 3	1.58785	2.16876
CD55	CD55 molecule, decay accelerating factor for complement (Cromer blood group)	1.7142	-1.50861
IGFBPL1	Insulin-like growth factor binding protein-like 1	-1.70416	1.68164
LIX1	Lix1 homolog (chicken)	-2.03114	1.57
VPS8	Vacuolar protein sorting 8 homolog (S. cerevisiae)	-1.78746	-1.64178
CD24	CD24 molecule	-1.55722	1.55706

.

Discussion

In efforts to understand signaling patterns altered by expression of *FJX1*
we performed microarray analysis on the SW480 cell lines. The top genes
altered by *FJX1* expression were enriched in genes involved in RNA post
translational modification, cell cycle, and protein synthesis. As neither FJX1 nor
Drosophila fj have been found in the nucleus, we predict that FJX1 would
function downstream of transcription. By far the most robust changes in gene
expression were between SW480$^{\text{FJX1}}$ cells treated with scrambled or *FJX1*
specific siRNA. Raw expression data shows that *FJX1* mRNA was significantly
silenced after *FJX1* siRNA treatment of the SW480$^{\text{FJX1}}$, so much so that these
cells had lower expression that untreated SW480$^{\text{VEC}}$ control cells, suggesting
that cultured cell lines did express endogenous *FJX1* but at a level below our
limit of detection. Interestingly, genes altered with this treatment were involved in
cardiovascular system development and function. These data nicely correlate
with the angiogenesis driven biological effect we observe upon *FJX1*
manipulation. Additionally, the top network associated with gene changes
included *cysteine-rich angiogeneic inducer (CYR61)* as a central node, a gene
we also found to change concordantly with *FJX1* expression in our human CRC
datasets. Further, *CYR61* expression can be induced by hypoxia treatment or by
PGE$_2$ in various cell lines [109,110]. The known role of CYR61 in promoting
angiogenesis, and its association with inflammatory genes make it an exciting
candidate to analyze in our cell lines.

In chapter IV we described our findings that conditioned media from

SW480 cells transduced with *FJX1* promotes endothelial capillary tube formation *in vitro* in a HIF1-α dependent manner. Thus we hypothesized that global gene expression analysis of SW480 transduced with *FJX1* and subsequently treated with *HIF1A* siRNA might provide insight into potential candidates associated with this phenotype. There was one gene that fit this criteria*; CD55/decay accelerating factor (DAF)*. CD55 is a glycoprotein involved in the complement cascade; binding of CD55 to complement causes their rapid decay. Although the predominant isoform is transmembrane bound, smaller soluble peptides have been identified, but not attributed a biological function. *CD24* was uniquely found in all three gene lists: *CD24* was downregulated upon *FJX1* expression and upregulated with both *FJX1* and *HIF1A* specific siRNA.   Increased expression of *CD24* has been demonstrated in CRC [111,112] however studies in breast cancer have described putative cancer stem cells as being CD44+/CD24- [113]. Interestingly, CD44+/CD24- cells grow more rapidly *in vivo* and are associated with increased *COX-2* expression[114]. Further work will be needed to determine both the level of *CD55* and *CD24* mRNA and protein in CRC cell lines, and if they contribute to the biological phenotypes we observe *in vitro* and *in vivo*. Nevertheless, the global analysis of gene changes in the SW480 cell lines will provide a framework for reference of potential signaling pathways that are altered upon *FJX1* expression.

CHAPTER VII.

SUMMARY AND FUTURE DIRECTIONS

There is substantial experimental evidence in both mouse models and in humans documenting the effectiveness of non-steroidal anti-inflammatory drugs, particularly selective COX-2 inhibitors, in reducing both colorectal tumor formation and progression [24,25,115,116]. The studies described herein have contributed to our understanding of the biological responses to one such selective COX-2 inhibitor, celecoxib, by analyzing human tumor gene expression *in vivo*. To date this is the first genome wide analysis of human rectal tumors in response to celecoxib treatment *in vivo*. Through this screen we were able to identify a novel protein, Four jointed box 1, that was previously uncharacterized in human tumor biology. We generated a variety of reagents, including expression vectors and specific polyclonal antibodies that are applicable to ELISA, immunoblotting, immunofluorescence, and immunohistochemistry. Whereas previous studies had only analyzed *FJX1* mRNA, we have provided the first evidence that FJX1 protein expression is increased in the epithelial cell compartment of advanced colorectal cancers. It will be interesting to determine if protein levels are indeed increased in some of these other cancers, and if our antibody can demonstrate epithelial expression. Also, as we were only able to screen a dozen or so human tumor samples using FJX1 IHC, it will be of use to stain more tissues to strengthen our current data. Since FJX1 protein is a secreted molecule, FJX1 protein levels might be detectable in patient blood or urinary samples and serve as a biomarker for colorectal or other cancers.

117

Interestingly, despite our findings that rectal tumors expressed moderate to high levels of FJX1 protein, we were unable to detect endogenous FJX1 protein expression in cultured colon cancer, human embryonic kidney or endothelial cells, and thus were unable to demonstrate an effect of celecoxib on *FJX1* expression. Our ability to reliably detect endogenous FJX1 in the epithelial cells of colon tumor specimens, but not in immortalized colon cancer cell lines suggests that expression of *FJX1* may require paracrine signaling or matrix interactions not supported through standard cell culture conditions. Since we also failed to detect expression of FJX1 in SW480 vector-transduced cells grown as subcutaneous tumor xenografts, but detected FJX1 protein in human colorectal tumors, it is highly likely that some component of the colonic niche is crucial in maintaining FJX1 expression in colonic cells. Similarly, despite COX-2 expression being upregulated in the majority of CRC, expression in cell lines is much more limited. One study identified a common sequence in both the *COX-2* and *FJX1* promoters although the factors binding this type of element are unknown. Perhaps there is a common paracrine factor that regulates expression of both *COX-2* and *FJX1 in vivo* that is absent from cell cultures.

We postulated that our observation that patients with higher *FJX1* mRNA expression have worse survival outcomes is related to the pro-angiogenic effects of *FJX1* on tumor formation. In both xenograft and inflammatory/carcinogen induced mouse models of tumorigenesis we found an association between vascularization and *FJX1* expression; colonic sections and tumor xenografts lacking FJX1 had fewer blood vessels. It is well recognized that without

118

angiogenesis, tumors remain limited in both size and location, thus posing limited threat to the overall health of the individual [80]. Converging evidence supports the role of axon-guidance cues in both normal vasculature development (for review, [117]) and tumor associated angiogenesis [118,119]. *FJX1* is highly expressed throughout the central nervous system during development and in the adult mouse [64,65]. In *Fjx1* KO mice, specific subsets of hippocampal neurons exhibit either increased dendrite length or decreased arborization [65]. The observation that neuronal cues (neuropilins, ephrins, netrins, slits) are also expressed in certain tumors raised questions as to how these proteins might influence tumor development. Our observations suggest that FJX1 may represent another protein that exhibits a dual function in neuron/endothelial biology.

In vitro, conditioned media from *FJX1* expressing cells was able to stimulate endothelial capillary tube formation. This non-autonomous phenotype was maintained even upon exclusion of secreted FJX1 protein, suggesting that *FJX1* regulates secretion of other angiogenic factors. The cell lines used in our studies, SW480, KM12C and HEK293T, do not express detectable levels of COX-2, arguing that the pro-angiogenic phenotype is FJX1 specific and not due to previously described angiogenic effects of COX-2 [40]. We also found strong correlations between expression of *FJX1* and known angiogenic genes in two human colorectal cancer datasets, supporting our experimental data showing FJX1 regulates tumor angiogenesis.

We detected increased HIF1-α protein in FJX1 transduced cells and

119

experimentally linked HIF1-α levels to increased capillary tube formation. HIF1-α

has been shown to induce pro-angiogenic programs through modulation of a

variety of molecules including but not limited to VEGF, FLT1, ANGPT2, THBS1

and CYR61 [87-89,91,95,96]. Some of these proteins can undergo proteolytic

processing into smaller peptides that are functionally distinct from the full length

form, i.e. VEGF and COL18A1 [99,100]. Although we detected increased

expression of the HIF1-α-regulated VEGF and annexin A1 in conditioned media

from *FJX1* transduced cell lines, these proteins were excluded from the flow

through fraction of conditioned media that contained the angiogenic stimulus

associated with *FJX1* expression.   We have argued that smaller processed

forms of VEGF or annexin A1 might not be detectable with the antibodies used in

our study, but may contribute to the endothelial phenotype. Although one could

argue that this may also be true for FJX1, our proteomics data on the flow

through fraction only detected annexin A1 peptides, but not VEGF or FJX1.

Inhibition of *annexin A1* in our *FJX1* transduced cell lines will help determine if

annexin A1 does contribute to the capillary tube phenotype.

We found that FJX1 increases HIF1-α protein stability. Post

transcriptionally, HIF1- α is tightly regulated by oxygen levels in the cell, as

molecular oxygen is absolutely required for PHD and FIH-mediated modification

of HIF1-α. We will need to assess if cellular oxygen levels are altered in our

FJX1 expressing cells. Altered cellular oxygen levels may be due to an alteration

of mitochondrial function which has been proposed to interfere with PHD activity

in either a ROS dependent or independent fashion. The addition of mitochondrial

inhibitors (i.e. sodium azide) or anti-oxidant reagents (i.e. n-acetyl cysteine) to our cell lines will help us tease out where FJX1 may be limiting the ability to degrade HIF1-α. It will also be necessary to determine if FJX1 regulates the interaction of HIF1-α with components of its degradation complex, including VHL.

Our FJX1-specific antibodies allowed us to characterize FJX1 localization and processing. Despite the development of commercially available antibodies since the onset of these studies, our reagents seem much more specific and widely effective thereby enabling us to characterize human FJX1. Like *Drosophila* fj [56], human FJX1 protein is found to localize to the Golgi apparatus where it is processed by glycosylation and phosphorylation, before secretion. It is interesting that fj retains function in a Golgi tethered form [56] while murine FJX1 was shown to function as a secreted protein [65]. In our experiments, we found that FJX1 induces secretion of other molecules that were responsible for effects on endothelial cells *in vitro*. Expression of *FJX1* in *Drosophila* failed to show any activity (David Strutt, personal communication), which may be due to a divergence of sequence or perhaps altered function altogether. The residues in fj that are required for kinase activity are completed conserved across numerous species, including vertebrate. Mutation of these conserved regions in FJX1 did not affect the ability of FJX1 to stimulate endothelial cells or increase HIF1-α protein. Thus more experimental testing will be required if FJX1 is indeed a kinase, and if so what domains are required for function.

In conclusion, we have identified a novel, pro-angiogenic protein in colorectal carcinoma. Our discovery of *FJX1* as a potential COX-2 regulated

gene *in vivo* is of particular interest since numerous studies show the benefits of COX-2 inhibition in the formation and progression of CRC. The ability of FJX1 protein to enhance angiogenesis is particularly intriguing, especially if this biological function holds true in other cancers where increased *FJX1* mRNA has been observed. The large amount of expression data from our FJX1 manipulated cell lines provides a wide array of potential mechanisms to explore to help explain the biological function of FJX1.

Table 1. Genes inhibited in human rectal tumor biopsies after celecoxib treatment. Affymetrix probe ID, Gene ID, symbol and name for the 96 expression elements inhibited after celecoxib treatment.

Affymetrix Probe ID	Entrez Gene ID	Gene Symbol	Gene Name
219249_s_at	60681	FKBP10	FK506 binding protein 10, 65 kDa
242444_at	114904	C1QTNF6	C1q and tumor necrosis factor related protein 6
230281_at	123775	C16orf46	chromosome 16 open reading frame 46
240258_at	2023	ENO1	enolase 1
218410_s_at	283871	PGP	phosphoglycolate phosphatase
223001_at	58505	OSTC	oligosaccharyltransferase complex subunit
230440_at	84627	ZNF469	zinc finger protein 469
219785_s_at	79791	FBXO31	F-box protein 31
241903_at		NA	
221932_s_at	51218	GLRX5	glutaredoxin 5
213230_at	30850	CDR2L	cerebellar degeneration-related protein 2-like
228655_at		NA	
201052_s_at	9491	PSMF1	proteasome (prosome, macropain) inhibitor subunit 1 (PI31)
241392_at	55254	TMEM39A	transmembrane protein 39A
225484_at	95681	TSGA14	testis specific, 14
222768_s_at	51605	TRMT6	tRNA methyltransferase 6 homolog (S. cerevisiae)
205406_s_at	53340	SPA17	sperm autoantigenic protein 17
218739_at	51099	ABHD5	abhydrolase domain containing 5
217831_s_at	55968	NSFL1C	NSFL1 (p97) cofactor (p47)
1565644_at		NA	
206514_s_at		NA	
223748_at	83959	SLC4A11	solute carrier family 4, sodium borate transporter, member 11
201695_s_at		NP	
210187_at	2280	FKBP1A	FK506 binding protein 1A, 12kDa
218809_at	80025	PANK2	pantothenate kinase 2
217958_at	51399	TRAPPC4	trafficking protein particle complex 4
217042_at	51109	RDH11	retinol dehydrogenase 11 (all-trans/9-cis/11-cis)
212072_s_at	1457	CSNK2A1	casein kinase 2, alpha 1 polypeptide
219324_at		NA	
226276_at	153339	TMEM167A	transmembrane protein 167A
225819_at	84897	TBRG1	transforming growth factor beta regulator 1

236901_at		NA	
213419_at	323	APBB2	amyloid beta (A4) precursor protein-binding, family B, member 2
1555778_a_at	10631	POSTN	periostin, osteoblast specific factor
1558487_a_at	222068	TMED4	transmembrane emp24 protein transport domain containing 4
225648_at	140901	STK35	serine/threonine kinase 35
57703_at	205564	SENP5	SUMO1/sentrin specific peptidase 5
238542_at	80328	ULBP2	UL16 binding protein 2
227628_at	493869	GPX8	glutathione peroxidase 8 (putative)
209596_at	25878	MXRA5	matrix-remodelling associated 5
218840_s_at	55191	NADSYN1	NAD synthetase 1
225196_s_at	64949	MRPS26	mitochondrial ribosomal protein S26
232150_at		NA	
213425_at	7474	WNT5A	wingless-type MMTV integration site family, member 5A
222040_at	3178	HNRNPA1	heterogeneous nuclear ribonucleoprotein A1
220969_s_at		NA	
208823_s_at	5127	PCTK1	cyclin-dependent kinase 16
205990_s_at	7474	WNT5A	wingless-type MMTV integration site family, member 5A
204327_s_at	7753	ZNF202	zinc finger protein 202
213799_s_at	5786	PTPRA	protein tyrosine phosphatase, receptor type, A
231227_at		NA	
235588_at	157570	ESCO2	establishment of cohesion 1 homolog 2 (S. cerevisiae)
223278_at	2706	GJB2	gap junction protein, beta 2, 26kDa
200825_s_at	10525	HYOU1	hypoxia up-regulated 1
201692_at	10280	SIGMAR1	sigma non-opioid intracellular receptor 1
216175_at		NA	
210809_s_at	10631	POSTN	periostin, osteoblast specific factor
218357_s_at	26521	TIMM8B	translocase of inner mitochondrial membrane 8 homolog B (yeast)
203325_s_at	1289	COL5A1	collagen, type V, alpha 1
219522_at	24147	FJX1	four jointed box 1 (Drosophila)
220002_at	55083	KIF26B	kinesin family member 26B
214074_s_at	2017	CTTN	cortactin
203459_s_at	64601	VPS16	vacuolar protein sorting 16 homolog (S. cerevisiae)
201715_s_at	22985	ACIN1	apoptotic chromatin condensation inducer 1
226572_at	30837	SOCS7	suppressor of cytokine signaling 7
218159_at	65992	DDRGK1	DDRGK domain containing 1
225554_s_at	51434	ANAPC7	anaphase promoting complex subunit 7
226899_at	219699	UNC5B	unc-5 homolog B (C. elegans)

235511_at		NA	
234111_at		NA	
205543_at	22824	HSPA4L	heat shock 70kDa protein 4-like
239228_at		NA	
212691_at	23511	NUP188	nucleoporin 188kDa
222380_s_at	10016	PDCD6	programmed cell death 6
1556055_at		NA	
200874_s_at	10528	NOP56	NOP56 ribonucleoprotein homolog (yeast)
209246_at	10061	ABCF2	ATP-binding cassette, sub-family F (GCN20), member 2
212624_s_at	1123	CHN1	chimerin (chimaerin) 1
215011_at	8420	SNHG3	small nucleolar RNA host gene 3 (non-protein coding)
1562352_at		NA	
219709_x_at	65990	FAM173A	family with sequence similarity 173, member A
1565786_x_at	645566	FLJ45482	hypothetical LOC645566
219678_x_at	64421	DCLRE1C	DNA cross-link repair 1C
230469_at	219790	RTKN2	rhotekin 2
238732_at	255631	COL24A1	collagen, type XXIV, alpha 1
221637_s_at	79081	C11orf48	chromosome 11 open reading frame 48
236250_at	172	AFG3L1	AFG3 ATPase family gene 3-like 1 (S. cerevisiae)
206336_at	6372	CXCL6	chemokine (C-X-C motif) ligand 6 (granulocyte chemotactic protein 2)
217841_s_at	51400	PPME1	protein phosphatase methylesterase 1
232278_s_at	55635	DEPDC1	DEP domain containing 1
225649_s_at	140901	STK35	serine/threonine kinase 35
233216_at	340481	ZDHHC21	zinc finger, DHHC-type containing 21
221598_s_at	9442	MED27	mediator complex subunit 27
210532_s_at	9556	C14orf2	chromosome 14 open reading frame 2
1556111_s_at		NA	
237486_at		NA	

Table 2. Genes stimulated in human rectal tumor biopsies after celecoxib treatment. Affymetrix probe ID, Gene ID, symbol and name for the 96 expression elements stimulated after celecoxib treatment.

Affymetrix Probe ID	Entrez Gene ID	Gene Symbol	Gene Name
201369_s_at	678	ZFP36L2	zinc finger protein 36, C3H type-like 2
239066_at		NA	
214156_at	25924	MYRIP	myosin VIIA and Rab interacting protein
226525_at	9262	STK17B	serine/threonine kinase 17b
223469_at	54858	PGPEP1	pyroglutamyl-peptidase
225207_at	5166	PDK4	pyruvate dehydrogenase kinase, isozyme 4
221756_at	113791	PIK3IP1	phosphoinositide-3-kinase interacting protein 1
219195_at	10891	PPARGC1A	peroxisome proliferator-activated receptor gamma, coactivator 1 alpha
229146_at	136895	C7orf31	chromosome 7 open reading frame 31
236235_at	83737	ITCH	itchy E3 ubiquitin protein ligase homolog
205066_s_at	5167	ENPP1	ectonucleotide pyrophosphatase/phosphodiesterase 1
225498_at	128866	CHMP4B	chromatin modifying protein 4B
201368_at		ZFP36L2	
209221_s_at	9885	OSBPL2	oxysterol binding protein-like 2
213268_at	23261	CAMTA1	calmodulin binding transcription activator 1
201367_s_at		ZFP36L2	
210482_x_at	5607	MAP2K5	mitogen-activated protein kinase kinase 5
223169_s_at	58480	RHOU	ras homolog gene family, member U
205960_at	5166	PDK4	pyruvate dehydrogenase kinase, isozyme 4

126

203719_at	2067	ERCC1	excision repair cross-complementing rodent repair deficiency, complementation group 1
205997_at	10863	ADAM28	a disintegrin and metalloproteinase domain 28
1553704_x_at	163049	ZNF791	zinc finger protein 791
201466_s_at	3725	JUN	jun oncogene
239934_x_at		NA	
225380_at	91461	SGK493 (PKDCC)	protein kinase domain containing, cytoplasmic homolog
229026_at	56990	CDC42SE2	CDC42 small effector 2
205094_at	5193	PEX12	peroxisomal biogenesis factor 12
219132_at	57161	PELI2	pellino homolog 2
223130_s_at	29116	MYLIP	myosin regulatory light chain interacting protein
228788_at	29799	YPEL1	yippee-like 1
213385_at	1124	CHN2	chimerin (chimaerin) 2
201360_at	1471	CST3	cystatin C
216871_at	23390	ZDHHC17	zinc finger, DHHC-type containing 17
212929_s_at		NA	
202080_s_at	22906	TRAK1	trafficking protein, kinesin binding 1
222891_s_at	53335	BCL11A	B-cell CLL/lymphoma 11A (zinc finger protein)
225130_at	54764	ZRANB1	zinc finger, RAN-binding domain containing 1
219801_at	80778	ZNF34	zinc finger protein 34
215315_at	256051	ZNF549	zinc finger protein 549
211504_x_at	9475	ROCK2	Rho-associated, coiled-coil containing protein kinase 2
215559_at	368	ABCC6	ATP-binding cassette, sub-family C (CFTR/MRP), member 6
226470_at	2686	GGT7	gamma-glutamyltransferase 7
229984_at	56986	DTWD1	DTW domain containing 1
211370_s_at	5607	MAP2K5	mitogen-activated protein kinase kinase 5

223044_at	30061	SLC40A1	solute carrier family 40 (iron-regulated transporter), member 1
241962_at		NA	
1552455_at	158471	PRUNE2	prune homolog 2
223283_s_at	10194	TSHZ1	teashirt zinc finger homeobox 1
205236_x_at	6649	SOD3	superoxide dismutase 3, extracellular
203187_at	1793	DOCK1	dedicator of cytokinesis 1
225132_at	26224	FBXL3	F-box and leucine-rich repeat protein 3
1558293_at	23285	KIAA1107	KIAA1107
223897_at	91661	ZNF765	zinc finger protein 765
232336_at	57643	ZSWIM5	zinc finger, SWIM-type containing 5
201236_s_at	7832	BTG2	BTG family, member 2
203697_at	2487	FRZB	frizzled-related protein
219497_s_at	53335	BCL11A	B-cell CLL/lymphoma 11A (zinc finger protein)
226555_at	54891	INO80D	INO80 complex subunit D
228503_at		NA	
219548_at	7564	ZNF16	zinc finger protein 16
1553375_at	114781	BTBD9	BTB (POZ) domain containing 9
226679_at	284129	SLC26A11	solute carrier family 26, member 11
213263_s_at	5094	PCBP2	poly(rC) binding protein 2

Table 7. Probeset ID, gene symbol, refseq transcript ID and fold change from microarray analysis of SW480^{VEC} versus SW480^{FJX1} colon cancer cells.

Probeset ID	Gene Symbol	RefSeq Transcript ID	Fold-Change (FJX1 UT vs. VEC UT)
229777_PM_at	CLRN3	NM_152311	-3.03735
234989_PM_at	---	---	-2.79504
227062_PM_at	---	---	-2.57087
205347_PM_s_at	TMSB15A	NM_021992	-2.48453
236752_PM_at	---	---	-2.36989
201667_PM_at	GJA1	NM_000165	-2.35028
215795_PM_at	MYH7B	NM_020884	-2.26467
236114_PM_at	---	---	-2.2604
229899_PM_s_at	NCRNA00275	NR_003604 /// NR_003605 /// NR_003606 /// NR_036658 /// NR_036659	-2.24961
205549_PM_at	PCP4	NM_006198	-2.24821
205267_PM_at	POU2AF1	NM_006235	-2.24541
236610_PM_at	---	---	-2.21907
218162_PM_at	OLFML3	NM_020190	-2.21508
231199_PM_at	---	---	-2.20488
202831_PM_at	GPX2	NM_002083	-2.19997
1556606_PM_at	NAV2	NM_001111018 /// NM_001111019 /// NM_145117 /// NM_182964	-2.18961
232528_PM_at	---	---	-2.13577
229147_PM_at	RASSF6	NM_177532 /// NM_201431	-2.09525
235028_PM_at	---	---	-2.07442
242671_PM_at	---	---	-2.0559
240690_PM_at	---	---	-2.0495
236163_PM_at	LIX1	NM_153234	-2.03114
1556331_PM_a_at	---	---	-2.0198
238883_PM_at	---	---	-2.01325

243541_PM_at	IL31RA	NM_139017	-1.99815
206002_PM_at	GPR64	NM_001079858 /// NM_001079859 /// NM_001079860 /// NM_001184833 /// NM_001184834 /// NM	-1.96597
236961_PM_at	---	---	-1.95339
241425_PM_at	NUPL1	NM_001008564 /// NM_014089	-1.93167
240452_PM_at	GSPT1	NM_001130006 /// NM_001130007 /// NM_002094	-1.92388
233303_PM_at	---	---	-1.91824
239653_PM_at	---	---	-1.91582
232979_PM_at	---	---	-1.91179
223746_PM_at	STK4	NM_006282	-1.90884
242918_PM_at	NASP	NM_001195193 /// NM_002482 /// NM_152298	-1.90822
243768_PM_at	---	---	-1.90306
237992_PM_at	---	---	-1.89083
235693_PM_at	---	---	-1.88934
215599_PM_at	GUSBP3	NR_027386	-1.88831
232347_PM_x_at	---	---	-1.88548
239811_PM_at	---	---	-1.88479
230256_PM_at	C1orf104	NM_001039517	-1.88323
230712_PM_at	NBPF1	NM_017940	-1.8774
242837_PM_at	SFRS4	NM_005626	-1.87292
213517_PM_at	PCBP2	NM_001098620 /// NM_001128911 /// NM_001128912 /// NM_001128913 /// NM_001128914 /// NM	-1.85011
209458_PM_x_at	HBA1 /// HBA2	NM_000517 /// NM_000558	-1.8429
243435_PM_at	KCNQ1OT1	NR_002728	-1.84055
230332_PM_at	ZCCHC7	NM_032226	-1.82788
1552423_PM_at	ETV3	NM_001145312 /// NM_005240	-1.82479
1557527_PM_at	---	---	-1.8186

235172_PM_at	---	---	-1.81355
225667_PM_s_at	FAM84A	NM_145175	-1.81051
242110_PM_at	---	---	-1.80345
206488_PM_s_at	CD36	NM_000072 /// NM_001001547 /// NM_001001548 /// NM_001127443 /// NM_001127444	-1.80282
222310_PM_at	SFRS15	NM_001145444 /// NM_001145445 /// NM_020706	-1.80274
211653_PM_x_at	AKR1C2	NM_001135241 /// NM_001354 /// NM_205845	-1.79476
239917_PM_at	VPS8	NM_001009921 /// NM_015303	-1.78746
229467_PM_at	PCBP2	NM_001098620 /// NM_001128911 /// NM_001128912 /// NM_001128913 /// NM_001128914 /// NM	-1.78444
236229_PM_at	---	---	-1.78304
233300_PM_at	---	---	-1.77553
229434_PM_at	---	---	-1.77548
202409_PM_at	IGF2 /// INS-IGF2	NM_000612 /// NM_001007139 /// NM_001042376 /// NM_001127598 /// NR_003512	-1.7717
204561_PM_x_at	APOC2	NM_000483	-1.77042
205348_PM_s_at	DYNC1I1	NM_001135556 /// NM_001135557 /// NM_004411	-1.77011
206785_PM_s_at	KLRC1 /// KLRC2	NM_002259 /// NM_002260 /// NM_007328 /// NM_213657 /// NM_213658	-1.76422
241865_PM_at	---	---	-1.76234
212980_PM_at	USP34	NM_014709	-1.75969
205506_PM_at	VIL1	NM_007127	-1.75953

		NM_001136007 /// NM_001136008 /// NM_001136009 /// NM_001136010 /// NM_001136011 ///	
202489_PM_s_at	FXYD3	NM	-1.75854
241786_PM_at	---	---	-1.75822
242121_PM_at	NCRNA00182	NR_028379	-1.75602
214375_PM_at	PPFIBP1	NM_003622 /// NM_177444	-1.75598
241905_PM_at	PIK3C2A	NM_002645	-1.75475
229193_PM_at	LUC7L3	NM_006107 /// NM_016424	-1.75458
230964_PM_at	FREM2	NM_207361	-1.75257
237591_PM_at	NCRNA00173	NR_027345 /// NR_027346	-1.74915
243489_PM_at	---	---	-1.74248
228455_PM_at	RBM15	NM_022768	-1.74161
230099_PM_at	---	---	-1.74055
242233_PM_at	---	---	-1.73861
205431_PM_s_at	BMP5	NM_021073	-1.73747
242389_PM_at	LUC7L3	NM_006107 /// NM_016424	-1.73482
215012_PM_at	ZNF451	NM_001031623 /// NM_015555	-1.73275
241838_PM_at	---	---	-1.72584
210306_PM_at	L3MBTL1	NM_015478 /// NM_032107	-1.72529
236404_PM_at	---	---	-1.72378
216069_PM_at	---	---	-1.72072
232478_PM_at	---	---	-1.71932
229858_PM_at	---	---	-1.71772
244766_PM_at	LOC100271836 /// LOC440354 /// LOC595101 /// LOC641298 /// SMG1	NM_015092 /// NR_002453 /// NR_002473 /// NR_027154 /// NR_027155	-1.71696
213593_PM_s_at	TRA2A	NM_013293	-1.71253
238642_PM_at	ANKRD13D	NM_207354 /// NR_030767	-1.71205
243514_PM_at	---	---	-1.71196

205472_PM_s_at	DACH1	NM_004392 /// NM_080759 /// NM_080760	-1.70995
230885_PM_at	SPG7	NM_003119 /// NM_199367	-1.70717
217414_PM_x_at	HBA1 /// HBA2	NM_000517 /// NM_000558	-1.70587
227760_PM_at	IGFBPL1	NM_001007563	-1.70416
242550_PM_at	EIF3B	NM_001037283 /// NM_003751	-1.69214
226766_PM_at	ROBO2	NM_001128929 /// NM_002942	-1.68602
232783_PM_at	---	---	-1.68513
213931_PM_at	ID2 /// ID2B	NM_002166 /// NR_026582	-1.68098
235803_PM_at	---	---	-1.68086
205673_PM_s_at	ASB9	NM_001031739 /// NM_001168530 /// NM_001168531 /// NM_024087	-1.67782
1557810_PM_at	---	---	-1.67719
238549_PM_at	CBFA2T2	NM_001032999 /// NM_001039709 /// NM_005093	-1.67661
236907_PM_at	---	---	-1.67562
230064_PM_at	---	---	-1.67288
211980_PM_at	COL4A1	NM_001845	-1.67279
233198_PM_at	GOLGA2B	NR_024261 /// NR_036632	-1.67045
221860_PM_at	HNRNPL	NM_001005335 /// NM_001533	-1.6682
212384_PM_at	ATP6V1G2 /// BAT1	NM_004640 /// NM_080598 /// NM_130463 /// NM_138282	-1.66576
204260_PM_at	CHGB	NM_001819	-1.66094
225786_PM_at	NCRNA00201	NR_026778	-1.65919
1556568_PM_a_at	---	---	-1.65795
1557384_PM_at	ZNF131	NM_003432	-1.65457

221768_PM_at	LOC100506168	XR_110484 /// XR_110485 /// XR_110486 /// XR_112062 /// XR_112063 /// XR_112064 /// XR_	-1.64742
226318_PM_at	TBRG1	NM_032811 /// NR_016021	-1.64726
229574_PM_at	TRA2A	NM_013293	-1.64498
239040_PM_at	HNRNPD	NM_001003810 /// NM_002138 /// NM_031369 /// NM_031370	-1.64438
1562722_PM_at	PRR20A /// PRR20B /// PRR20C /// PRR20D /// PRR20E	NM_001130404 /// NM_001130405 /// NM_001130406 /// NM_001130407 /// NM_198441	-1.64367
226783_PM_at	AGXT2L2	NM_153373	-1.64162
227388_PM_at	TUSC1	NM_001004125	-1.63602
235551_PM_at	WDR4	NM_018669 /// NM_033661	-1.63564
239102_PM_s_at	---	---	-1.63552
226848_PM_at	---	---	-1.6353
243431_PM_at	---	---	-1.63503
235123_PM_at	---	---	-1.63485
239841_PM_at	---	---	-1.63469
242146_PM_at	SNRPA1	NM_003090	-1.63369
239937_PM_at	ZNF207	NM_001032293 /// NM_001098507 /// NM_003457	-1.63211
229593_PM_at	---	---	-1.63147
1556821_PM_x_at	DLEU2	NR_002612	-1.63104
217042_PM_at	RDH11	NM_016026	-1.63083
232476_PM_at	---	---	-1.62932
231848_PM_x_at	ZNF207	NM_001032293 /// NM_001098507 /// NM_003457	-1.62839
236841_PM_at	LOC100134445	XM_001720526	-1.62647
207154_PM_at	DIO3	NM_001362	-1.62509
237398_PM_at	---	---	-1.62387

243759_PM_at	SFRS15	NM_001145444 /// NM_001145445 /// NM_020706	-1.62268
225815_PM_at	CPLX2	NM_001008220 /// NM_006650	-1.62194
243608_PM_at	COG2	NM_001145036 /// NM_007357	-1.61733
1552348_PM_at	PRSS33	NM_152891	-1.61552
236368_PM_at	KIAA0368	NM_001080398	-1.61505
239027_PM_at	DOCK8	NM_001190458 /// NM_001193536 /// NM_203447	-1.61482
239516_PM_at	---	---	-1.61463
242467_PM_at	---	---	-1.61418
207981_PM_s_at	ESRRG	NM_001134285 /// NM_001438 /// NM_206594 /// NM_206595 /// NR_024099	-1.61302
205825_PM_at	PCSK1	NM_000439 /// NM_001177875 /// NM_001177876	-1.61285
227394_PM_at	NCAM1	NM_000615 /// NM_001076682 /// NM_181351	-1.61251
1557521_PM_a_at	---	---	-1.60944
230312_PM_at	---	---	-1.60637
1557081_PM_at	RBM25	NM_021239	-1.60477
236149_PM_at	---	---	-1.6035
1569540_PM_at	---	---	-1.60277
1565786_PM_x_at	FLJ45482	XR_040445 /// XR_040446 /// XR_040447	-1.59368
236428_PM_at	---	---	-1.59361
209757_PM_s_at	MYCN	NM_005378	-1.5922
228338_PM_at	C11orf93	NM_001136105	-1.59205
227952_PM_at	---	---	-1.59184
226419_PM_s_at	FLJ44342	XR_109412 /// XR_115130	-1.59042

217523_PM_at	CD44	NM_000610 /// NM_001001389 /// NM_001001390 /// NM_001001391 /// NM_001001392	-1.59008
213700_PM_s_at	---	---	-1.58934
239232_PM_at	MSI2	NM_138962 /// NM_170721	-1.58872
209006_PM_s_at	C1orf63	NM_020317	-1.58676
233599_PM_at	LOC728061	XR_040680 /// XR_040681 /// XR_040682	-1.58504
230961_PM_at	---	---	-1.58439
1559883_PM_s_at	SAMHD1	NM_015474	-1.58404
217585_PM_at	NEBL	NM_001173484 /// NM_006393 /// NM_213569	-1.58306
1556035_PM_s_at	ZNF207	NM_001032293 /// NM_001098507 /// NM_003457	-1.58238
205471_PM_s_at	DACH1	NM_004392 /// NM_080759 /// NM_080760	-1.58155
230057_PM_at	LOC285178	---	-1.57783
239219_PM_at	AURKB	NM_004217	-1.57699
240908_PM_at	LOC100507153	XR_110384	-1.57655
240221_PM_at	---	---	-1.57638
1559490_PM_at	LRCH3	NM_032773	-1.57547
222371_PM_at	---	---	-1.57507
239432_PM_at	FLJ31306	NR_029434 /// NR_029435	-1.57419
215828_PM_at	---	---	-1.57363
233539_PM_at	NAPEPLD	NM_001122838 /// NM_198990	-1.57324
1570259_PM_at	LIMS1	NM_001193482 /// NM_001193483 /// NM_001193484 /// NM_001193485 /// NM_001193488 /// NM	-1.57309
238453_PM_at	FGFBP3	NM_152429	-1.57169
242111_PM_at	METTL3	NM_019852	-1.57098

232571_PM_at	---	---	-1.56708
242447_PM_at	C3orf70	NM_001025266	-1.5664
243112_PM_at	---	---	-1.56635
1556336_PM_at	RBMX	NM_001164803 /// NM_002139 /// NR_028476 /// NR_028477	-1.56601
1561079_PM_at	ANKRD28	NM_001195098 /// NM_001195099 /// NM_015199	-1.56462
240494_PM_at	---	---	-1.56413
228173_PM_at	---	---	-1.56215
223679_PM_at	CTNNB1	NM_001098209 /// NM_001098210 /// NM_001904	-1.56152
232134_PM_at	---	---	-1.56052
1569353_PM_at	CP110	NM_014711	-1.55986
244075_PM_at	---	---	-1.55906
243282_PM_at	CCDC93	NM_019044	-1.55885
1560622_PM_at	---	---	-1.55747
204687_PM_at	PARM1	NM_015393	-1.55735
216983_PM_s_at	ZNF224	NM_013398	-1.55735
216379_PM_x_at	CD24	NM_013230	-1.55722
228912_PM_at	VIL1	NM_007127	-1.55577
1560297_PM_at	---	---	-1.55496
235190_PM_at	---	---	-1.55451
226663_PM_at	ANKRD10	NM_017664	-1.55274
242040_PM_at	GCNT7	NM_080615	-1.55248
228762_PM_at	LFNG	NM_001040167 /// NM_001040168 /// NM_001166355 /// NM_002304	-1.55154
236808_PM_at	FGFR1OP2	NM_001171887 /// NM_001171888 /// NM_015633	-1.54983
1569142_PM_at	TRIM13	NM_001007278 /// NM_005798 /// NM_052811 /// NM_213590	-1.54752
1557780_PM_at	---	---	-1.54735
244342_PM_at	PATL1	NM_152716	-1.54671
241435_PM_at	---	---	-1.54543

137

219255_PM_x_at	IL17RB	NM_018725	-1.54441
1559993_PM_at	SFXN3	NM_030971	-1.54432
232141_PM_at	U2AF1	NM_001025203 /// NM_001025204 /// NM_006758	-1.54422
204798_PM_at	MYB	NM_001130172 /// NM_001130173 /// NM_001161656 /// NM_001161657 /// NM_001161658 /// NM	-1.54325
213326_PM_at	VAMP1	NM_014231 /// NM_016830 /// NM_199245	-1.54311
240383_PM_at	UBE2D3	NM_003340 /// NM_181886 /// NM_181887 /// NM_181888 /// NM_181889 /// NM_181890 /// NM_	-1.54061
220796_PM_x_at	SLC35E1	NM_024881	-1.5402
244174_PM_at	---	---	-1.54014
1570248_PM_at	---	---	-1.53989
221973_PM_at	LOC100506076 /// LOC100506123	XR_109917 /// XR_109918 /// XR_109919 /// XR_109920 /// XR_109921 /// XR_109922 /// XR_	-1.53809
243618_PM_s_at	ZNF827	NM_178835	-1.53626
208798_PM_x_at	GOLGA8A	NM_181077 /// NR_027409	-1.53411
241699_PM_at	---	---	-1.53312
206619_PM_at	DKK4	NM_014420	-1.53236
219049_PM_at	CSGALNACT1	NM_001130518 /// NM_018371 /// NR_024040	-1.53201
232601_PM_at	---	---	-1.53014
221831_PM_at	LUZP1	NM_001142546 /// NM_033631	-1.52959
233055_PM_at	---	---	-1.52877
235511_PM_at	---	---	-1.52789

238456_PM_at	LOC100289230	NR_036530	-1.52633
209446_PM_s_at	C7orf44	NM_018224	-1.5259
213194_PM_at	ROBO1	NM_001145845 /// NM_002941 /// NM_133631	-1.52572
232291_PM_at	MIR17HG	NR_027349 /// NR_027350	-1.52529
206224_PM_at	CST1	NM_001898	-1.52523
230464_PM_at	S1PR5	NM_001166215 /// NM_030760	-1.52433
228180_PM_at	---	---	-1.52319
1560556_PM_a_at	PLEKHA8	NM_001197026 /// NM_001197027 /// NM_032639	-1.52257
239445_PM_at	---	---	-1.52253
206822_PM_s_at	L3MBTL1	NM_015478 /// NM_032107	-1.52251
226362_PM_at	---	---	-1.52158
242131_PM_at	ATP6	---	-1.52022
1557267_PM_s_at	LOC284952	XM_001126137 /// XM_001722633	-1.51949
235732_PM_at	ZNF704	NM_001033723	-1.51929
230998_PM_at	---	---	-1.51851
244648_PM_at	---	---	-1.51851
215470_PM_at	GTF2H2B	NR_033417	-1.51656
242431_PM_at	---	---	-1.51612
235879_PM_at	MBNL1	NM_021038 /// NM_207292 /// NM_207293 /// NM_207294 /// NM_207295 /// NM_207296 /// NM_	-1.51499
235314_PM_at	RPL32P3	NR_003111	-1.51422
242576_PM_x_at	N4BP2L2	NM_014887 /// NM_033111	-1.51418
219229_PM_at	SLCO3A1	NM_001145044 /// NM_013272	-1.51317
1556432_PM_at	---	---	-1.51173
230180_PM_at	---	---	-1.51108
243691_PM_at	---	---	-1.50955

221584_PM_s_at	KCNMA1	NM_001014797 /// NM_001161352 /// NM_001161353 /// NM_002247	-1.50899
233976_PM_at	---	---	-1.50884
244849_PM_at	SEMA3A	NM_006080	-1.50728
236411_PM_at	---	---	-1.50641
1565689_PM_at	---	---	-1.50435
229707_PM_at	ZNF606	NM_025027	-1.50358
242059_PM_at	---	---	-1.50245
232529_PM_at	SP3	NM_001017371 /// NM_001172712 /// NM_003111	-1.50184
238876_PM_at	---	---	-1.50183
1555372_PM_at	BCL2L11	NM_006538 /// NM_138621 /// NM_207002	-1.50165
204966_PM_at	BAI2	NM_001703	-1.50112
1553396_PM_a_at	CCDC13	NM_144719	-1.50085
244503_PM_at	---	---	-1.50019
239195_PM_at	---	---	1.50072
242313_PM_at	LOC728730	XR_109973 /// XR_112311 /// XR_115530	1.50244
1559584_PM_a_at	C16orf54	NM_175900	1.50332
228966_PM_at	PANK2	NM_024960 /// NM_153638 /// NM_153640	1.5059
204984_PM_at	GPC4	NM_001448	1.50633
213994_PM_s_at	SPON1	NM_006108	1.50703
205796_PM_at	TCP11L1	NM_001145541 /// NM_018393	1.50719
1554424_PM_at	FIP1L1	NM_001134937 /// NM_001134938 /// NM_030917	1.51532
1553590_PM_at	FAM27E1 /// FAM27E3	XM_001720463 /// XR_110794 /// XR_113221	1.51584
232202_PM_at	---	---	1.52145
219232_PM_s_at	EGLN3	NM_022073	1.52208

204982_PM_at	GIT2	NM_001135213 /// NM_001135214 /// NM_014776 /// NM_057169 /// NM_057170 /// NM_139201	1.52394
229984_PM_at	DTWD1	NM_001144955 /// NM_020234	1.52436
225940_PM_at	EIF4E3	NM_001134649 /// NM_001134650 /// NM_001134651 /// NM_173359	1.52459
223799_PM_at	KIAA1826	NM_032424	1.52611
1554283_PM_at	CCRN4L	NM_012118	1.52653
1555785_PM_a_at	XRN1	NM_001042604 /// NM_019001	1.52754
230974_PM_at	DDX19B	NM_001014449 /// NM_001014451 /// NM_007242	1.53024
235352_PM_at	MR1	NM_001194999 /// NM_001195000 /// NM_001195035 /// NM_001531	1.53488
239468_PM_at	MKX	NM_173576	1.53601
239515_PM_at	---	---	1.53671
1553768_PM_a_at	DCBLD1	NM_173674	1.54817
217127_PM_at	CTH	NM_001190463 /// NM_001902 /// NM_153742	1.54891
1558692_PM_at	C1orf85	NM_144580	1.55024
223349_PM_s_at	BOK	NM_032515	1.55057
209062_PM_x_at	NCOA3	NM_001174087 /// NM_001174088 /// NM_006534 /// NM_181659	1.55834
210004_PM_at	OLR1	NM_001172632 /// NM_001172633 /// NM_002543	1.56132
1555787_PM_at	C11orf63	NM_024806 /// NM_199124	1.56286
1561347_PM_a_at	---	---	1.56883
219619_PM_at	DIRAS2	NM_017594	1.57376

1569470_PM_a_at	FRMD5	NM_032892	1.57505
212096_PM_s_at	MTUS1	NM_001001924 /// NM_001001925 /// NM_001001931 /// NM_001166393 /// NM_020749	1.57703
221577_PM_x_at	GDF15	NM_004864	1.57893
241984_PM_at	FOXN3	NM_001085471 /// NM_005197	1.57986
201312_PM_s_at	SH3BGRL	NM_003022	1.58002
206667_PM_s_at	SCAMP1	NM_004866	1.58151
1565823_PM_at	7-Sep	NM_001011553 /// NM_001788	1.58158
227752_PM_at	SPTLC3	NM_018327	1.58785
231765_PM_at	ZFYVE20	NM_022340	1.59765
226695_PM_at	PRRX1	NM_006902 /// NM_022716	1.60043
242062_PM_at	SAMD8	NM_001174156 /// NM_144660	1.6036
229927_PM_at	LEMD1	NM_001001552	1.60472
1556176_PM_at	TAF8	NM_138572	1.60548
222862_PM_s_at	AK5	NM_012093 /// NM_174858	1.60558
229393_PM_at	L3MBTL3	NM_001007102 /// NM_032438	1.60835
213806_PM_at	PURA	NM_005859	1.61156
244353_PM_s_at	SLC2A12	NM_145176	1.62088
205239_PM_at	AREG	NM_001657	1.63475
1553318_PM_at	RIBC1	NM_001031745 /// NM_144968	1.63611
1564220_PM_a_at	---	---	1.64288
223292_PM_s_at	MRPS15	NM_031280	1.64681
230383_PM_x_at	---	---	1.64805
206085_PM_s_at	CTH	NM_001190463 /// NM_001902 /// NM_153742	1.64874
1554003_PM_at	RGNEF	NM_001080479 /// NM_001177693	1.69981
201925_PM_s_at	CD55	NM_000574 /// NM_001114752	1.7142
236646_PM_at	C12orf59	NM_153022	1.7346
229441_PM_at	PRSS23	NM_007173	1.75382

220266_PM_s_at	KLF4	NM_004235	1.77572
243999_PM_at	SLFN5	NM_144975	1.78294
226725_PM_at	---	---	1.79124
205767_PM_at	EREG	NM_001432	1.81392
202672_PM_s_at	ATF3	NM_001030287 /// NM_001040619 /// NM_001674	1.81546
1554969_PM_x_at	DIP2A	NM_001146114 /// NM_001146115 /// NM_001146116 /// NM_015151 /// NM_206889 /// NM_20689	1.81723
228360_PM_at	LYPD6B	NM_177964	1.88046
234462_PM_at	---	---	1.92308
210587_PM_at	INHBE	NM_031479	1.93314
202014_PM_at	PPP1R15A	NM_014330	2.04829
202620_PM_s_at	PLOD2	NM_000935 /// NM_182943	2.08166
231265_PM_at	COX7B2	NM_130902	2.32161
228038_PM_at	SOX2	NM_003106	2.36521

Table 8. Probeset ID, gene symbol, refseq transcript ID and fold change from microarray analysis of SW480^{FJX1} treated with scramble siRNA (siSCR) versus SW480^{FJX1} treated with *FJX1* specific siRNA (*siFJX1*) colon cancer cells.

Probeset ID	Gene Symbol	RefSeq Transcript ID	Fold-Change (FJX1 siFJX1 vs. FJX1 siSCR)
210587_PM_at	INHBE	NM_031479	-4.16243
227959_PM_at	---	---	-3.9682
219522_PM_at	FJX1	NM_014344	-3.46637
1555339_PM_at	RAP1A	NM_001010935 /// NM_002884	-3.23984
1555340_PM_x_at	RAP1A	NM_001010935 /// NM_002884	-2.85722
208760_PM_at	UBE2I	NM_003345 /// NM_194259 /// NM_194260 /// NM_194261	-2.70226
204079_PM_at	TPST2	NM_001008566 /// NM_003595	-2.62307
209695_PM_at	PTP4A3	NM_007079 /// NM_032611	-2.56625
238604_PM_at	---	---	-2.45679
202409_PM_at	IGF2 /// INS-IGF2	NM_000612 /// NM_001007139 /// NM_001042376 /// NM_001127598 /// NR_003512	-2.39021
205549_PM_at	PCP4	NM_006198	-2.37463
225671_PM_at	SPNS2	NM_001124758	-2.3391
224578_PM_at	RCC2	NM_001136204 /// NM_018715	-2.33736
219429_PM_at	FA2H	NM_024306	-2.27513
241367_PM_at	TEX19	NM_207459	-2.27388
222764_PM_at	ASRGL1	NM_001083926 /// NM_025080	-2.17904
202967_PM_at	GSTA4	NM_001512	-2.17295
200917_PM_s_at	SRPR	NM_001177842 /// NM_003139	-2.16542

225897_PM_at	MARCKS	NM_002356	-2.15615
229912_PM_at	SDK1	NM_152744 /// NR_027816	-2.15188
202887_PM_s_at	DDIT4	NM_019058	-2.10614
203397_PM_s_at	GALNT3	NM_004482	-2.07615
200918_PM_s_at	SRPR	NM_001177842 /// NM_003139	-2.07377
226181_PM_at	TUBE1	NM_016262	-2.05642
215795_PM_at	MYH7B	NM_020884	-2.03838
225556_PM_at	VMA21	NM_001017980	-2.0319
225096_PM_at	C17orf79	NM_018405	-2.0188
209409_PM_at	GRB10	NM_001001549 /// NM_001001550 /// NM_001001555 /// NM_005311	-1.99853
233949_PM_s_at	MYH7B	NM_020884	-1.97874
1555867_PM_at	GNG4	NM_001098721 /// NM_001098722 /// NM_004485	-1.9721
219032_PM_x_at	OPN3	NM_014322	-1.96509
243718_PM_at	---	---	-1.96328
229125_PM_at	KANK4	NM_181712	-1.96257
207529_PM_at	DEFA5	NM_021010	-1.95514
1555788_PM_a_at	TRIB3	NM_021158	-1.95101
208725_PM_at	EIF2S2	NM_003908	-1.93676
208510_PM_s_at	PPARG	NM_005037 /// NM_015869 /// NM_138711 /// NM_138712	-1.9332
209395_PM_at	CHI3L1	NM_001276	-1.92938
229354_PM_at	AHRR	NM_020731	-1.91806
226403_PM_at	TMC4	NM_001145303 /// NM_144686	-1.9044
223167_PM_s_at	USP25	NM_013396	-1.90212
223339_PM_at	ATPIF1	NM_016311 /// NM_178190 /// NM_178191	-1.89871
212816_PM_s_at	CBS	NM_000071 /// NM_001178008 /// NM_001178009	-1.89476
218974_PM_at	SOBP	NM_018013	-1.89462
218872_PM_at	TESC	NM_001168325 /// NM_017899 /// NR_031766	-1.89383

240152_PM_at	---	---	-1.89234
218857_PM_s_at	ASRGL1	NM_001083926 /// NM_025080	-1.88064
219497_PM_s_at	BCL11A	NM_018014 /// NM_022893 /// NM_138559	-1.88048
227506_PM_at	SLC16A9	NM_194298	-1.87927
226126_PM_at	TBCK	NM_001163435 /// NM_001163436 /// NM_001163437 /// NM_033115	-1.87503
225111_PM_s_at	NAPB	NM_022080	-1.86992
238681_PM_at	GDPD1	NM_001165993 /// NM_001165994 /// NM_182569	-1.85574
222256_PM_s_at	JMJD7	NM_001114632	-1.83753
226519_PM_s_at	AGXT2L2	NM_153373	-1.83542
226552_PM_at	IER5L	NM_203434	-1.82281
204394_PM_at	SLC43A1	NM_001198810 /// NM_003627	-1.82098
228006_PM_at	---	---	-1.80843
1555890_PM_at	OR2A20P /// OR2A9P	NR_002157 /// NR_002158	-1.80708
226560_PM_at	---	---	-1.80366
223464_PM_at	OSBPL5	NM_001144063 /// NM_020896 /// NM_145638	-1.80351
203256_PM_at	CDH3	NM_001793	-1.80335
213558_PM_at	PCLO	NM_014510 /// NM_033026	-1.80035
229544_PM_at	---	---	-1.79352
225704_PM_at	FBRSL1	NM_001142641	-1.78371
200952_PM_s_at	CCND2	NM_001759	-1.78091
227074_PM_at	LOC100131564	NR_034089	-1.77972
229407_PM_at	SDK1	NM_152744 /// NR_027816	-1.77729
201670_PM_s_at	MARCKS	NM_002356	-1.76539
235962_PM_at	AZI2	NM_001134432 /// NM_001134433 /// NM_022461	-1.76146
226012_PM_at	ANKRD11	NM_013275	-1.75877
1552789_PM_at	SEC62	NM_003262	-1.75521
220609_PM_at	LOC202181	NR_026921	-1.75166

210650_PM_s_at	PCLO	NM_014510 /// NM_033026	-1.74953
227174_PM_at	WDR72	NM_182758	-1.74705
229963_PM_at	BEX5	NM_001012978 /// NM_001159560	-1.7446
201010_PM_s_at	TXNIP	NM_006472	-1.74344
239694_PM_at	TRIM7	NM_033342 /// NM_203293 /// NM_203294 /// NM_203295 /// NM_203296 /// NM_203297	-1.74072
219188_PM_s_at	MACROD1	NM_014067	-1.7395
240180_PM_at	---	---	-1.73858
225527_PM_at	CEBPG	NM_001806	-1.73717
201008_PM_s_at	TXNIP	NM_006472	-1.73636
228999_PM_at	CHD2	NM_001042572 /// NM_001271	-1.73398
235476_PM_at	TRIM59	NM_173084	-1.73154
217997_PM_at	PHLDA1	NM_007350	-1.73046
207236_PM_at	ZNF345	NM_003419	-1.72877
237213_PM_at	---	---	-1.72849
213002_PM_at	MARCKS	NM_002356	-1.72395
1559132_PM_at	TMEM80	NM_001042463 /// NM_174940	-1.72171
226820_PM_at	ZNF362	NM_152493	-1.72142
226548_PM_at	SBK1	NM_001024401	-1.71667
204134_PM_at	PDE2A	NM_001143839 /// NM_001146209 /// NM_002599 /// NR_026572	-1.71487
204718_PM_at	EPHB6	NM_004445	-1.71449
212307_PM_s_at	OGT	NM_181672 /// NM_181673	-1.71252
206082_PM_at	HCP5	NM_006674	-1.71116
221969_PM_at	PAX5	NM_016734	-1.70843
213601_PM_at	SLIT1	NM_003061	-1.7079
235309_PM_at	RPS15A	NM_001019 /// NM_001030009	-1.70684

1564907_PM_s_at	MATR3 /// SNHG4	NM_001194954 /// NM_001194955 /// NM_001194956 /// NM_018834 /// NM_199189 /// NR_00314	-1.70424
205531_PM_s_at	GLS2	NM_013267	-1.70377
228108_PM_at	PPM1L	NM_139245	-1.70331
224784_PM_at	MLLT6	NM_005937	-1.69987
221840_PM_at	PTPRE	NM_006504 /// NM_130435	-1.699
217999_PM_s_at	PHLDA1	NM_007350	-1.69827
242998_PM_at	RDH12	NM_152443	-1.69812
218848_PM_at	THOC6	NM_001142350 /// NM_024339	-1.69766
230486_PM_at	---	---	-1.69632
243209_PM_at	KCNQ4	NM_004700 /// NM_172163	-1.69604
236453_PM_at	---	---	-1.69587
209083_PM_at	CORO1A	NM_001193333 /// NM_007074	-1.69254
1558740_PM_s_at	---	---	-1.69253
226412_PM_at	SFRS18	NM_015491 /// NM_032870	-1.68923
227404_PM_s_at	EGR1	NM_001964	-1.68866
227867_PM_at	C2orf89	NM_001080824	-1.68844
238029_PM_s_at	SLC16A14	NM_152527	-1.68769
238151_PM_at	---	---	-1.686
235275_PM_at	BMP8B	NM_001720	-1.68311
226925_PM_at	ACPL2	NM_001037172 /// NM_152282	-1.68256
203570_PM_at	LOXL1	NM_005576	-1.67946
226431_PM_at	FAM117B	NM_173511	-1.67802
226457_PM_at	---	---	-1.67723
225942_PM_at	NLN	NM_020726	-1.67554
221963_PM_x_at	---	---	-1.67504
243179_PM_at	LOC100130360	---	-1.67504
210410_PM_s_at	C6orf26 /// MSH5	NM_001039651 /// NM_002441 /// NM_025259 /// NM_172165 /// NM_172166	-1.67276
1559222_PM_at	---	---	-1.67098
221878_PM_at	C2orf68	NM_001013649	-1.67053

213889_PM_at	---	---	-1.66683
218902_PM_at	NOTCH1	NM_017617	-1.66654
1559227_PM_s_at	VHL	NM_000551 /// NM_198156	-1.66632
228461_PM_at	SH3RF3	NM_001099289	-1.66466
242053_PM_at	---	---	-1.66457
201009_PM_s_at	TXNIP	NM_006472	-1.66361
207173_PM_x_at	CDH11	NM_001797	-1.6636
228686_PM_at	FLJ33630	NR_015360	-1.66359
235772_PM_at	---	---	-1.66349
213285_PM_at	TMEM30B	NM_001017970	-1.66332
1554250_PM_s_at	TRIM73	NM_198924	-1.65704
207760_PM_s_at	NCOR2	NM_001077261 /// NM_006312	-1.65449
227641_PM_at	FBXL16	NM_153350	-1.65431
1557348_PM_at	---	---	-1.65427
230467_PM_at	TMEM52	NM_178545	-1.65282
1553972_PM_a_at	CBS	NM_000071 /// NM_001178008 /// NM_001178009	-1.65091
202454_PM_s_at	ERBB3	NM_001005915 /// NM_001982	-1.65075
212843_PM_at	NCAM1	NM_000615 /// NM_001076682 /// NM_181351	-1.6493
238853_PM_at	RAB3IP	NM_001024647 /// NM_022456 /// NM_175623 /// NM_175624 /// NM_175625	-1.64749
218145_PM_at	TRIB3	NM_021158	-1.64634
223630_PM_at	C7orf13	NR_026865	-1.64601
208291_PM_s_at	TH	NM_000360 /// NM_199292 /// NM_199293	-1.64585
229983_PM_at	TIGD2	NM_145715	-1.64528
230752_PM_at	---	---	-1.64526
215785_PM_s_at	CYFIP2	NM_001037332 /// NM_001037333 /// NM_014376	-1.64381
205402_PM_x_at	PRSS2	NM_002770	-1.64275

231399_PM_at	RAB3IP	NM_001024647 /// NM_022456 /// NM_175623 /// NM_175624 /// NM_175625	-1.64265
227708_PM_at	EEF1A1	NM_001402	-1.64244
204788_PM_s_at	PPOX	NM_000309 /// NM_001122764	-1.63854
222360_PM_at	DPH5	NM_001077394 /// NM_001077395 /// NM_015958	-1.63497
202847_PM_at	PCK2	NM_001018073 /// NM_004563	-1.63171
230782_PM_at	SORD	NM_003104 /// NR_034039	-1.62999
228771_PM_at	ADRBK2	NM_005160	-1.62651
240983_PM_s_at	CARS	NM_001014437 /// NM_001194997 /// NM_001751 /// NM_139273 /// NR_036542	-1.62618
214110_PM_s_at	---	---	-1.62133
235191_PM_at	LOC148189	NR_027301	-1.62114
220196_PM_at	MUC16	NM_024690	-1.61943
229215_PM_at	ASCL2	NM_005170	-1.61825
203438_PM_at	STC2	NM_003714	-1.61662
209846_PM_s_at	BTN3A2	NM_001197246 /// NM_001197247 /// NM_001197248 /// NM_001197249 /// NM_007047	-1.6149
200951_PM_s_at	CCND2	NM_001759	-1.61442
212192_PM_at	KCTD12	NM_138444	-1.61434
243356_PM_at	---	---	-1.61348
228090_PM_at	NMNAT3	NM_178177	-1.61226
213194_PM_at	ROBO1	NM_001145845 /// NM_002941 /// NM_133631	-1.61176
242673_PM_at	---	---	-1.61063
242546_PM_at	FLJ39632	XR_110291 /// XR_112214	-1.61015
218080_PM_x_at	FAF1	NM_007051	-1.60982
225812_PM_at	C6orf225	NM_001033564	-1.60939
226590_PM_at	ZNF618	NM_133374	-1.60905

206463_PM_s_at	DHRS2	NM_005794 /// NM_182908	-1.60884
226213_PM_at	ERBB3	NM_001005915 /// NM_001982	-1.60867
205047_PM_s_at	ASNS	NM_001178075 /// NM_001178076 /// NM_001178077 /// NM_001673 /// NM_133436 /// NM_18335	-1.60816
207610_PM_s_at	EMR2	NM_013447 /// NM_152916 /// NM_152917 /// NM_152918 /// NM_152919 /// NM_152920 /// NM_	-1.60806
214823_PM_at	ZNF204P	NR_002722 /// NR_024553	-1.60465
220762_PM_s_at	GNB1L	NM_053004	-1.60154
225949_PM_at	NRBP2	NM_178564	-1.60138
207076_PM_s_at	ASS1	NM_000050 /// NM_054012	-1.59987
242835_PM_s_at	LOC728730	XR_109973 /// XR_112311 /// XR_115530	-1.59774
210482_PM_x_at	MAP2K5	NM_002757 /// NM_145160	-1.59745
228156_PM_at	---	---	-1.59619
224156_PM_x_at	IL17RB	NM_018725	-1.59545
201048_PM_x_at	RAB6A	NM_002869 /// NM_198896	-1.59506
204351_PM_at	S100P	NM_005980	-1.59441
235123_PM_at	---	---	-1.59374
228397_PM_at	TUG1	NR_002323	-1.59288
221951_PM_at	TMEM80	NM_001042463 /// NM_174940	-1.59018
242558_PM_at	---	---	-1.59001
212942_PM_s_at	KIAA1199	NM_018689	-1.59
212512_PM_s_at	CARM1	NM_199141	-1.58835
201508_PM_at	IGFBP4	NM_001552	-1.58827

227179_PM_at	STAU2	NM_001164380 /// NM_001164381 /// NM_001164382 /// NM_001164383 /// NM_001164384 /// NM	-1.58755
225846_PM_at	ESRP1	NM_001034915 /// NM_001122825 /// NM_001122826 /// NM_001122827 /// NM_017697	-1.5868
242064_PM_at	SDK2	NM_001144952	-1.58575
236219_PM_at	TMEM20	NM_001134658 /// NM_153226	-1.5841
201505_PM_at	LAMB1	NM_002291	-1.58369
231311_PM_at	---	---	-1.58291
220459_PM_at	MCM3AP-AS	NR_002776	-1.58265
226124_PM_at	ZFP90	NM_133458	-1.58126
239082_PM_at	FZD3	NM_017412	-1.58096
224995_PM_at	SPIRE1	NM_001128626 /// NM_001128627 /// NM_020148	-1.57882
227293_PM_at	---	---	-1.57803
213848_PM_at	DUSP7	NM_001947	-1.57451
1569923_PM_s_at	LOC285708	---	-1.57435
201694_PM_s_at	EGR1	NM_001964	-1.57369
235470_PM_at	NAA38	NM_016200	-1.57364
228066_PM_at	C17orf96	NM_001130677	-1.57344
222746_PM_s_at	BSPRY	NM_017688	-1.57325
230606_PM_at	LOC100287525	XM_002343549 /// XM_002345023 /// XM_002347757	-1.57283
214434_PM_at	HSPA12A	NM_025015	-1.5726
229545_PM_at	FERMT1	NM_017671	-1.5719
220668_PM_s_at	DNMT3B	NM_006892 /// NM_175848 /// NM_175849 /// NM_175850	-1.57142
220177_PM_s_at	TMPRSS3	NM_024022 /// NM_032405 /// NR_027348	-1.57077
209368_PM_at	EPHX2	NM_001979	-1.57033
202148_PM_s_at	PYCR1	NM_006907 /// NM_153824	-1.56876
203831_PM_at	R3HDM2	NM_014925	-1.56843

205162_PM_at	ERCC8	NM_000082	-1.56699
229748_PM_x_at	LOC100132288	NM_001033515	-1.56683
218789_PM_s_at	C11orf71	NM_019021	-1.56592
209816_PM_at	PTCH1	NM_000264 /// NM_001083602 /// NM_001083603 /// NM_001083604 /// NM_001083605 /// NM_00	-1.56587
218537_PM_at	HCFC1R1	NM_001002017 /// NM_001002018 /// NM_017885	-1.56474
219270_PM_at	CHAC1	NM_001142776 /// NM_024111	-1.56473
221582_PM_at	HIST3H2A	NM_033445	-1.56443
224392_PM_s_at	OPN3	NM_014322	-1.56425
224694_PM_at	ANTXR1	NM_018153 /// NM_032208 /// NM_053034	-1.56375
204411_PM_at	KIF21B	NM_017596	-1.56178
236780_PM_at	---	---	-1.56143
211651_PM_s_at	LAMB1	NM_002291	-1.56142
225220_PM_at	SNHG8	NR_003584 /// NR_034010 /// NR_034011	-1.56117
207291_PM_at	PRRG4	NM_024081	-1.5592
226534_PM_at	KITLG	NM_000899 /// NM_003994	-1.55836
202597_PM_at	IRF6	NM_006147	-1.55685
217998_PM_at	PHLDA1	NM_007350	-1.55558
242111_PM_at	METTL3	NM_019852	-1.55455
225018_PM_at	SPIRE1	NM_001128626 /// NM_001128627 /// NM_020148	-1.55365
224466_PM_s_at	MAFG	NM_002359 /// NM_032711	-1.55239
213113_PM_s_at	SLC43A3	NM_014096 /// NM_017611 /// NM_199329	-1.55225
203180_PM_at	ALDH1A3	NM_000693	-1.55157
226652_PM_at	USP3	NM_006537	-1.54975
221430_PM_s_at	RNF146	NM_030963	-1.54946
232396_PM_at	---	---	-1.54906
201693_PM_s_at	EGR1	NM_001964	-1.54838

228341_PM_at	NUDT16	NM_001171905 /// NM_001171906 /// NM_152395 /// NR_033268	-1.54709
209396_PM_s_at	CHI3L1	NM_001276	-1.54702
1554079_PM_at	GALNTL4	NM_198516	-1.54682
210341_PM_at	MYT1	NM_004535	-1.54521
221858_PM_at	TBC1D12	NM_015188	-1.54462
227801_PM_at	TRIM59	NM_173084	-1.54308
241114_PM_s_at	---	---	-1.54303
216867_PM_s_at	PDGFA	NM_002607 /// NM_033023	-1.54278
239697_PM_x_at	C3orf67	NM_198463	-1.54262
224186_PM_s_at	RNF123	NM_022064	-1.54262
1553180_PM_at	ADAMTS19	NM_133638	-1.54254
230488_PM_s_at	NCRNA00118	NR_002783	-1.54251
214907_PM_at	CEACAM21	NM_001098506 /// NM_033543	-1.54215
237299_PM_at	---	---	-1.54174
223541_PM_at	HAS3	NM_005329 /// NM_138612	-1.54016
204199_PM_at	RALGPS1	NM_001190728 /// NM_001190729 /// NM_001190730 /// NM_014636	-1.53972
232069_PM_at	KIF26A	NM_015656	-1.53907
211370_PM_s_at	MAP2K5	NM_002757 /// NM_145160	-1.53804
241972_PM_at	LOC401588	NR_015378	-1.53794
227446_PM_s_at	C14orf167	NR_023921 /// NR_023922 /// NR_023923 /// NR_023924	-1.53758
238513_PM_at	PRRG4	NM_024081	-1.53738
236967_PM_at	LOC645249	XR_108719 /// XR_110785 /// XR_113097 /// XR_114128	-1.53709
206574_PM_s_at	PTP4A3	NM_007079 /// NM_032611	-1.53693
226849_PM_at	DENND1A	NM_020946 /// NM_024820	-1.53462
243009_PM_at	---	---	-1.53353
226614_PM_s_at	FAM167A	NM_053279	-1.53253

207564_PM_x_at	OGT	NM_181672 /// NM_181673	-1.5324
210999_PM_s_at	GRB10	NM_001001549 /// NM_001001550 /// NM_001001555 /// NM_005311	-1.53219
211126_PM_s_at	CSRP2	NM_001321	-1.53099
210915_PM_x_at	TRBC2	---	-1.53097
218839_PM_at	HEY1	NM_001040708 /// NM_012258	-1.53036
241687_PM_at	---	---	-1.53009
229058_PM_at	ANKRD16	NM_001009941 /// NM_001009943 /// NM_019046	-1.52968
227250_PM_at	KREMEN1	NM_001039570 /// NM_032045	-1.52906
229954_PM_at	CHDH	NM_018397	-1.5289
225520_PM_at	MTHFD1L	NM_015440	-1.52887
47560_PM_at	LPHN1	NM_001008701 /// NM_014921	-1.52871
204875_PM_s_at	GMDS	NM_001500	-1.52812
202157_PM_s_at	CELF2	NM_001025076 /// NM_001025077 /// NM_001083591 /// NM_006561	-1.52812
229332_PM_at	HPDL	NM_032756	-1.52809
218689_PM_at	FANCF	NM_022725	-1.5278
227864_PM_s_at	FAM125A	NM_138401	-1.52728
241234_PM_at	LOC100506797	XR_109881 /// XR_109882 /// XR_109883 /// XR_112377 /// XR_112378 /// XR_113370 /// XR_	-1.52688
213411_PM_at	ADAM22	NM_004194 /// NM_016351 /// NM_021721 /// NM_021722 /// NM_021723	-1.52666
224428_PM_s_at	CDCA7	NM_031942 /// NM_145810	-1.526

		NM_001197246 ///	
		NM_001197247 ///	
		NM_001197248 ///	
	BTN3A2 ///	NM_001197249 ///	
204820_PM_s_at	BTN3A3	NM_006994 /// NM_00	-1.52578
218677_PM_at	S100A14	NM_020672	-1.52558
		NM_001185022 ///	
		NM_001185023 ///	
202790_PM_at	CLDN7	NM_001307	-1.52435
		NM_001032999 ///	
		NM_001039709 ///	
238549_PM_at	CBFA2T2	NM_005093	-1.52391
		NM_001178138 ///	
		NM_001178139 ///	
		NM_001178140 ///	
		NM_001178141 ///	
226157_PM_at	TFDP2	NM_001178142 /// NM	-1.52327
223196_PM_s_at	SESN2	NM_031459	-1.52307
224217_PM_s_at	FAF1	NM_007051	-1.52239
222445_PM_at	SLC39A9	NM_018375	-1.52204
		NM_001193493 ///	
209610_PM_s_at	SLC1A4	NM_003038	-1.52198
		NM_001193493 ///	
212811_PM_x_at	SLC1A4	NM_003038	-1.52174
1569973_PM_at	SEPT7P2	NR_024271	-1.52064
		NM_001143781 ///	
		NM_001143782 ///	
219117_PM_s_at	FKBP11	NM_016594	-1.52054
242857_PM_at	---	---	-1.52035
		NM_001007102 ///	
229393_PM_at	L3MBTL3	NM_032438	-1.52025
		NM_001159673 ///	
		NM_001159674 ///	
		NM_001159675 ///	
		NM_001159676 ///	
217833_PM_at	SYNCRIP	NM_001159677 /// NM	-1.51865
		NM_001142386 ///	
230085_PM_at	PDK3	NM_005391	-1.51628
		NM_001030272 ///	
		NM_001030273 ///	
209824_PM_s_at	ARNTL	NM_001178	-1.51571
218792_PM_s_at	BSPRY	NM_017688	-1.51519
226388_PM_at	TCEA3	NM_003196	-1.51312

228752_PM_at	EFCAB4B	NM_001144958 /// NM_001144959 /// NM_032680	-1.51295
204123_PM_at	LIG3	NM_002311 /// NM_013975	-1.5129
223093_PM_at	ANKH	NM_054027	-1.51223
229830_PM_at	PDGFA	NM_002607 /// NM_033023	-1.51174
235583_PM_at	ILDR1	NM_175924	-1.51151
207413_PM_s_at	SCN5A	NM_000335 /// NM_001099404 /// NM_001099405 /// NM_001160160 /// NM_001160161 /// NM_19	-1.51131
228200_PM_at	ZNF252	NR_023392	-1.51107
212810_PM_s_at	SLC1A4	NM_001193493 /// NM_003038	-1.51105
223125_PM_s_at	C1orf21	NM_030806	-1.50996
225193_PM_at	---	---	-1.50944
1562013_PM_a_at	---	---	-1.50854
226301_PM_at	C6orf192	NM_052831	-1.50774
233016_PM_at	---	---	-1.50769
225928_PM_at	VTI1B	NM_006370	-1.50715
203867_PM_s_at	NLE1	NM_001014445 /// NM_018096	-1.50553
243747_PM_at	ZNF599	NM_001007248	-1.50523
219743_PM_at	HEY2	NM_012259	-1.50508
214095_PM_at	SHMT2	NM_001166356 /// NM_001166357 /// NM_001166358 /// NM_001166359 /// NM_005412 /// NR_02	-1.50499
223184_PM_s_at	AGPAT3	NM_001037553 /// NM_020132	-1.50448
235577_PM_at	ZNF652	NM_001145365 /// NM_014897	-1.50437
224367_PM_at	BEX2	NM_001168399 /// NM_001168400 /// NM_001168401 /// NM_032621	-1.50398
205258_PM_at	INHBB	NM_002193	-1.50394
227417_PM_at	MOSC2	NM_017898	-1.50379
1564706_PM_s_at	GLS2	NM_013267	-1.50313

214571_PM_at	FGF3	NM_005247	-1.50309
243224_PM_at	---	---	-1.50233
222930_PM_s_at	AGMAT	NM_024758	-1.50182
205352_PM_at	SERPINI1	NM_001122752 /// NM_005025	-1.50168
244769_PM_at	---	---	-1.50136
208886_PM_at	H1F0	NM_005318	-1.5005
205411_PM_at	STK4	NM_006282	1.50071
235235_PM_s_at	PATL1	NM_152716	1.50121
232083_PM_at	KIF16B	NM_024704	1.50123
235371_PM_at	GXYLT2	NM_001080393	1.50156
230493_PM_at	SHISA2	NM_001007538	1.50205
238476_PM_at	C5orf41	NM_001168393 /// NM_001168394 /// NM_153607	1.50212
213343_PM_s_at	GDPD5	NM_030792	1.50229
AFFX-r2-Bs-phe-M_at	---	---	1.50356
219471_PM_at	C13orf18	NM_025113	1.50497
201700_PM_at	CCND3	NM_001136017 /// NM_001136125 /// NM_001136126 /// NM_001760	1.50501
210426_PM_x_at	RORA	NM_002943 /// NM_134260 /// NM_134261 /// NM_134262	1.5055
209387_PM_s_at	TM4SF1	NM_014220	1.50605
37966_PM_at	PARVB	NM_001003828 /// NM_013327	1.50607
228097_PM_at	MYLIP	NM_013262	1.50608
217560_PM_at	GGA1	NM_001001560 /// NM_001001561 /// NM_001172687 /// NM_001172688 /// NM_013365	1.50623
209459_PM_s_at	ABAT	NM_000663 /// NM_001127448 /// NM_020686	1.50667
228260_PM_at	ELAVL2	NM_001171195 /// NM_001171197 /// NM_004432	1.50677
230104_PM_s_at	TPPP	NM_007030	1.50806
1556826_PM_s_at	C1orf187	NM_198545	1.50825

229881_PM_at	KLF12	NM_007249	1.50903
210987_PM_x_at	TPM1	NM_000366 /// NM_001018004 /// NM_001018005 /// NM_001018006 /// NM_001018007 /// NM_00	1.51085
229106_PM_at	DYNLL2	NM_080677	1.51157
219210_PM_s_at	RAB8B	NM_016530	1.51383
217585_PM_at	NEBL	NM_001173484 /// NM_006393 /// NM_213569	1.51457
211756_PM_at	PTHLH	NM_002820 /// NM_198964 /// NM_198965 /// NM_198966	1.51513
230955_PM_s_at	C20orf112	NM_080616	1.51543
208926_PM_at	NEU1	NM_000434	1.51552
208596_PM_s_at	UGT1A1 /// UGT1A10 /// UGT1A3 /// UGT1A4 /// UGT1A5 /// UGT1A6 /// UGT1A7 /// UGT1A8 /// UGT1A9	NM_000463 /// NM_001072 /// NM_007120 /// NM_019075 /// NM_019076 /// NM_019077 /// NM_	1.51589
212758_PM_s_at	ZEB1	NM_001128128 /// NM_001174093 /// NM_001174094 /// NM_001174095 /// NM_001174096 /// NM	1.51634
224128_PM_at	C20orf43	NM_016407	1.51658
208678_PM_at	ATP6V1E1	NM_001039366 /// NM_001039367 /// NM_001696	1.51664
212602_PM_at	WDFY3	NM_014991	1.51722
203158_PM_s_at	GLS	NM_014905	1.51857
208869_PM_s_at	GABARAPL1	NM_031412	1.51871
225372_PM_at	C10orf54	NM_022153	1.51885
238842_PM_at	---	---	1.51927
231221_PM_at	CLEC16A	NM_015226	1.51941
224790_PM_at	ASAP1	NM_018482	1.51963
203650_PM_at	PROCR	NM_006404	1.51973
36552_PM_at	C2CD3	NM_015531	1.52148

210964_PM_s_at	GYG2	NM_001079855 /// NM_001184702 /// NM_001184703 /// NM_001184704 /// NM_003918	1.52193
215495_PM_s_at	SAMD4A	NM_001161576 /// NM_001161577 /// NM_015589	1.52233
238419_PM_at	PHLDB2	NM_001134437 /// NM_001134438 /// NM_001134439 /// NM_145753	1.52329
206518_PM_s_at	RGS9	NM_001081955 /// NM_001165933 /// NM_003835	1.52348
224916_PM_at	TMEM173	NM_198282	1.52421
203870_PM_at	USP46	NM_001134223 /// NM_022832	1.52501
204929_PM_s_at	VAMP5	NM_006634	1.52511
1555716_PM_a_at	CXADR	NM_001338	1.52532
209290_PM_s_at	NFIB	NM_001190737 /// NM_001190738 /// NM_005596	1.52541
209909_PM_s_at	TGFB2	NM_001135599 /// NM_003238	1.52554
222045_PM_s_at	PCIF1	NM_022104	1.52575
215058_PM_at	DENND5B	NM_144973	1.52667
221946_PM_at	C9orf116	NM_001048265 /// NM_144654	1.52731
230035_PM_at	BOC	NM_033254	1.5295
242439_PM_s_at	ASXL1	NM_001164603 /// NM_015338	1.53045
202637_PM_s_at	ICAM1	NM_000201	1.53071
232206_PM_at	ULK4	NM_017886	1.53089
227019_PM_at	C1orf226	NM_001085375 /// NM_001135240	1.53172
225093_PM_at	UTRN	NM_007124	1.53187
201625_PM_s_at	INSIG1	NM_005542 /// NM_198336 /// NM_198337	1.5328
228448_PM_at	MAP6	NM_033063 /// NM_207577	1.53303
239825_PM_at	---	---	1.53364

		NM_001142648 /// NM_020150	1.53413
201543_PM_s_at	SAR1A	NM_013358	1.53517
223739_PM_at	PADI1	NM_013358	1.53517
204220_PM_at	GMFG	NM_004877	1.53568
238890_PM_at	BRWD1	NM_001007246 /// NM_018963 /// NM_033656	1.53701
217176_PM_s_at	ZFX	NM_001178084 /// NM_001178085 /// NM_001178086 /// NM_001178095 /// NM_003410	1.53714
235230_PM_at	PLCXD2	NM_001185106 /// NM_153268	1.53735
227278_PM_at	---	---	1.53784
1566671_PM_a_at	PDXK	NM_003681	1.53876
228098_PM_s_at	MYLIP	NM_013262	1.5397
235088_PM_at	C4orf46	NM_001008393	1.5408
212095_PM_s_at	MTUS1	NM_001001924 /// NM_001001925 /// NM_001001931 /// NM_001166393 /// NM_020749	1.54118
235672_PM_at	MAP6	NM_033063 /// NM_207577	1.54157
230492_PM_s_at	GPCPD1	NM_019593	1.54192
238917_PM_s_at	DENND5B	NM_144973	1.54208
220766_PM_at	BTG4	NM_017589	1.54221
242322_PM_at	---	---	1.54238
205805_PM_s_at	ROR1	NM_001083592 /// NM_005012	1.54252
220254_PM_at	LRP12	NM_001135703 /// NM_013437	1.54366
227410_PM_at	FAM43A	NM_153690	1.54513
219403_PM_s_at	HPSE	NM_001098540 /// NM_001166498 /// NM_006665	1.5453
224828_PM_at	CPEB4	NM_030627	1.54543
230747_PM_s_at	TTC39C	NM_001135993 /// NM_153211 /// NR_024232	1.54641
223689_PM_at	IGF2BP1	NM_001160423 /// NM_006546	1.54662
228185_PM_at	ZNF25	NM_145011	1.54733

204633_PM_s_at	RPS6KA5	NM_004755 /// NM_182398	1.54763
240369_PM_at	---	---	1.54774
1563229_PM_at	DLEU2	NR_002612	1.54891
230962_PM_at	DCLK1	NM_001195415 /// NM_001195416 /// NM_001195430 /// NM_004734	1.54945
227375_PM_at	ANKRD13C	NM_030816	1.55041
242438_PM_at	ASXL1	NM_001164603 /// NM_015338	1.55059
202368_PM_s_at	TRAM2	NM_012288	1.55064
212003_PM_at	C1orf144	NM_001114600 /// NM_015609	1.55095
217234_PM_s_at	EZR	NM_001111077 /// NM_003379	1.55145
219282_PM_s_at	TRPV2	NM_016113	1.55151
203913_PM_s_at	HPGD	NM_000860 /// NM_001145816 /// NR_027332	1.55217
221766_PM_s_at	FAM46A	NM_017633	1.55284
235004_PM_at	RBM24	NM_001143941 /// NM_001143942 /// NM_153020	1.55288
242414_PM_at	QPRT	NM_014298	1.55451
202082_PM_s_at	SEC14L1	NM_001039573 /// NM_001143998 /// NM_001143999 /// NM_001144001 /// NM_003003	1.55493
232341_PM_x_at	HABP4	NM_014282	1.55591
222715_PM_s_at	SYNRG	NM_001163544 /// NM_001163545 /// NM_001163546 /// NM_001163547 /// NM_007247 /// NM_08	1.5561
223185_PM_s_at	BHLHE41	NM_030762	1.55643
217763_PM_s_at	RAB31	NM_006868	1.5574
212844_PM_at	RRP1B	NM_015056	1.55861
206907_PM_at	TNFSF9	NM_003811	1.55861
203429_PM_s_at	C1orf9	NM_014283 /// NM_016227	1.55975
1559893_PM_at	CCDC75	NM_174931	1.5605

		NM_001190918 /// NM_001190919 /// NM_003250 /// NM_021724 ///	
204760_PM_s_at	NR1D1 /// THRA	NM_199334	1.56059
226968_PM_at	KIF1B	NM_015074 /// NM_183416	1.56126
201627_PM_s_at	INSIG1	NM_005542 /// NM_198336 /// NM_198337	1.56141
203708_PM_at	PDE4B	NM_001037339 /// NM_001037340 /// NM_001037341 /// NM_002600	1.56207
222692_PM_s_at	FNDC3B	NM_001135095 /// NM_022763	1.56254
214719_PM_at	SLC46A3	NM_001135919 /// NM_181785	1.56301
213407_PM_at	PHLPP2	NM_015020	1.56311
231121_PM_at	HPS3	NM_032383	1.56324
208481_PM_at	ASB4	NM_016116 /// NM_145872	1.56468
227828_PM_s_at	FAM176A	NM_001135032 /// NM_032181	1.5647
226810_PM_at	OGFRL1	NM_024576	1.5657
225856_PM_at	---	---	1.56594
214108_PM_at	MAX	NM_002382 /// NM_145112 /// NM_145113 /// NM_145114 /// NM_145116 /// NM_197957	1.56638
208881_PM_x_at	IDI1	NM_004508	1.5672
206022_PM_at	NDP	NM_000266	1.56747
209420_PM_s_at	SMPD1	NM_000543 /// NM_001007593	1.56823
232591_PM_s_at	TMEM30A	NM_001143958 /// NM_018247	1.56827
239190_PM_at	VRK3	NM_001025778 /// NM_016440	1.56841
229952_PM_at	---	---	1.56979
1555358_PM_a_at	ENTPD4	NM_001128930 /// NM_004901	1.56999

		NM_032857 /// NM_171846	
1552485_PM_at	LACTB		1.57085
207056_PM_s_at	SLC4A8	NM_001039960 /// NM_004858	1.57088
213711_PM_at	KRT81	NM_002281	1.57174
59437_PM_at	C9orf116	NM_001048265 /// NM_144654	1.57483
205443_PM_at	SNAPC1	NM_003082	1.57552
239212_PM_at	LTV1	NM_032860	1.57559
222847_PM_s_at	EGLN3	NM_022073	1.57587
221511_PM_x_at	CCPG1	NM_004748 /// NM_020739	1.57761
1565558_PM_at	---	---	1.57772
227840_PM_at	C2orf76	NM_001017927	1.57944
208427_PM_s_at	ELAVL2	NM_001171195 /// NM_001171197 /// NM_004432	1.58109
202581_PM_at	HSPA1A /// HSPA1B	NM_005345 /// NM_005346	1.58261
1557129_PM_a_at	FAM111B	NM_001142703 /// NM_001142704 /// NM_198947	1.58263
244637_PM_at	---	---	1.58316
202438_PM_x_at	IDS	NM_000202 /// NM_001166550 /// NM_006123	1.58447
229317_PM_at	KPNA5	NM_002269	1.58455
227236_PM_at	TSPAN2	NM_005725	1.58549
204602_PM_at	DKK1	NM_012242	1.58619
226222_PM_at	KIAA1432	NM_001135920 /// NM_020829	1.58634
210510_PM_s_at	NRP1	NM_001024628 /// NM_001024629 /// NM_003873	1.58793
217762_PM_s_at	RAB31	NM_006868	1.59086
203729_PM_at	EMP3	NM_001425	1.5914
213603_PM_s_at	RAC2	NM_002872	1.5918
220198_PM_s_at	EIF5A2	NM_020390	1.59333
202458_PM_at	PRSS23	NM_007173	1.59356
227750_PM_at	KALRN	NM_001024660 /// NM_003947 /// NM_007064 /// NR_028136	1.59512
204615_PM_x_at	IDI1	NM_004508	1.59561

225912_PM_at	TP53INP1	NM_001135733 /// NM_033285	1.59618
1554004_PM_a_at	RGNEF	NM_001080479 /// NM_001177693	1.59647
221676_PM_s_at	CORO1C	NM_014325	1.59694
218196_PM_at	OSTM1	NM_014028	1.5973
228121_PM_at	TGFB2	NM_001135599 /// NM_003238	1.59781
204830_PM_x_at	PSG5	NM_001130014 /// NM_002781	1.59832
213956_PM_at	CEP350	NM_014810	1.59854
206429_PM_at	F2RL1	NM_005242	1.60018
212944_PM_at	SLC5A3	NM_006933	1.60046
236719_PM_at	---	---	1.60142
231270_PM_at	CA13	NM_198584	1.60172
203914_PM_x_at	HPGD	NM_000860 /// NM_001145816 /// NR_027332	1.6034
210830_PM_s_at	PON2	NM_000305 /// NM_001018161	1.60586
233587_PM_s_at	SIPA1L2	NM_020808	1.60683
222670_PM_s_at	MAFB	NM_005461	1.60801
213199_PM_at	C2CD3	NM_015531	1.60823
208622_PM_s_at	EZR	NM_001111077 /// NM_003379	1.61055
224823_PM_at	MYLK	NM_053025 /// NM_053026 /// NM_053027 /// NM_053028 /// NM_053031 /// NM_053032	1.61067
202213_PM_s_at	CUL4B	NM_001079872 /// NM_003588	1.61124
1558501_PM_at	DNM3	NM_001136127 /// NM_015569	1.61152
233085_PM_s_at	OBFC2A	NM_001031716 /// NR_024415	1.61173
204682_PM_at	LTBP2	NM_000428	1.61227
225059_PM_at	AGTRAP	NM_001040194 /// NM_001040195 /// NM_001040196 /// NM_001040197 /// NM_020350	1.61276
1554471_PM_a_at	ANKRD13C	NM_030816	1.61354

235264_PM_at	HCFC2	NM_013320	1.61357
221903_PM_s_at	CYLD	NM_001042355 /// NM_001042412 /// NM_015247	1.6143
211741_PM_x_at	PSG3	NM_021016	1.61435
212444_PM_at	---	---	1.6145
206117_PM_at	TPM1	NM_000366 /// NM_001018004 /// NM_001018005 /// NM_001018006 /// NM_001018007 /// NM_00	1.61481
214696_PM_at	C17orf91	NR_028502 /// NR_028503 /// NR_028504 /// NR_028505	1.61483
222717_PM_at	SDPR	NM_004657	1.61643
205767_PM_at	EREG	NM_001432	1.61777
210619_PM_s_at	HYAL1	NM_007312 /// NM_033159 /// NM_153281 /// NM_153282 /// NM_153283 /// NM_153285	1.61841
201108_PM_s_at	THBS1	NM_003246	1.61859
226189_PM_at	ITGB8	NM_002214	1.6188
238738_PM_at	PSMD7	NM_002811	1.61946
211260_PM_at	BMP7	NM_001719	1.61997
209506_PM_s_at	NR2F1	NM_005654	1.62112
223388_PM_s_at	ZFYVE1	NM_021260 /// NM_178441	1.62187
228596_PM_at	LOC728377	NR_033942	1.62193
208191_PM_x_at	PSG4	NM_002780 /// NM_213633	1.6222
208134_PM_x_at	PSG2	NM_031246	1.62244
203394_PM_s_at	HES1	NM_005524	1.62341
202551_PM_s_at	CRIM1	NM_016441	1.62395
229242_PM_at	---	---	1.62466
204401_PM_at	KCNN4	NM_002250	1.6247
201995_PM_at	EXT1	NM_000127	1.62524
222747_PM_s_at	SCML1	NM_001037535 /// NM_001037536 /// NM_001037540 /// NM_006746	1.626

1560818_PM_at	LOC100288701	---	1.62648
200800_PM_s_at	HSPA1A /// HSPA1B	NM_005345 /// NM_005346	1.62679
226462_PM_at	STXBP6	NM_014178	1.62929
236083_PM_at	BCL2L15	NM_001010922	1.62963
212327_PM_at	LIMCH1	NM_001112717 /// NM_001112718 /// NM_001112719 /// NM_001112720 /// NM_014988	1.63109
230050_PM_at	NACC2	NM_144653	1.63115
206584_PM_at	LY96	NM_001195797 /// NM_015364	1.63257
239155_PM_at	CXADR	NM_001338	1.63352
222942_PM_s_at	TIAM2	NM_001010927 /// NM_012454	1.63422
206570_PM_s_at	PSG11	NM_001113410 /// NM_002785 /// NM_203287	1.63526
223208_PM_at	KCTD10	NM_031954	1.63551
221566_PM_s_at	NOL3	NM_001185057 /// NM_001185058 /// NM_003946	1.63674
204635_PM_at	RPS6KA5	NM_004755 /// NM_182398	1.63958
215150_PM_at	YOD1	NM_018566	1.63974
214022_PM_s_at	IFITM1	NM_003641	1.63977
201564_PM_s_at	FSCN1	NM_003088	1.64052
219321_PM_at	MPP5	NM_022474	1.64218
224999_PM_at	EGFR	NM_005228 /// NM_201282 /// NM_201283 /// NM_201284	1.64329
228369_PM_at	CNPY3	NM_006586	1.64396
214663_PM_at	DSTYK	NM_015375 /// NM_199462	1.644
223595_PM_at	TMEM133	NM_032021	1.64463
212919_PM_at	DCP2	NM_152624	1.645
204077_PM_x_at	ENTPD4	NM_001128930 /// NM_004901	1.64554
229493_PM_at	LOC100506783	XR_108398 /// XR_112435 /// XR_113393	1.64794
227803_PM_at	ENPP5	NM_021572	1.64795

223232_PM_s_at	CGN	NM_020770	1.64967
235558_PM_at	RBMS2	NM_002898	1.65352
219181_PM_at	LIPG	NM_006033	1.65467
214183_PM_s_at	TKTL1	NM_001145933 /// NM_001145934 /// NM_012253	1.65796
214455_PM_at	HIST1H2BC	NM_003526	1.65829
202547_PM_s_at	ARHGEF7	NM_001113511 /// NM_001113512 /// NM_001113513 /// NM_003899 /// NM_145735	1.65981
203504_PM_s_at	ABCA1	NM_005502	1.66276
236979_PM_at	BCL2L15	NM_001010922	1.66342
209738_PM_x_at	PSG6	NM_001031850 /// NM_002782	1.66484
209568_PM_s_at	RGL1	NM_015149	1.66508
212190_PM_at	SERPINE2	NM_001136528 /// NM_001136530 /// NM_006216	1.66535
243610_PM_at	C9orf135	NM_001010940	1.66535
200632_PM_s_at	NDRG1	NM_001135242 /// NM_006096	1.66833
223418_PM_x_at	ANKRD13C	NM_030816	1.66859
210164_PM_at	GZMB	NM_004131	1.66866
222872_PM_x_at	OBFC2A	NM_001031716 /// NR_024415	1.66968
209146_PM_at	SC4MOL	NM_001017369 /// NM_006745	1.67077
221696_PM_s_at	STYK1	NM_018423	1.67147
235970_PM_at	LCORL	NM_001166139 /// NM_153686	1.67167
223233_PM_s_at	CGN	NM_020770	1.6717
203382_PM_s_at	APOE	NM_000041	1.673
226248_PM_s_at	KIAA1324	NM_020775	1.67341
214285_PM_at	FABP3	NM_004102	1.6735
227927_PM_at	---	---	1.67427
205645_PM_at	REPS2	NM_001080975 /// NM_004726	1.6748
1554757_PM_a_at	INPP5A	NM_005539	1.67813
225681_PM_at	CTHRC1	NM_138455	1.67814
227531_PM_at	---	---	1.67866

202439_PM_s_at	IDS	NM_000202 /// NM_001166550 /// NM_006123	1.67894
212298_PM_at	NRP1	NM_001024628 /// NM_001024629 /// NM_003873	1.67934
211333_PM_s_at	FASLG	NM_000639	1.68114
217230_PM_at	EZR	NM_001111077 /// NM_003379	1.68177
76897_PM_s_at	FKBP15	NM_015258	1.68228
202067_PM_s_at	LDLR	NM_000527 /// NM_001195798 /// NM_001195799 /// NM_001195800 /// NM_001195802 /// NM_00	1.68272
229017_PM_s_at	DSTYK	NM_015375 /// NM_199462	1.68275
221567_PM_at	NOL3	NM_001185057 /// NM_001185058 /// NM_003946	1.6954
203167_PM_at	TIMP2	NM_003255	1.69748
1555978_PM_s_at	---	---	1.69767
204823_PM_at	NAV3	NM_014903	1.69804
227370_PM_at	FAM171B	NM_177454	1.70096
203474_PM_at	IQGAP2	NM_006633	1.70099
229838_PM_at	NUCB2	NM_005013	1.7022
206706_PM_at	NTF3	NM_001102654 /// NM_002527	1.70395
205602_PM_x_at	PSG7	NM_002783	1.70465
211549_PM_s_at	HPGD	NM_000860 /// NM_001145816 /// NR_027332	1.70516
243362_PM_s_at	LOC641518	NR_029373 /// NR_029374	1.70535
209348_PM_s_at	MAF	NM_001031804 /// NM_005360	1.70592
205214_PM_at	STK17B	NM_004226	1.70606
215821_PM_x_at	PSG3	NM_021016	1.70717
1558208_PM_at	TARDBP	NM_007375	1.70762
1557128_PM_at	FAM111B	NM_001142703 /// NM_001142704 /// NM_198947	1.70834
203706_PM_s_at	FZD7	NM_003507	1.71008

201109_PM_s_at	THBS1	NM_003246	1.71212
242037_PM_at	---	---	1.71356
202965_PM_s_at	CAPN6	NM_014289	1.71441
203705_PM_s_at	FZD7	NM_003507	1.71471
225328_PM_at	---	---	1.71792
224279_PM_s_at	CABYR	NM_012189 /// NM_138643 /// NM_138644 /// NM_153768 /// NM_153769 /// NM_153770	1.7181
207279_PM_s_at	NEBL	NM_001173484 /// NM_006393 /// NM_213569	1.71868
242762_PM_s_at	FAM171B	NM_177454	1.71874
229256_PM_at	PGM2L1	NM_173582	1.7192
226625_PM_at	TGFBR3	NM_001195683 /// NM_001195684 /// NM_003243 /// NR_036634	1.72004
210257_PM_x_at	CUL4B	NM_001079872 /// NM_003588	1.72112
211538_PM_s_at	HSPA2	NM_021979	1.72396
202083_PM_s_at	SEC14L1	NM_001039573 /// NM_001143998 /// NM_001143999 /// NM_001144001 /// NM_003003	1.72594
49077_PM_at	PPME1	NM_016147	1.72813
222173_PM_s_at	TBC1D2	NM_018421	1.72921
214091_PM_s_at	GPX3	NM_002084	1.73137
203471_PM_s_at	PLEK	NM_002664	1.73224
209594_PM_x_at	PSG9	NM_002784	1.73245
214247_PM_s_at	DKK3	NM_001018057 /// NM_013253 /// NM_015881	1.73366
227752_PM_at	SPTLC3	NM_018327	1.73475
225373_PM_at	C10orf54	NM_022153	1.73546
207433_PM_at	IL10	NM_000572	1.73588
208257_PM_x_at	PSG1	NM_001184825 /// NM_001184826 /// NM_006905	1.74035
209772_PM_s_at	CD24	NM_013230	1.7406

202086_PM_at	MX1	NM_001144925 /// NM_001178046 /// NM_002462	1.74128
200799_PM_at	HSPA1A	NM_005345	1.74239
1554327_PM_a_at	CANT1	NM_001159772 /// NM_001159773 /// NM_138793	1.74611
219603_PM_s_at	ZNF226	NM_001032372 /// NM_001032373 /// NM_001032374 /// NM_001146220 /// NM_015919	1.74648
220921_PM_at	SPANXB1 /// SPANXB2 /// SPANXF1	NM_032461 /// NM_139019 /// NM_145664	1.74956
202196_PM_s_at	DKK3	NM_001018057 /// NM_013253 /// NM_015881	1.74986
211671_PM_s_at	NR3C1	NM_000176 /// NM_001018074 /// NM_001018075 /// NM_001018076 /// NM_001018077 /// NM_00	1.74999
229004_PM_at	ADAMTS15	NM_139055	1.75429
218793_PM_s_at	SCML1	NM_001037535 /// NM_001037536 /// NM_001037540 /// NM_006746	1.75447
230954_PM_at	C20orf112	NM_080616	1.75541
209879_PM_at	SELPLG	NM_003006	1.75575
205034_PM_at	CCNE2	NM_057749	1.75741
229999_PM_at	LOC100128416	---	1.75742
227123_PM_at	RAB3B	NM_002867	1.75792
226460_PM_at	FNIP2	NM_020840	1.75936
239814_PM_at	LOC100506860	XR_108813 /// XR_108814 /// XR_110749 /// XR_110750 /// XR_113050 /// XR_113051 /// XR_	1.76244
208621_PM_s_at	EZR	NM_001111077 /// NM_003379	1.76316
202510_PM_s_at	TNFAIP2	NM_006291	1.76588

171

217173_PM_s_at	LDLR	NM_000527 /// NM_001195798 /// NM_001195799 /// NM_001195800 /// NM_001195802 /// NM_00	1.76869
230831_PM_at	FRMD5	NM_032892	1.77459
239303_PM_at	PIWIL2	NM_001135721 /// NM_018068	1.77582
227566_PM_at	NTM	NM_001048209 /// NM_001144058 /// NM_001144059 /// NM_016522	1.77609
206132_PM_at	MCC	NM_001085377 /// NM_002387	1.77724
244321_PM_at	PGAP1	NM_024989	1.78204
235619_PM_at	ASB4 /// LOC285986	NM_016116 /// NM_145872	1.7829
230047_PM_at	ARHGAP42	NM_152432	1.78304
204588_PM_s_at	SLC7A7	NM_001126105 /// NM_001126106 /// NM_003982	1.78428
225941_PM_at	EIF4E3	NM_001134649 /// NM_001134650 /// NM_001134651 /// NM_173359	1.78576
1554493_PM_s_at	THADA	NM_001083953 /// NM_022065	1.78635
210935_PM_s_at	WDR1	NM_005112 /// NM_017491	1.79493
210538_PM_s_at	BIRC3	NM_001165 /// NM_182962	1.7952
204044_PM_at	QPRT	NM_014298	1.79525
201983_PM_s_at	EGFR	NM_005228 /// NM_201282 /// NM_201283 /// NM_201284	1.79635
1553313_PM_s_at	SLC5A3	NM_006933	1.79686
204415_PM_at	IFI6	NM_002038 /// NM_022872 /// NM_022873	1.80067
221127_PM_s_at	DKK3	NM_001018057 /// NM_013253 /// NM_015881	1.80079

		NM_001003715 /// NM_001003716 ///	
211468_PM_s_at	RECQL5	NM_004259	1.80674
218559_PM_s_at	MAFB	NM_005461	1.81066
202627_PM_s_at	SERPINE1	NM_000602 /// NM_001165413	1.81117
1556309_PM_s_at	C1orf86 /// LOC100128003	NM_001146310 /// NM_182533 /// NR_024445	1.81448
1554114_PM_s_at	SSH2	NM_033389	1.81568
219687_PM_at	HHAT	NM_001122834 /// NM_001170564 /// NM_001170580 /// NM_001170587 /// NM_001170588 /// NM	1.81886
214329_PM_x_at	TNFSF10	NM_001190942 /// NM_001190943 /// NM_003810 /// NR_033994	1.82518
207980_PM_s_at	CITED2	NM_001168388 /// NM_001168389 /// NM_006079	1.82668
205399_PM_at	DCLK1	NM_001195415 /// NM_001195416 /// NM_001195430 /// NM_004734	1.83121
210002_PM_at	GATA6	NM_005257	1.83152
201012_PM_at	ANXA1	NM_000700	1.83359
230652_PM_at	ARAF	NM_001654	1.83472
202901_PM_x_at	CTSS	NM_004079	1.83697
228158_PM_at	LOC645166	NR_027354 /// NR_027355 /// NR_027356	1.83819
229759_PM_s_at	VEPH1	NM_001167911 /// NM_001167912 /// NM_001167915 /// NM_001167916 /// NM_001167917 /// NM	1.84169
217841_PM_s_at	PPME1	NM_016147	1.85263
229441_PM_at	PRSS23	NM_007173	1.85366
208115_PM_x_at	C10orf137	NM_015608	1.85539
203505_PM_at	ABCA1	NM_005502	1.85581
203108_PM_at	GPRC5A	NM_003979	1.85855

212325_PM_at	LIMCH1	NM_001112717 /// NM_001112718 /// NM_001112719 /// NM_001112720 /// NM_014988	1.86241
212845_PM_at	SAMD4A	NM_001161576 /// NM_001161577 /// NM_015589	1.86244
230363_PM_s_at	INPP5F	NM_014937 /// NR_003251 /// NR_003252	1.86522
237145_PM_at	EIF2AK4	NM_001013703	1.86588
222693_PM_at	FNDC3B	NM_001135095 /// NM_022763	1.87117
232397_PM_at	LOC100507039	XR_108413 /// XR_108414	1.8742
222810_PM_s_at	RASAL2	NM_004841 /// NM_170692	1.87442
227926_PM_s_at	NBPF11 /// NBPF12 /// NBPF24	NM_001101663 /// NM_183372 /// XM_001715810	1.87788
228284_PM_at	TLE1	NM_005077	1.88123
218717_PM_s_at	LEPREL1	NM_001134418 /// NM_018192	1.88172
202628_PM_s_at	SERPINE1	NM_000602 /// NM_001165413	1.88325
219655_PM_at	C7orf10	NM_001193311 /// NM_001193312 /// NM_001193313 /// NM_024728	1.88405
214748_PM_at	N4BP2L2	NM_014887 /// NM_033111	1.88411
225922_PM_at	FNIP2	NM_020840	1.88729
205801_PM_s_at	RASGRP3	NM_001139488 /// NM_015376 /// NM_170672	1.88847
204437_PM_s_at	FOLR1	NM_000802 /// NM_016724 /// NM_016725 /// NM_016729	1.88905
207733_PM_x_at	PSG9	NM_002784	1.88921

216442_PM_x_at	FN1	NM_002026 /// NM_054034 /// NM_212474 /// NM_212476 /// NM_212478 /// NM_212482	1.89031
225924_PM_at	FNIP2	NM_020840	1.89039
239678_PM_at	---	---	1.89085
219014_PM_at	PLAC8	NM_001130715 /// NM_001130716 /// NM_016619	1.89713
220265_PM_at	GPR107	NM_001136557 /// NM_001136558 /// NM_020960	1.90845
220111_PM_s_at	ANO2	NM_020373	1.92518
211719_PM_x_at	FN1	NM_002026 /// NM_054034 /// NM_212474 /// NM_212476 /// NM_212478 /// NM_212482	1.92606
225123_PM_at	---	---	1.92757
204471_PM_at	GAP43	NM_001130064 /// NM_002045	1.93104
219836_PM_at	ZBED2	NM_024508	1.93603
210004_PM_at	OLR1	NM_001172632 /// NM_001172633 /// NM_002543	1.93603
211548_PM_s_at	HPGD	NM_000860 /// NM_001145816 /// NR_027332	1.93877
213069_PM_at	HEG1	NM_020733	1.94034
241014_PM_at	LOC339400	XR_108352 /// XR_111940 /// XR_114805	1.94662
219944_PM_at	CLIP4	NM_024692	1.95057
215997_PM_s_at	CUL4B	NM_001079872 /// NM_003588	1.95074
222963_PM_s_at	IL1RAPL1	NM_014271	1.95879
216379_PM_x_at	CD24	NM_013230	1.96449
1562960_PM_at	LOC338653	---	1.97664
202803_PM_s_at	ITGB2	NM_000211 /// NM_001127491	1.9771
206508_PM_at	CD70	NM_001252	1.97794

		NM_001112717 /// NM_001112718 /// NM_001112719 /// NM_001112720 ///	
212328_PM_at	LIMCH1	NM_014988	1.98133
201110_PM_s_at	THBS1	NM_003246	1.98482
204731_PM_at	TGFBR3	NM_001195683 /// NM_001195684 /// NM_003243 /// NR_036634	1.98529
212464_PM_s_at	FN1	NM_002026 /// NM_054034 /// NM_212474 /// NM_212476 /// NM_212478 /// NM_212482	1.98766
230487_PM_at	C6orf99	NM_001195032	1.99526
203381_PM_s_at	APOE	NM_000041	1.99638
228551_PM_at	DENND5B	NM_144973	1.99957
236656_PM_s_at	LOC100288911	XR_108260 /// XR_109968 /// XR_115525	2.00259
203305_PM_at	F13A1	NM_000129	2.00397
209357_PM_at	CITED2	NM_001168388 /// NM_001168389 /// NM_006079	2.0084
210495_PM_x_at	FN1	NM_002026 /// NM_054034 /// NM_212474 /// NM_212476 /// NM_212478 /// NM_212482	2.01481
266_PM_s_at	CD24	NM_013230	2.01694
229412_PM_at	TAF8	NM_138572	2.01998
1553708_PM_at	MGC16075	XR_000600 /// XR_000617 /// XR_001277	2.02565
212822_PM_at	HEG1	NM_020733	2.0337
202638_PM_s_at	ICAM1	NM_000201	2.03569
225491_PM_at	SLC1A2	NM_001195728 /// NM_004171	2.03903

208228_PM_s_at	FGFR2	NM_000141 /// NM_001144913 /// NM_001144914 /// NM_001144915 /// NM_001144916 /// NM_00	2.04227
205104_PM_at	SNPH	NM_014723	2.04294
202688_PM_at	TNFSF10	NM_001190942 /// NM_001190943 /// NM_003810 /// NR_033994	2.04891
207761_PM_s_at	METTL7A	NM_014033	2.05926
202800_PM_at	SLC1A3	NM_001166695 /// NM_001166696 /// NM_004172	2.06912
225847_PM_at	NCEH1	NM_001146276 /// NM_001146277 /// NM_001146278 /// NM_020792	2.07182
209771_PM_x_at	CD24	NM_013230	2.07521
239203_PM_at	C7orf53	NM_001134468 /// NM_182597	2.07597
225207_PM_at	PDK4	NM_002612	2.0782
1554364_PM_at	PPP2R5C	NM_001161725 /// NM_001161726 /// NM_002719 /// NM_178586 /// NM_178587	2.08137
222862_PM_s_at	AK5	NM_012093 /// NM_174858	2.08229
202687_PM_s_at	TNFSF10	NM_001190942 /// NM_001190943 /// NM_003810 /// NR_033994	2.10634
214476_PM_at	TFF2	NM_005423	2.10699
206523_PM_at	CYTH3	NM_004227	2.11618
239202_PM_at	RAB3B	NM_002867	2.14163
230508_PM_at	DKK3	NM_001018057 /// NM_013253 /// NM_015881	2.14737
230121_PM_at	C1orf133	NR_024337	2.15723
228885_PM_at	MAMDC2	NM_153267	2.17373
220663_PM_at	IL1RAPL1	NM_014271	2.21768

		NM_012189 /// NM_138643 /// NM_138644 /// NM_153768 /// NM_153769 ///	
219928_PM_s_at	CABYR	NM_153770	2.22377
203845_PM_at	KAT2B	NM_003884	2.2336
204818_PM_at	HSD17B2	NM_002153	2.23849
201163_PM_s_at	IGFBP7	NM_001553	2.23967
227484_PM_at	SRGAP1	NM_020762	2.24848
240089_PM_at	---	---	2.25269
209037_PM_s_at	EHD1	NM_006795	2.2843
1552546_PM_a_at	LETM2	NM_144652	2.33461
1569470_PM_a_at	FRMD5	NM_032892	2.3398
202902_PM_s_at	CTSS	NM_004079	2.35946
1554010_PM_at	NDST1	NM_001543	2.38454
208651_PM_x_at	CD24	NM_013230	2.39914
214456_PM_x_at	SAA1 /// SAA2	NM_000331 /// NM_001127380 /// NM_001178006 /// NM_030754 /// NM_199161	2.40256
229041_PM_s_at	---	---	2.41547
208650_PM_s_at	CD24	NM_013230	2.41638
211814_PM_s_at	CCNE2	NM_057749	2.4419
201162_PM_at	IGFBP7	NM_001553	2.49832
232060_PM_at	ROR1	NM_001083592 /// NM_005012	2.50328
205924_PM_at	RAB3B	NM_002867	2.51551
209904_PM_at	TNNC1	NM_003280	2.53513
201289_PM_at	CYR61	NM_001554	2.54444
226425_PM_at	CLIP4	NM_024692	2.62045
227345_PM_at	TNFRSF10D	NM_003840	2.64458
232914_PM_s_at	SYTL2	NM_001162951 /// NM_001162952 /// NM_001162953 /// NM_032379 /// NM_032943 /// NM_20692	2.67453
209684_PM_at	RIN2	NM_018993	2.6756
210764_PM_s_at	CYR61	NM_001554	2.70487

208607_PM_s_at	SAA1 /// SAA2	NM_000331 /// NM_001127380 /// NM_001178006 /// NM_030754 /// NM_199161	2.76187
220158_PM_at	LGALS14	NM_020129 /// NM_203471	2.81139
233537_PM_at	KRTAP3-1	NM_031958	2.86541
217228_PM_s_at	ASB4	NM_016116 /// NM_145872	2.96288
229380_PM_at	---	---	2.98811
200665_PM_s_at	SPARC	NM_003118	3.29503
1552348_PM_at	PRSS33	NM_152891	3.32338
1562722_PM_at	PRR20A /// PRR20B /// PRR20C /// PRR20D /// PRR20E	NM_001130404 /// NM_001130405 /// NM_001130406 /// NM_001130407 /// NM_198441	3.3548
239201_PM_at	CDK15	NM_139158	3.43917
207096_PM_at	SAA4	NM_006512	3.47118
225496_PM_s_at	SYTL2	NM_001162951 /// NM_001162952 /// NM_001162953 /// NM_032379 /// NM_032943 /// NM_20692	3.55404
237732_PM_at	PRR9	NM_001195571	3.60694
1553995_PM_a_at	NT5E	NM_002526	3.71625
203939_PM_at	NT5E	NM_002526	3.99018
235818_PM_at	VSTM1	NM_198481	4.65915
1553994_PM_at	NT5E	NM_002526	5.96951

Table 9. **Probeset ID, gene symbol, refseq transcript ID and fold change from microarray analysis of SW480^{FJX1} treated with scramble siRNA (siSCR) versus SW480^{FJX1} treated with *HIF1A* specific siRNA (*siHIF*) colon cancer cells.**

Probeset ID	Gene Symbol	RefSeq Transcript ID	Fold-Change (FJX1 siIHIF vs. FJX1 siSCR)
200989_PM_at	HIF1A	NM_001530 /// NM_181054	-2.47572
212992_PM_at	AHNAK2	NM_138420	-1.74224
215785_PM_s_at	CYFIP2	NM_001037332 /// NM_001037333 /// NM_014376	-1.71622
212343_PM_at	YIPF6	NM_001195214 /// NM_173834	-1.70336
235023_PM_at	VPS13C	NM_001018088 /// NM_017684 /// NM_018080 /// NM_020821	-1.69819
241367_PM_at	TEX19	NM_207459	-1.66703
232890_PM_at	---	---	-1.64772
239917_PM_at	VPS8	NM_001009921 /// NM_015303	-1.64178
203542_PM_s_at	KLF9	NM_001206	-1.64177
237119_PM_at	---	---	-1.63131
209695_PM_at	PTP4A3	NM_007079 /// NM_032611	-1.61265
211184_PM_s_at	USH1C	NM_005709 /// NM_153676	-1.60949
232549_PM_at	RBM11	NM_144770	-1.60642
241624_PM_at	LOC389834	NR_027420	-1.5903
225812_PM_at	C6orf225	NM_001033564	-1.58729
243356_PM_at	---	---	-1.57508
204698_PM_at	ISG20	NM_002201	-1.57446
212340_PM_at	YIPF6	NM_001195214 /// NM_173834	-1.57377
228771_PM_at	ADRBK2	NM_005160	-1.57376
222375_PM_at	---	---	-1.5659
240180_PM_at	---	---	-1.56173

201540_PM_at	FHL1	NM_001159699 /// NM_001159700 /// NM_001159701 /// NM_001159702 /// NM_001159703 /// NM	-1.55843
1553502_PM_a_at	PALM2	NM_001037293 /// NM_053016	-1.54023
212843_PM_at	NCAM1	NM_000615 /// NM_001076682 /// NM_181351	-1.54008
231024_PM_at	LOC572558	NR_015423	-1.53683
212342_PM_at	YIPF6	NM_001195214 /// NM_173834	-1.53234
227417_PM_at	MOSC2	NM_017898	-1.52879
226576_PM_at	ARHGAP26	NM_001135608 /// NM_015071	-1.52555
220576_PM_at	PGAP1	NM_024989	-1.52462
229011_PM_at	---	---	-1.52389
211157_PM_at	---	---	-1.5201
231964_PM_at	---	---	-1.5194
232796_PM_at	---	---	-1.51873
242869_PM_at	---	---	-1.51805
210718_PM_s_at	ARL17A /// LOC100294341	NM_001113738 /// NM_016632 /// XM_002344068	-1.51668
222061_PM_at	CD58	NM_001144822 /// NM_001779 /// NR_026665	-1.5158
210102_PM_at	VWA5A	NM_001130142 /// NM_014622 /// NM_198315	-1.51549
1570588_PM_at	---	---	-1.51274
219726_PM_at	NLGN3	NM_001166660 /// NM_018977 /// NM_181303	-1.51234
214660_PM_at	ITGA1	NM_181501	-1.51162
1556951_PM_at	---	---	-1.50907
236322_PM_at	---	---	-1.50895
201925_PM_s_at	CD55	NM_000574 /// NM_001114752	-1.50861
203158_PM_s_at	GLS	NM_014905	-1.50727
225912_PM_at	TP53INP1	NM_001135733 /// NM_033285	1.5002
218954_PM_s_at	BRF2	NM_018310	1.50162
207702_PM_s_at	MAGI2	NM_012301	1.50256

235762_PM_at	TAS2R14	NM_023922	1.50851
216255_PM_s_at	GRM8	NM_000845 /// NM_001127323 /// NR_028041	1.50973
204653_PM_at	TFAP2A	NM_001032280 /// NM_001042425 /// NM_003220	1.5099
225990_PM_at	BOC	NM_033254	1.51277
1555543_PM_a_at	CLCC1	NM_001048210 /// NM_015127	1.51338
231538_PM_at	C11orf1	NM_022761	1.51414
235424_PM_at	---	---	1.51449
219517_PM_at	ELL3 /// SERINC4	NM_001033517 /// NM_025165	1.5226
222484_PM_s_at	CXCL14	NM_004887	1.52742
206022_PM_at	NDP	NM_000266	1.52755
220394_PM_at	FGF20	NM_019851	1.52981
238528_PM_at	UBR1	NM_174916	1.53069
228915_PM_at	DACH1	NM_004392 /// NM_080759 /// NM_080760	1.53556
208228_PM_s_at	FGFR2	NM_000141 /// NM_001144913 /// NM_001144914 /// NM_001144915 /// NM_001144916 /// NM_00	1.537
215358_PM_x_at	ZNF37BP	NR_026777	1.53709
241239_PM_at	---	---	1.53914
206706_PM_at	NTF3	NM_001102654 /// NM_002527	1.54019
228325_PM_at	KIAA0146	NM_001080394	1.54893
230755_PM_at	RHBDL3	NM_138328	1.55084
226775_PM_at	ENY2	NM_001193557 /// NM_020189 /// NR_036471 /// NR_036472	1.55461
230278_PM_at	---	---	1.55478
215283_PM_at	LOC339290	NR_015389	1.55666
216379_PM_x_at	CD24	NM_013230	1.55706
203221_PM_at	TLE1	NM_005077	1.55708
236213_PM_at	---	---	1.56203
209684_PM_at	RIN2	NM_018993	1.5636
236163_PM_at	LIX1	NM_153234	1.57
218002_PM_s_at	CXCL14	NM_004887	1.57267

182

206432_PM_at	HAS2	NM_005328	1.57506
1559382_PM_at	C19orf42	NM_024104	1.57526
1562736_PM_at	LHX9	NM_001014434 /// NM_020204	1.57781
208998_PM_at	UCP2	NM_003355	1.58208
228284_PM_at	TLE1	NM_005077	1.58477
225491_PM_at	SLC1A2	NM_001195728 /// NM_004171	1.58593
1557149_PM_at	---	---	1.58937
229041_PM_s_at	---	---	1.59153
241709_PM_s_at	DOCK1	NM_001380	1.5962
236656_PM_s_at	LOC100288911	XR_108260 /// XR_109968 /// XR_115525	1.60813
200974_PM_at	ACTA2	NM_001141945 /// NM_001613	1.61099
213169_PM_at	SEMA5A	NM_003966	1.61139
227124_PM_at	LOC221710	NM_001135575	1.6175
242923_PM_at	ZNF678	NM_178549 /// NR_033184	1.62247
210964_PM_s_at	GYG2	NM_001079855 /// NM_001184702 /// NM_001184703 /// NM_001184704 /// NM_003918	1.62362
236937_PM_at	LOC100505729	XR_108524 /// XR_112552 /// XR_113551	1.63659
213830_PM_at	TRD@	---	1.64197
239482_PM_x_at	ZNF708	NM_021269	1.65647
238761_PM_at	ELK4	NM_001973 /// NM_021795	1.66864
227760_PM_at	IGFBPL1	NM_001007563	1.68164
209348_PM_s_at	MAF	NM_001031804 /// NM_005360	1.68749
211814_PM_s_at	CCNE2	NM_057749	1.70147
208651_PM_x_at	CD24	NM_013230	1.70962
214456_PM_x_at	SAA1 /// SAA2	NM_000331 /// NM_001127380 /// NM_001178006 /// NM_030754 /// NM_199161	1.75096
207096_PM_at	SAA4	NM_006512	1.75267
209771_PM_x_at	CD24	NM_013230	1.77005

208650_PM_s_at	CD24	NM_013230	1.7919
208607_PM_s_at	SAA1 /// SAA2	NM_000331 /// NM_001127380 /// NM_001178006 /// NM_030754 /// NM_199161	1.94786
206363_PM_at	MAF	NM_001031804 /// NM_005360	2.01026
212909_PM_at	LYPD1	NM_001077427 /// NM_144586	2.06227
227566_PM_at	NTM	NM_001048209 /// NM_001144058 /// NM_001144059 /// NM_016522	2.08625
208399_PM_s_at	EDN3	NM_000114 /// NM_207032 /// NM_207033 /// NM_207034	2.12032
227752_PM_at	SPTLC3	NM_018327	2.16876

REFERENCES

1. Siegel R, Naishadham D, Jemal A Cancer statistics, 2013. CA Cancer J Clin 63: 11-30.
2. Fearon ER, Vogelstein B (1990) A genetic model for colorectal tumorigenesis. Cell 61: 759-767.
3. Tai HH, Ensor CM, Tong M, Zhou H, Yan F (2002) Prostaglandin catabolizing enzymes. Prostaglandins Other Lipid Mediat 68-69: 483-493.
4. Eberhart CE, Coffey RJ, Radhika A, Giardiello FM, Ferrenbach S, et al. (1994) Up-regulation of cyclooxygenase 2 gene expression in human colorectal adenomas and adenocarcinomas. Gastroenterology 107: 1183-1188.
5. Kargman SL, O'Neill GP, Vickers PJ, Evans JF, Mancini JA, et al. (1995) Expression of prostaglandin G/H synthase-1 and -2 protein in human colon cancer. Cancer Res 55: 2556-2559.
6. Sano H, Kawahito Y, Wilder RL, Hashiramoto A, Mukai S, et al. (1995) Expression of cyclooxygenase-1 and -2 in human colorectal cancer. Cancer Res 55: 3785-3789.
7. Rigas B, Goldman IS, Levine L (1993) Altered eicosanoid levels in human colon cancer. J Lab Clin Med 122: 518-523.
8. Yaqub S, Henjum K, Mahic M, Jahnsen FL, Aandahl EM, et al. (2008) Regulatory T cells in colorectal cancer patients suppress anti-tumor immune activity in a COX-2 dependent manner. Cancer Immunol Immunother 57: 813-821.
9. Murphey LJ, Williams MK, Sanchez SC, Byrne LM, Csiki I, et al. (2004) Quantification of the major urinary metabolite of PGE2 by a liquid chromatographic/mass spectrometric assay: determination of cyclooxygenase-specific PGE2 synthesis in healthy humans and those with lung cancer. Anal Biochem 334: 266-275.
10. Johnson JC, Schmidt CR, Shrubsole MJ, Billheimer DD, Joshi PR, et al. (2006) Urine PGE-M: A metabolite of prostaglandin E2 as a potential biomarker of advanced colorectal neoplasia. Clin Gastroenterol Hepatol 4: 1358-1365.
11. Shrubsole MJ, Cai Q, Wen W, Milne G, Smalley WE, et al. (2012) Urinary prostaglandin E2 metabolite and risk for colorectal adenoma. Cancer Prev Res (Phila) 5: 336-342.
12. Ogino S, Kirkner GJ, Nosho K, Irahara N, Kure S, et al. (2008) Cyclooxygenase-2 expression is an independent predictor of poor prognosis in colon cancer. Clin Cancer Res 14: 8221-8227.
13. Oshima M, Dinchuk JE, Kargman SL, Oshima H, Hancock B, et al. (1996) Suppression of intestinal polyposis in Apc delta716 knockout mice by inhibition of cyclooxygenase 2 (COX-2). Cell 87: 803-809.
14. Chulada PC, Thompson MB, Mahler JF, Doyle CM, Gaul BW, et al. (2000) Genetic disruption of Ptgs-1, as well as Ptgs-2, reduces intestinal tumorigenesis in Min mice. Cancer Res 60: 4705-4708.
15. Sonoshita M, Takaku K, Sasaki N, Sugimoto Y, Ushikubi F, et al. (2001) Acceleration of intestinal polyposis through prostaglandin receptor EP2 in Apc(Delta 716) knockout mice. Nat Med 7: 1048-1051.
16. Mutoh M, Watanabe K, Kitamura T, Shoji Y, Takahashi M, et al. (2002) Involvement of prostaglandin E receptor subtype EP(4) in colon carcinogenesis. Cancer Res 62: 28-32.
17. Watanabe K, Kawamori T, Nakatsugi S, Ohta T, Ohuchida S, et al. (1999) Role of the prostaglandin E receptor subtype EP1 in colon carcinogenesis. Cancer Res 59: 5093-5096.

18. Wang D, Wang H, Shi Q, Katkuri S, Walhi W, et al. (2004) Prostaglandin E(2) promotes colorectal adenoma growth via transactivation of the nuclear peroxisome proliferator-activated receptor delta. Cancer Cell 6: 285-295.

19. Kawamori T, Uchiya N, Sugimura T, Wakabayashi K (2003) Enhancement of colon carcinogenesis by prostaglandin E2 administration. Carcinogenesis 24: 985-990.

20. Yan M, Rerko RM, Platzer P, Dawson D, Willis J, et al. (2004) 15-Hydroxyprostaglandin dehydrogenase, a COX-2 oncogene antagonist, is a TGF-beta-induced suppressor of human gastrointestinal cancers. Proc Natl Acad Sci U S A 101: 17468-17473.

21. Backlund MG, Mann JR, Holla VR, Buchanan FG, Tai HH, et al. (2005) 15-Hydroxyprostaglandin dehydrogenase is down-regulated in colorectal cancer. J Biol Chem 280: 3217-3223.

22. Myung SJ, Rerko RM, Yan M, Platzer P, Guda K, et al. (2006) 15-Hydroxyprostaglandin dehydrogenase is an in vivo suppressor of colon tumorigenesis. Proc Natl Acad Sci U S A 103: 12098-12102.

23. Rostom A, Dube C, Lewin G, Tsertsvadze A, Barrowman N, et al. (2007) Nonsteroidal anti-inflammatory drugs and cyclooxygenase-2 inhibitors for primary prevention of colorectal cancer: a systematic review prepared for the U.S. Preventive Services Task Force. Ann Intern Med 146: 376-389.

24. Bertagnolli MM, Eagle CJ, Zauber AG, Redston M, Solomon SD, et al. (2006) Celecoxib for the prevention of sporadic colorectal adenomas. N Engl J Med 355: 873-884.

25. Arber N, Eagle CJ, Spicak J, Racz I, Dite P, et al. (2006) Celecoxib for the prevention of colorectal adenomatous polyps. N Engl J Med 355: 885-895.

26. Steinbach G, Lynch PM, Phillips RK, Wallace MH, Hawk E, et al. (2000) The effect of celecoxib, a cyclooxygenase-2 inhibitor, in familial adenomatous polyposis. N Engl J Med 342: 1946-1952.

27. Baron JA, Cole BF, Sandler RS, Haile RW, Ahnen D, et al. (2003) A randomized trial of aspirin to prevent colorectal adenomas. N Engl J Med 348: 891-899.

28. Baron JA, Sandler RS, Bresalier RS, Quan H, Riddell R, et al. (2006) A randomized trial of rofecoxib for the chemoprevention of colorectal adenomas. Gastroenterology 131: 1674-1682.

29. Benamouzig R, Deyra J, Martin A, Girard B, Jullian E, et al. (2003) Daily soluble aspirin and prevention of colorectal adenoma recurrence: one-year results of the APACC trial. Gastroenterology 125: 328-336.

30. Sandler RS, Halabi S, Baron JA, Budinger S, Paskett E, et al. (2003) A randomized trial of aspirin to prevent colorectal adenomas in patients with previous colorectal cancer. N Engl J Med 348: 883-890.

31. Yan M, Myung SJ, Fink SP, Lawrence E, Lutterbaugh J, et al. (2009) 15-Hydroxyprostaglandin dehydrogenase inactivation as a mechanism of resistance to celecoxib chemoprevention of colon tumors. Proc Natl Acad Sci U S A 106: 9409-9413.

32. Hansen-Petrik MB, McEntee MF, Jull B, Shi H, Zemel MB, et al. (2002) Prostaglandin E(2) protects intestinal tumors from nonsteroidal anti-inflammatory drug-induced regression in Apc(Min/+) mice. Cancer Res 62: 403-408.

33. Kober L, Swedberg K, McMurray JJ, Pfeffer MA, Velazquez EJ, et al. (2006) Previously known and newly diagnosed atrial fibrillation: a major risk indicator after a myocardial infarction complicated by heart failure or left ventricular dysfunction. Eur J Heart Fail 8: 591-598.

34. Folkman J, Watson K, Ingber D, Hanahan D (1989) Induction of angiogenesis during the transition from hyperplasia to neoplasia. Nature 339: 58-61.

35. Takebayashi Y, Aklyama S, Yamada K, Akiba S, Aikou T (1996) Angiogenesis as an unfavorable prognostic factor in human colorectal carcinoma. Cancer 78: 226-231.
36. Vermeulen PB, Van den Eynden GG, Huget P, Goovaerts G, Weyler J, et al. (1999) Prospective study of intratumoral microvessel density, p53 expression and survival in colorectal cancer. Br J Cancer 79: 316-322.
37. Brown LF, Berse B, Jackman RW, Tognazzi K, Manseau EJ, et al. (1993) Expression of vascular permeability factor (vascular endothelial growth factor) and its receptors in adenocarcinomas of the gastrointestinal tract. Cancer Res 53: 4727-4735.
38. Amaya H, Tanigawa N, Lu C, Matsumura M, Shimomatsuya T, et al. (1997) Association of vascular endothelial growth factor expression with tumor angiogenesis, survival and thymidine phosphorylase/platelet-derived endothelial cell growth factor expression in human colorectal cancer. Cancer Lett 119: 227-235.
39. Stoeltzing O, Liu W, Reinmuth N, Parikh A, Ahmad SA, et al. (2003) Angiogenesis and antiangiogenic therapy of colon cancer liver metastasis. Ann Surg Oncol 10: 722-733.
40. Tsujii M, Kawano S, Tsuji S, Sawaoka H, Hori M, et al. (1998) Cyclooxygenase regulates angiogenesis induced by colon cancer cells. Cell 93: 705-716.
41. Williams CS, Tsujii M, Reese J, Dey SK, DuBois RN (2000) Host cyclooxygenase-2 modulates carcinoma growth. J Clin Invest 105: 1589-1594.
42. Masferrer JL, Leahy KM, Koki AT, Zweifel BS, Settle SL, et al. (2000) Antiangiogenic and antitumor activities of cyclooxygenase-2 inhibitors. Cancer Res 60: 1306-1311.
43. Leahy KM, Ornberg RL, Wang Y, Zweifel BS, Koki AT, et al. (2002) Cyclooxygenase-2 inhibition by celecoxib reduces proliferation and induces apoptosis in angiogenic endothelial cells in vivo. Cancer Res 62: 625-631.
44. Zhong H, De Marzo AM, Laughner E, Lim M, Hilton DA, et al. (1999) Overexpression of hypoxia-inducible factor 1alpha in common human cancers and their metastases. Cancer Res 59: 5830-5835.
45. Keith B, Johnson RS, Simon MC (2012) HIF1alpha and HIF2alpha: sibling rivalry in hypoxic tumour growth and progression. Nat Rev Cancer 12: 9-22.
46. Semenza GL (2003) Targeting HIF-1 for cancer therapy. Nat Rev Cancer 3: 721-732.
47. Forsythe JA, Jiang BH, Iyer NV, Agani F, Leung SW, et al. (1996) Activation of vascular endothelial growth factor gene transcription by hypoxia-inducible factor 1. Mol Cell Biol 16: 4604-4613.
48. Kaidi A, Qualtrough D, Williams AC, Paraskeva C (2006) Direct transcriptional up-regulation of cyclooxygenase-2 by hypoxia-inducible factor (HIF)-1 promotes colorectal tumor cell survival and enhances HIF-1 transcriptional activity during hypoxia. Cancer Res 66: 6683-6691.
49. Ravi R, Mookerjee B, Bhujwalla ZM, Sutter CH, Artemov D, et al. (2000) Regulation of tumor angiogenesis by p53-induced degradation of hypoxia-inducible factor 1alpha. Genes Dev 14: 34-44.
50. Fukuda R, Kelly B, Semenza GL (2003) Vascular endothelial growth factor gene expression in colon cancer cells exposed to prostaglandin E2 is mediated by hypoxia-inducible factor 1. Cancer Res 63: 2330-2334.
51. Smith JJ, Deane NG, Wu F, Merchant NB, Zhang B, et al. (2010) Experimentally derived metastasis gene expression profile predicts recurrence and death in patients with colon cancer. Gastroenterology 138: 958-968.
52. Blaine SA, Ray KC, Anunobi R, Gannon MA, Washington MK, et al. (2010) Adult pancreatic acinar cells give rise to ducts but not endocrine cells in response to growth factor signaling. Development 137: 2289-2296.

53. Solomon SD, Pfeffer MA, McMurray JJ, Fowler R, Finn P, et al. (2006) Effect of celecoxib on cardiovascular events and blood pressure in two trials for the prevention of colorectal adenomas. Circulation 114: 1028-1035.
54. Zeidler MP, Perrimon N, Strutt DI (1999) The four-jointed gene is required in the Drosophila eye for ommatidial polarity specification. Curr Biol 9: 1363-1372.
55. Zeidler MP, Perrimon N, Strutt DI (2000) Multiple roles for four-jointed in planar polarity and limb patterning. Dev Biol 228: 181-196.
56. Strutt H, Mundy J, Hofstra K, Strutt D (2004) Cleavage and secretion is not required for Four-jointed function in Drosophila patterning. Development 131: 881-890.
57. Ishikawa HO, Takeuchi H, Haltiwanger RS, Irvine KD (2008) Four-jointed is a Golgi kinase that phosphorylates a subset of cadherin domains. Science 321: 401-404.
58. Villano JL, Katz FN (1995) four-jointed is required for intermediate growth in the proximal-distal axis in Drosophila. Development 121: 2767-2777.
59. Buckles GR, Rauskolb C, Villano JL, Katz FN (2001) Four-jointed interacts with dachs, abelson and enabled and feeds back onto the Notch pathway to affect growth and segmentation in the Drosophila leg. Development 128: 3533-3542.
60. Simon MA, Xu A, Ishikawa HO, Irvine KD Modulation of FAt:Dachsous binding by the cadherin domain kinase four-jointed. Curr Biol 20: 811-817.
61. Brittle AL, Repiso A, Casal J, Lawrence PA, Strutt D Four-jointed modulates growth and planar polarity by reducing the affinity of dachsous for fat. Curr Biol 20: 803-810.
62. Lawrence PA, Casal J (2013) The mechanisms of planar cell polarity, growth and the Hippo pathway: some known unknowns. Dev Biol 377: 1-8.
63. Rock R, Heinrich AC, Schumacher N, Gessler M (2005) Fjx1: a notch-inducible secreted ligand with specific binding sites in developing mouse embryos and adult brain. Dev Dyn 234: 602-612.
64. Ashery-Padan R, Alvarez-Bolado G, Klamt B, Gessler M, Gruss P (1999) Fjx1, the murine homologue of the Drosophila four-jointed gene, codes for a putative secreted protein expressed in restricted domains of the developing and adult brain. Mech Dev 80: 213-217.
65. Probst B, Rock R, Gessler M, Vortkamp A, Puschel AW (2007) The rodent Four-jointed ortholog Fjx1 regulates dendrite extension. Dev Biol 312: 461-470.
66. Saburi S, Hester I, Fischer E, Pontoglio M, Eremina V, et al. (2008) Loss of Fat4 disrupts PCP signaling and oriented cell division and leads to cystic kidney disease. Nat Genet 40: 1010-1015.
67. Morikawa K, Walker SM, Nakajima M, Pathak S, Jessup JM, et al. (1988) Influence of organ environment on the growth, selection, and metastasis of human colon carcinoma cells in nude mice. Cancer Res 48: 6863-6871.
68. Snijders AM, Schmidt BL, Fridlyand J, Dekker N, Pinkel D, et al. (2005) Rare amplicons implicate frequent deregulation of cell fate specification pathways in oral squamous cell carcinoma. Oncogene 24: 4232-4242.
69. Jarvinen AK, Autio R, Kilpinen S, Saarela M, Leivo I, et al. (2008) High-resolution copy number and gene expression microarray analyses of head and neck squamous cell carcinoma cell lines of tongue and larynx. Genes Chromosomes Cancer 47: 500-509.
70. Buckanovich RJ, Sasaroli D, O'Brien-Jenkins A, Botbyl J, Hammond R, et al. (2007) Tumor vascular proteins as biomarkers in ovarian cancer. J Clin Oncol 25: 852-861.
71. Lu C, Bonome T, Li Y, Kamat AA, Han LY, et al. (2007) Gene alterations identified by expression profiling in tumor-associated endothelial cells from invasive ovarian carcinoma. Cancer Res 67: 1757-1768.

72. Aird WC (2009) Molecular heterogeneity of tumor endothelium. Cell Tissue Res 335: 271-281.

73. Tracey L, Villuendas R, Dotor AM, Spiteri I, Ortiz P, et al. (2003) Mycosis fungoides shows concurrent deregulation of multiple genes involved in the TNF signaling pathway: an expression profile study. Blood 102: 1042-1050.

74. Nam KT, Varro A, Coffey RJ, Goldenring JR (2007) Potentiation of oxyntic atrophy-induced gastric metaplasia in amphiregulin-deficient mice. Gastroenterology 132: 1804-1819.

75. Okayasu I, Ohkusa T, Kajiura K, Kanno J, Sakamoto S (1996) Promotion of colorectal neoplasia in experimental murine ulcerative colitis. Gut 39: 87-92.

76. Neufert C, Becker C, Neurath MF (2007) An inducible mouse model of colon carcinogenesis for the analysis of sporadic and inflammation-driven tumor progression. Nat Protoc 2: 1998-2004.

77. Dieleman LA, Palmen MJ, Akol H, Bloemena E, Pena AS, et al. (1998) Chronic experimental colitis induced by dextran sulphate sodium (DSS) is characterized by Th1 and Th2 cytokines. Clin Exp Immunol 114: 385-391.

78. Kubota Y, Kleinman HK, Martin GR, Lawley TJ (1988) Role of laminin and basement membrane in the morphological differentiation of human endothelial cells into capillary-like structures. J Cell Biol 107: 1589-1598.

79. Arnaoutova I, George J, Kleinman HK, Benton G (2009) The endothelial cell tube formation assay on basement membrane turns 20: state of the science and the art. Angiogenesis 12: 267-274.

80. Naumov GN, Akslen LA, Folkman J (2006) Role of angiogenesis in human tumor dormancy: animal models of the angiogenic switch. Cell Cycle 5: 1779-1787.

81. Roy S, Khanna S, Shah H, Rink C, Phillips C, et al. (2005) Human genome screen to identify the genetic basis of the anti-inflammatory effects of Boswellia in microvascular endothelial cells. DNA Cell Biol 24: 244-255.

82. Mayer H, Bilban M, Kurtev V, Gruber F, Wagner O, et al. (2004) Deciphering regulatory patterns of inflammatory gene expression from interleukin-1-stimulated human endothelial cells. Arterioscler Thromb Vasc Biol 24: 1192-1198.

83. Dower K, Ellis DK, Saraf K, Jelinsky SA, Lin LL (2008) Innate immune responses to TREM-1 activation: overlap, divergence, and positive and negative cross-talk with bacterial lipopolysaccharide. J Immunol 180: 3520-3534.

84. Huber A, Hudelist G, Knofler M, Saleh L, Huber JC, et al. (2007) Effect of highly purified human chorionic gonadotropin preparations on the gene expression signature of stromal cells derived from endometriotic lesions: potential mechanisms for the therapeutic effect of human chorionic gonadotropin in vivo. Fertil Steril 88: 1232-1239.

85. Zhang B, Kirov S, Snoddy J (2005) WebGestalt: an integrated system for exploring gene sets in various biological contexts. Nucleic Acids Research 33: W741-W748.

86. Subramanian A, Tamayo P, Mootha VK, Mukherjee S, Ebert BL, et al. (2005) Gene set enrichment analysis: a knowledge-based approach for interpreting genome-wide expression profiles. Proc Natl Acad Sci U S A 102: 15545-15550.

87. Simon MP, Tournaire R, Pouyssegur J (2008) The angiopoietin-2 gene of endothelial cells is up-regulated in hypoxia by a HIF binding site located in its first intron and by the central factors GATA-2 and Ets-1. J Cell Physiol 217: 809-818.

88. Wolf N, Yang W, Dunk CE, Gashaw I, Lye SJ, et al. (2010) Regulation of the matricellular proteins CYR61 (CCN1) and NOV (CCN3) by hypoxia-inducible factor-1{alpha} and transforming-growth factor-{beta}3 in the human trophoblast. Endocrinology 151: 2835-2845.

89. Wan J, Chai H, Yu Z, Ge W, Kang N, et al. (2011) HIF-1alpha effects on angiogenic potential in human small cell lung carcinoma. J Exp Clin Cancer Res 30: 77.

90. Sanchez-Elsner T, Botella LM, Velasco B, Langa C, Bernabeu C (2002) Endoglin expression is regulated by transcriptional cooperation between the hypoxia and transforming growth factor-beta pathways. J Biol Chem 277: 43799-43808.

91. Okuyama H, Krishnamachary B, Zhou YF, Nagasawa H, Bosch-Marce M, et al. (2006) Expression of vascular endothelial growth factor receptor 1 in bone marrow-derived mesenchymal cells is dependent on hypoxia-inducible factor 1. J Biol Chem 281: 15554-15563.

92. Elvidge GP, Glenny L, Appelhoff RJ, Ratcliffe PJ, Ragoussis J, et al. (2006) Concordant regulation of gene expression by hypoxia and 2-oxoglutarate-dependent dioxygenase inhibition: the role of HIF-1alpha, HIF-2alpha, and other pathways. J Biol Chem 281: 15215-15226.

93. Anelli V, Gault CR, Cheng AB, Obeid LM (2008) Sphingosine kinase 1 is up-regulated during hypoxia in U87MG glioma cells. Role of hypoxia-inducible factors 1 and 2. J Biol Chem 283: 3365-3375.

94. Lai VK, Afzal MR, Ashraf M, Jiang S, Haider H (2012) Non-hypoxic stabilization of HIF-Ialpha during coordinated interaction between Akt and angiopoietin-1 enhances endothelial commitment of bone marrow stem cells. J Mol Med (Berl) 90: 719-730.

95. Osada-Oka M, Ikeda T, Akiba S, Sato T (2008) Hypoxia stimulates the autocrine regulation of migration of vascular smooth muscle cells via HIF-1alpha-dependent expression of thrombospondin-1. J Cell Biochem 104: 1918-1926.

96. Spinella F, Garrafa E, Di Castro V, Rosano L, Nicotra MR, et al. (2009) Endothelin-1 stimulates lymphatic endothelial cells and lymphatic vessels to grow and invade. Cancer Res 69: 2669-2676.

97. Maisonpierre PC, Suri C, Jones PF, Bartunkova S, Wiegand SJ, et al. (1997) Angiopoietin-2, a natural antagonist for Tie2 that disrupts in vivo angiogenesis. Science 277: 55-60.

98. Lobov IB, Brooks PC, Lang RA (2002) Angiopoietin-2 displays VEGF-dependent modulation of capillary structure and endothelial cell survival in vivo. Proc Natl Acad Sci U S A 99: 11205-11210.

99. Ferrara N (2010) Binding to the extracellular matrix and proteolytic processing: two key mechanisms regulating vascular endothelial growth factor action. Mol Biol Cell 21: 687-690.

100. Seppinen L, Pihlajaniemi T (2011) The multiple functions of collagen XVIII in development and disease. Matrix Biol 30: 83-92.

101. Epstein AC, Gleadle JM, McNeill LA, Hewitson KS, O'Rourke J, et al. (2001) C. elegans EGL-9 and mammalian homologs define a family of dioxygenases that regulate HIF by prolyl hydroxylation. Cell 107: 43-54.

102. Maxwell PH, Wiesener MS, Chang GW, Clifford SC, Vaux EC, et al. (1999) The tumour suppressor protein VHL targets hypoxia-inducible factors for oxygen-dependent proteolysis. Nature 399: 271-275.

103. Chandel NS, McClintock DS, Feliciano CE, Wood TM, Melendez JA, et al. (2000) Reactive oxygen species generated at mitochondrial complex III stabilize hypoxia-inducible factor-1alpha during hypoxia: a mechanism of O2 sensing. J Biol Chem 275: 25130-25138.

104. Guzy RD, Hoyos B, Robin E, Chen H, Liu L, et al. (2005) Mitochondrial complex III is required for hypoxia-induced ROS production and cellular oxygen sensing. Cell Metab 1: 401-408.

105. Hagen T, Taylor CT, Lam F, Moncada S (2003) Redistribution of intracellular oxygen in hypoxia by nitric oxide: effect on HIF1alpha. Science 302: 1975-1978.
106. Chua YL, Dufour E, Dassa EP, Rustin P, Jacobs HT, et al. (2010) Stabilization of hypoxia-inducible factor-1alpha protein in hypoxia occurs independently of mitochondrial reactive oxygen species production. J Biol Chem 285: 31277-31284.
107. Lim LH, Pervaiz S (2007) Annexin 1: the new face of an old molecule. FASEB J 21: 968-975.
108. Yi M, Schnitzer JE (2009) Impaired tumor growth, metastasis, angiogenesis and wound healing in annexin A1-null mice. Proc Natl Acad Sci U S A 106: 17886-17891.
109. Gashaw I, Stiller S, Boing C, Kimmig R, Winterhager E (2008) Premenstrual regulation of the pro-angiogenic factor CYR61 in human endometrium. Endocrinology 149: 2261-2269.
110. Meyuhas R, Pikarsky E, Tavor E, Klar A, Abramovitch R, et al. (2008) A Key role for cyclic AMP-responsive element binding protein in hypoxia-mediated activation of the angiogenesis factor CCN1 (CYR61) in Tumor cells. Mol Cancer Res 6: 1397-1409.
111. Wang W, Wang X, Peng L, Deng Q, Liang Y, et al. (2010) CD24-dependent MAPK pathway activation is required for colorectal cancer cell proliferation. Cancer Sci 101: 112-119.
112. Sagiv E, Memeo L, Karin A, Kazanov D, Jacob-Hirsch J, et al. (2006) CD24 is a new oncogene, early at the multistep process of colorectal cancer carcinogenesis. Gastroenterology 131: 630-639.
113. Marotta LL, Almendro V, Marusyk A, Shipitsin M, Schemme J, et al. (2011) The JAK2/STAT3 signaling pathway is required for growth of CD44(+)CD24(-) stem cell-like breast cancer cells in human tumors. J Clin Invest 121: 2723-2735.
114. Wang KH, Kao AP, Chang CC, Lee JN, Hou MF, et al. (2010) Increasing CD44+/CD24(-) tumor stem cells, and upregulation of COX-2 and HDAC6, as major functions of HER2 in breast tumorigenesis. Mol Cancer 9: 288.
115. Buchanan FG, Holla V, Katkuri S, Matta P, DuBois RN (2007) Targeting cyclooxygenase-2 and the epidermal growth factor receptor for the prevention and treatment of intestinal cancer. Cancer Res 67: 9380-9388.
116. Chan AT, Giovannucci EL, Meyerhardt JA, Schernhammer ES, Wu K, et al. (2008) Aspirin dose and duration of use and risk of colorectal cancer in men. Gastroenterology 134: 21-28.
117. Melani M, Weinstein BM Common factors regulating patterning of the nervous and vascular systems. Annu Rev Cell Dev Biol 26: 639-665.
118. Nasarre P, Potiron V, Drabkin H, Roche J (2010) Guidance molecules in lung cancer. Cell Adh Migr 4: 130-145.
119. Legg JA, Herbert JM, Clissold P, Bicknell R (2008) Slits and Roundabouts in cancer, tumour angiogenesis and endothelial cell migration. Angiogenesis 11: 13-21.